**European Commission**
**Research Programme of the Research Fund for Coal and Steel**

# ANGELHY

**Innovative solutions for design and strengthening of telecommunications and transmission lattice towers using large angles from high strength steel and hybrid techniques of angles with FRP strips**

# WORK PACKAGE 2 – DELIVERABLE 2.6

## Guidance on analysis models for complete towers

Coordinator:

National Technical University of Athens - NTUA, Greece

Beneficiaries:

ArcelorMittal Belval & Differdange SA - AMBD, Luxembourg

Universite de Liege - ULG, Belgium

COSMOTE Kinites Tilepikoinonies AE - COSMOTE, Greece

Centre Technique Industriel de la Construction Metallique - CTICM, France

SIKA France SAS - SIKA, France

Grant Agreement Number: 753993

03/07/2020

# AUTHORS:

CENTRE TECHNIQUE INDUSTRIEL DE LA CONSTRUCTION METALLIQUE - CTICM

Steel Construction Research Division
Espace Technologique – Immeuble Apollo
L'Orme des Merisiers – F-91193 Saint Aubin
Authors: André Beyer, Alain Bureau


NATIONAL TECHNICAL UNIVERSITY OF ATHENS

Institute of Steel Structures

15780 Athens, Greece

Authors: Ioannis Vayas, Pavlos Thanopoulos, Dimitrios Vamvatsikos, Konstantinos Vlachakis, Marios-Zois Bezas, Maria-Eleni Dasiou

# TABLE OF CONTENTS

# 1  Introduction

The type of analysis models for lattice towers evolved, depending on the available tools at each time. Before the application of electronic calculation, static calculations of lattice towers were performed by hand on the basis of 2D – models separately for each wall [1]. The forces on the members were determined using graphical methods, like the Cremona diagram, numerical methods, like the Ritter section method, or combined numerical-graphical methods. Evidently, the structure was considered as an ideal truss, where joints were considered as pinned. The introduction of electronic calculation brought a substantial improvement in tower analysis. The complete tower structure is indeed represented by a 3D – FE numerical model, composed of beam or truss elements. However, it is still the usual design practice to model the structure as an ideal truss, considering joints to behave as pinned and neglecting connection or load eccentricities resulting in braces from angle sections that are bolted to gusset plates. Accordingly, analysis results deliver only axial forces for members that have to be designed for pure compression/tension. The effects of load eccentricity and connection behavior, like partial restraint of braces, are incorporated in design by modification of the relevant buckling lengths [2], [3], [4].

For a further development of analysis models, it should be recognized that calculation models should reflect the anticipated type of behavior for cross sections, members, joints and bearings. Geometric properties and structural effects are considered either directly in the analysis model and method or design. For example, imperfections, eccentricities, or connection behavior may be introduced in the analysis model and stability problems may be directly checked by advanced analysis methods. Consequently, the implementation of refined analysis models and application of advanced analysis methods may replace some design checks.

In the following, current Code provisions for design of tower members composed of angle sections will be reviewed. This is followed by a presentation of alternative analysis and design models for telecommunication and transmission towers. The models are designated with **Level I** to **IV**, where increasing refinement in the analysis have been implemented to account for more effects in analysis and allow less effort in design. In addition, results of the back analysis for the six (6) experimental tower models that have been subjected to Laboratory testing at NTUA will be presented.

# 2   Code provisions for design of lattice tower members

In the following the provisions of selected Codes in respect to the design of tower legs and bracing members from angle sections will be presented. The provisions are based on analysis models that represent the structure as an ideal truss. Members are then designed to buckling due to pure compression. The effect of end-restraint of bracing members connected to the stiffer legs is considered by reduction of the relevant buckling length. The effect of load eccentricity through connection on one leg is considered by addition of a fixed term in the member slenderness. The effect of connection with one bolt is considered by direct reduction of the buckling resistance. More specifically the Code gives rules for the buckling length, possible modification in slenderness, the appropriate buckling curve and the design relation. These rules will be briefly presented for selected Codes.

## 2.1   Provisions of EN 1993-1-1 [5]

EN 1993-1-1 is the general part of Eurocode 3 and the part of buildings in general. In its Annex BB.1 it refers to design of lattice girders in general, providing design rules for chord members in general and web members from angle sections.

### 2.1.1   Chord members                                                    BB.1.1(1)B

- o   Buckling length in- and out-of plane        $L_{cr} = L$

- o   Design to compression and bending using §6.2.9 of EN 1993-1-1.

### 2.1.2   Web members connected through two bolts                    BB.1.2(1)B

- o   Buckling length

        Out of plane buckling  (minor axis v)        $L_{cr} = L$

        In plane buckling  (geometric axis y)        $L_{cr} = 0.9L$

- o   Effective slenderness

        Out of plane buckling  (minor axis v)        $\bar{\lambda}_{eff,v} = 0{,}35 + 0{,}7\bar{\lambda}_v$

        In plane buckling  (geometric axis y)        $\bar{\lambda}_{eff,y} = 0{,}50 + 0{,}7\bar{\lambda}_y$

- o   Design to compression, buckling curve b

$$N_{Ed} \leq \frac{\chi\, A\, f_y}{\gamma_{M1}}$$

### 2.1.3   Web members connected through one bolt                    BB.1.2(2)B

- o   Buckling length $L_{cr} = L$

- o   Member design by 2nd order analysis accounting for buckling curve b member imperfections and subsequent cross section design, as outlined in §6.2.9 of EN 1993-1-1.

## 2.2 Provisions of EN 1993-3-1 [4]

EN 1993-3-1 is the specific part of Eurocode 3 applicable to masts and towers. In its Annex G it refers to design of chord and bracing members from towers. These rules will be briefly presented for selected Codes.

### 2.2.1 Chord members

- Buckling length                                        Table G.1

    Out of plane buckling  (minor axis v)        $L_{cr} = L$

    In plane buckling  (geometric axis y)        $L_{cr} = L$

- Effective slenderness                                 Table G.1

    In plane buckling (minor axis v)            $\bar{\lambda}_{eff,v} = 0,10 + 0,8\bar{\lambda}_v$

    Out of plane buckling (geometric axis y)    $\bar{\lambda}_{eff,y} = \bar{\lambda}_y$

- Design to compression, buckling curve b

$$N_{Ed} \leq \frac{\chi\,A\,f_y}{\gamma_{M1}}$$

### 2.2.2 Bracing members connected through two bolts on both sides

- Buckling length                                        Table G.2

    Out of plane buckling  (minor axis v)        $L_{cr} = L$

    In plane buckling  (geometric axis y)        $L_{cr} = L$

- Effective slenderness                                 Table G.2

    In plane buckling (minor axis v)            $\bar{\lambda}_{eff,v} = 0,35 + 0,7\bar{\lambda}_v$

    Out of plane buckling (geometric axis y)    $\bar{\lambda}_{eff,y} = 0,40 + 0,7\bar{\lambda}_y$

- Design to compression, buckling curve b

$$N_{Ed} \leq \frac{\chi\,A\,f_y}{\gamma_{M1}}$$

### 2.2.3 Bracing members connected through one and two bolts          BB.1.2(2)B

- Buckling length                                        Table G.2

    Out of plane buckling  (minor axis v)        $L_{cr} = L$

    In plane buckling  (geometric axis y)        $L_{cr} = L$

- Effective slenderness                                 Table G.2

    In plane buckling (minor axis v)            $\bar{\lambda}_{eff,v} = 0,35 + 0,7\bar{\lambda}_v$

    Out of plane buckling (geometric axis y)    $\bar{\lambda}_{eff,y} = 0,40 + 0,7\bar{\lambda}_y$

- Design to compression, buckling curve b

$$N_{Ed} \leq \frac{0,9\,\chi\,A\,f_y}{\gamma_{M1}}$$                              G.1(3)

### 2.2.4  Bracing members connected through one bolt on both sides        BB.1.2(2)B

- o  Buckling length                                                  Table G.2

    Out of plane buckling  (minor axis v)        $L_{cr} = L$

    In plane buckling  (geometric axis y)        $L_{cr} = L$

- o  Effective slenderness        Table G2

    In plane buckling (minor axis v)                    $\bar{\lambda}_{eff,v} = 0{,}35 + 0{,}7\bar{\lambda}_v$

    Out of plane buckling (geometric axis y)            $\bar{\lambda}_{eff,y} = 0{,}58 + 0{,}7\bar{\lambda}_y$

- o  Design to compression, buckling curve b

    $$N_{Ed} \le \frac{0{,}8\,\chi\,A\,f_y}{\gamma_{M1}}$$                                      G.1(3)

## 2.3  Provisions of EN 50341 [6]

Finally, the European standard for the design of Overhead Transmission Lines EN 50341 also provides specific rules for the design of angle section members in lattice towers. These rules are presented next.

### 2.3.1  Web members connected through two bolts

- o  Buckling length

    Out of plane buckling  (minor axis v)        $L_{cr} = L$

    In plane buckling  (geometric axis y)        $L_{cr} = L$

- o  Effective slenderness

    Out of plane buckling  (minor axis v)              $\bar{\lambda}_{eff,v} = 0{,}30 + 0{,}68\bar{\lambda}_v$

    In plane buckling  (geometric axis y)              $\bar{\lambda}_{eff,y} = 0{,}52 + 0{,}68\bar{\lambda}_y$

- o  Design to compression, buckling curve b

    $$N_{Ed} \le \frac{\chi\,A\,f_y}{\gamma_{M1}}$$

### 2.3.2  Web members connected through one bolt

- o  Buckling length

    Out of plane buckling  (minor axis v)        $L_{cr} = L$

    In plane buckling  (geometric axis y)        $L_{cr} = L$

- o  Effective slenderness

    Out of plane buckling  (minor axis v)

      $\bar{\lambda}_{eff,v} = 0{,}30 + 0{,}68\bar{\lambda}_v$        if  $\bar{\lambda}_v \le \sqrt{2}$

      $\bar{\lambda}_{eff,v} = 1.091 - 0{,}287\bar{\lambda}_y$      if  $\bar{\lambda}_v > \sqrt{2}$

    In plane buckling  (geometric axis y)

$$\bar{\lambda}_{eff,v} = 0{,}52 + 0{,}68\bar{\lambda}_v \qquad \text{if } \bar{\lambda}_v \le \sqrt{2}$$

$$\bar{\lambda}_{eff,v} = 0{,}16 + 0{,}94\bar{\lambda}_y \qquad \text{if } \bar{\lambda}_v > \sqrt{2}$$

o Design to compression, buckling curve b

$$N_{Ed} \le \frac{\chi A f_y}{\gamma_{M1}}$$

## 2.4 Provisions of Canadian Code CAN/CSA-S37-94 [9]

According to the provisions of the Canadian Code for Antennas, masts and towers "Members composed of angles connected by one leg, with normal framing eccentricities, may be designed as axially loaded members using the effective slenderness ratio formulae given in Tables 6.1A and 6.1B. Normal framing eccentricities, means that the centroid of the bolt or weld pattern is located between the centroid of the angle and the centerline of the connected leg".

The effective slenderness ratio is determined from

- Angles connected through one bolt

$\lambda_v \le 120$: $\qquad\qquad\qquad\qquad \lambda_{v,eff} \le 60 + 0.5\,\lambda_v$

$\lambda_v > 120$ $\qquad\qquad\qquad\qquad \lambda_{v,eff} \le \lambda_v$

- Angles connected through two bolts

$\lambda_v \le 120$: $\qquad\qquad\qquad\qquad \lambda_{v,eff} \le 60 + 0.5\,\lambda_v$

$\lambda_v > 120$: $\qquad\qquad\qquad\qquad \lambda_{v,eff} \le 46.2 + 0.615\,\lambda_v$

The design resistance is determined from:

$C_r = \varphi\, A\, F_y'(1 + \lambda^{2n})^{-1/n}$

where:

$\varphi = 0{,}90$ safety factor

A cross section area

$F_y'$ yield stress, possibly modified to account for local buckling

$\lambda$ slenderness, modified as above

n = 1.34

## 3    Experimental validation of design provisions

### 3.1    Hajdar tests at UWindsor [7]

At the University of Windsor, Canada, 105 compression tests were carried out on equal angle sections loaded through two-bolts in one leg. The tests were performed during the MSc Thesis of Hajdar and reported in [7]. The cross sections were L 64.4.8, L64.6.4 and L76.6.4. The material was steel S 300. The bolts were snug-tight in 75 tests and preloaded in 30 tests. Figure 3.1 illustrates the test set-up. The tested angle was connected to stronger angles, from which the vertical one was continuously supported through U-clamps by the tested frame.
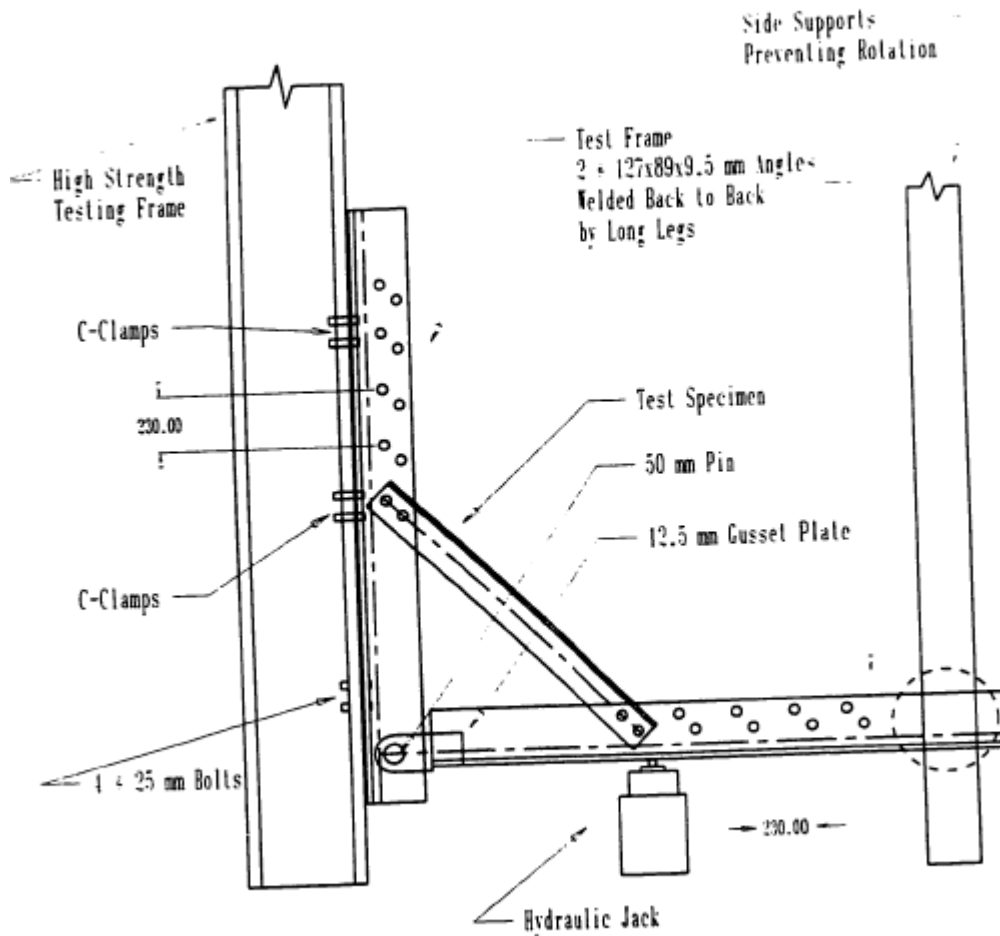


**Figure 3.1 Test set-up for Hajdar Windsor tests [7]**

The tested angle was connected to stronger angles, from which the vertical one was continuously supported through U-clamps by the tested frame. These boundary conditions provided fixity at the ends of the tested angle, which was considered in the re-analysis with the proposed formula through buckling length reduction.

Figure 3.2 presents the ratio between experimental and analytical load for the tests with snug-tight bolts and Figure 3.3 with preloaded bolts as a function of the weak axis slenderness λv. The analytical load was determined according to the proposed method as presented in Deliverable 2.2 of the current project and the provisions of EN 1993-3-1 using the actual geometrical and material properties without safety factors. These figures present also the mean minus one standard deviation value for the two analytical methods.
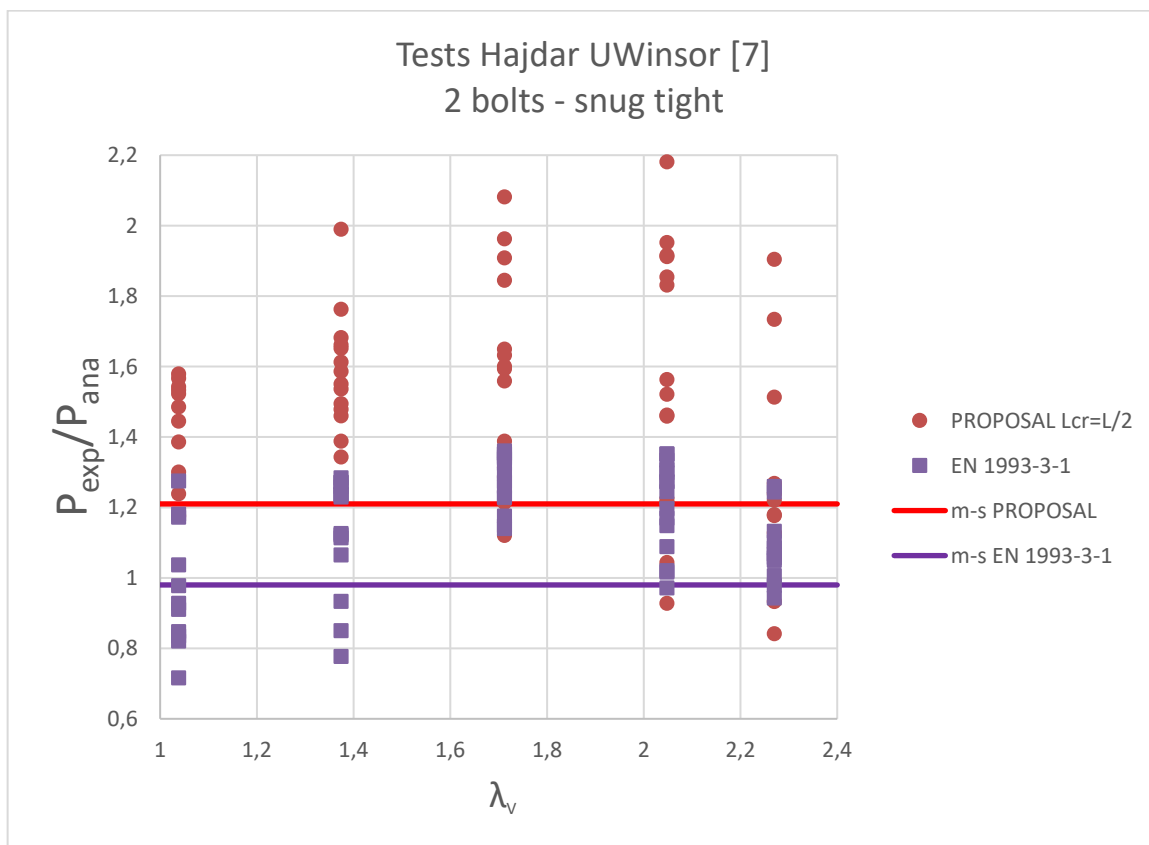
**Figure 3.2 Ratio between experimental and analytical load for the Hajdar/UWindsor tests with snug-tight bolts**
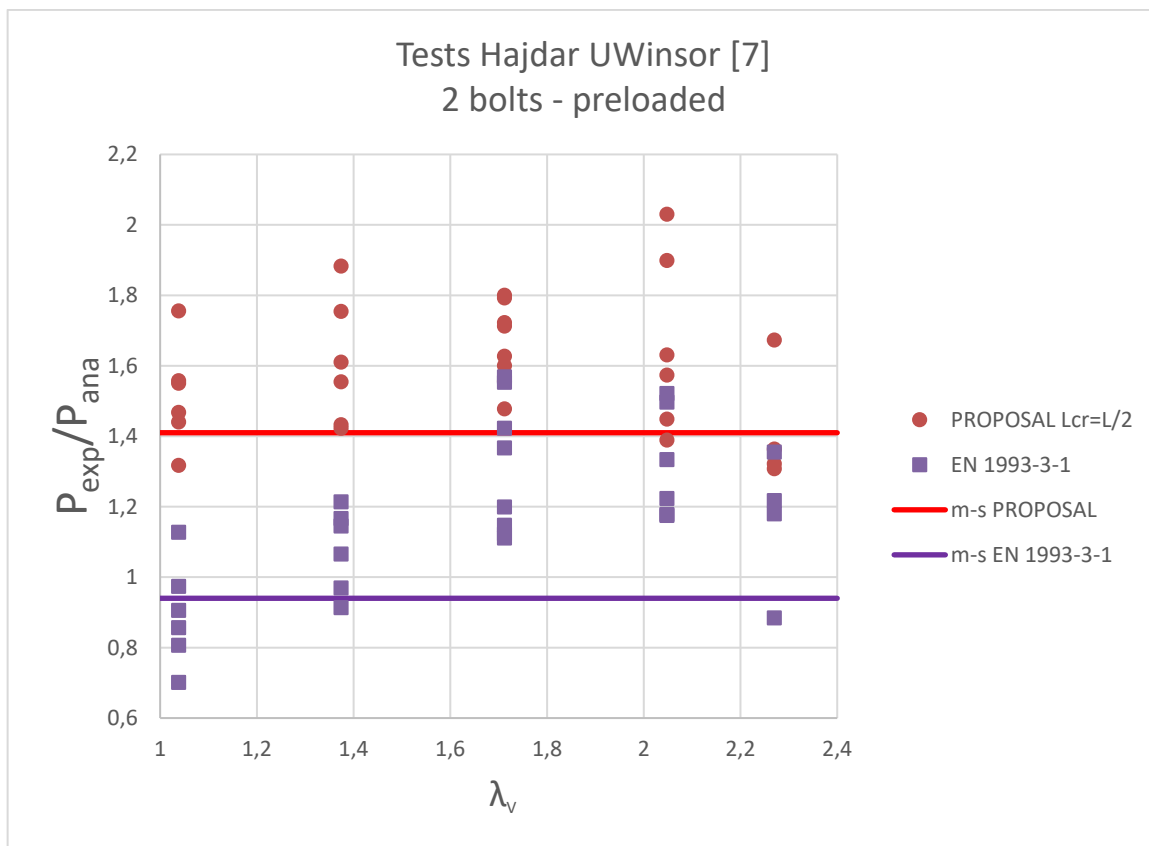


**Figure 3.3 Ratio between experimental and analytical load for the Hajdar/UWindsor tests with preloaded bolts**

The proposed method, checking the angle profile to compression and biaxial bending with following observations, the same as outlined in Deliverable 2.2:

a. The buckling length was set equal to ½ of the system length L due to the fixed end supports of the loaded specimen.

b. The load was introduced to the profile through one leg by the bolts. The relevant eccentricities are determined as following, Figure 3.4.

$$e_u = \frac{e}{\sqrt{2}} - u_G$$

$$e_v = e/\sqrt{2}$$

where:

$u_G$ is the distance of the angle's heel from its centroid along the strong axis

e is the distance of the angle's heel from the load introduction point along the leg.

The resulting moments are:

$M_u = N \cdot e_u$

$M_v = N \cdot e_v$

where N is the applied load.

The load introduction point is the center of the hole for connection with one bolt, or the center between the two holes for connection with two bolts.
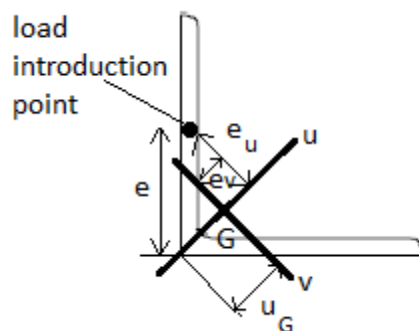


**Figure 3.4 Eccentricities due to load introduction in one leg**

Figures 3.2 and 3.3 lead to following observations:

1. The current proposal gives for all tests a safe prediction for the angle capacity.

2. Contrary, EN 1993-3-1 [4] does not provide safe estimations for a large number of tests.

3. The statistical estimates of the design rules are well on the safe side for the current proposal and a little on the unsafe side for the provisions of EN 1993-3-1. The latter appear to be adequate when the end support conditions provide fixity of the considered member.

## 3.2 Shani tests at UWindsor [8]

At the University of Windsor, Canada, 16 compression tests were carried out on equal angle sections loaded through one bolts in one leg. The tests were performed during the MSc Thesis of Shani and reported in [8]. The cross sections were L 51 in three thicknesses, 4.8, 6.4 and 7.9, L64 in two thicknesses, 6.4, 7.9 and L76.6.4. The material was steel S 300. Figure 3.5 illustrates the test set-up. It is the same as before, Figure 3.1, with the difference that the tested angle is connected through one bolt.
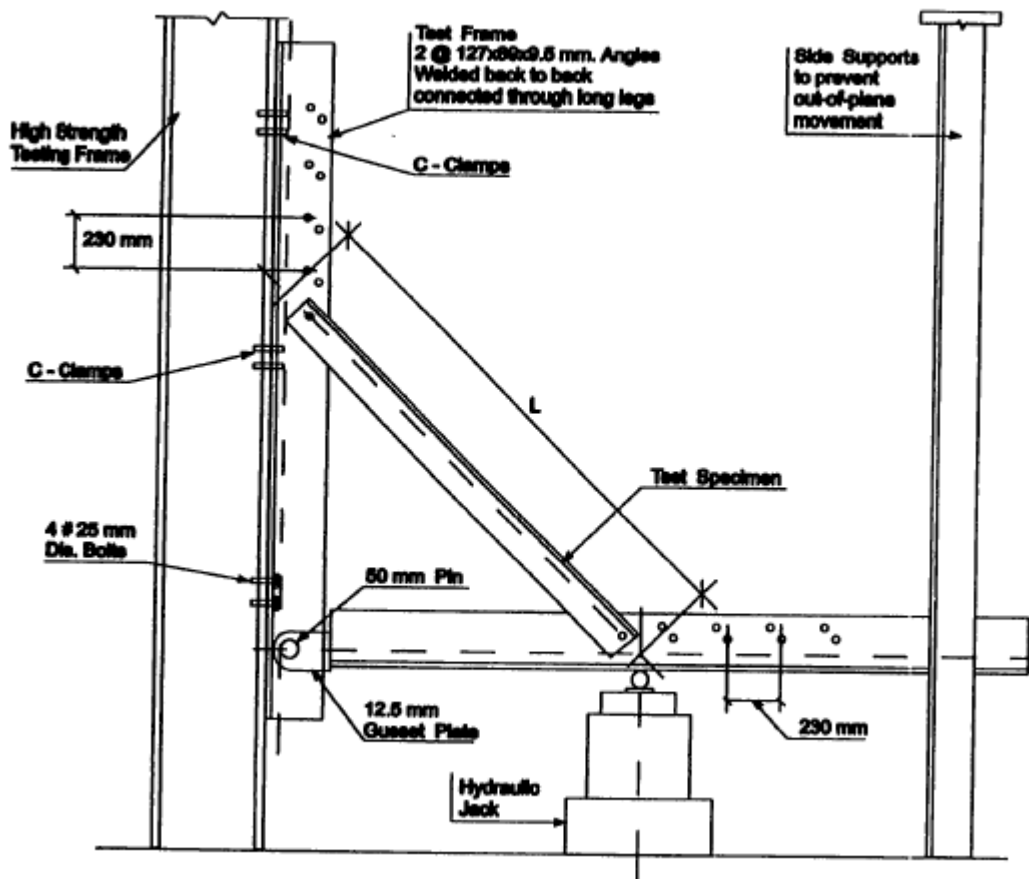


**Figure 3.5 Test set-up for Shani Windsor tests [8]**

Figure 3.6 presents the ratio between experimental and analytical load for the tests as a function of the weak axis slenderness $\lambda_v$. The analytical load was determined according to the proposed method setting the buckling length equal to 70% of the system length, as well as according to the provisions of EN 1993-3-1 Again the calculations were made using the actual geometrical and material properties without safety factors. Figure 3.7 presents the same ratio setting the buckling length equal to 50% of the system length.
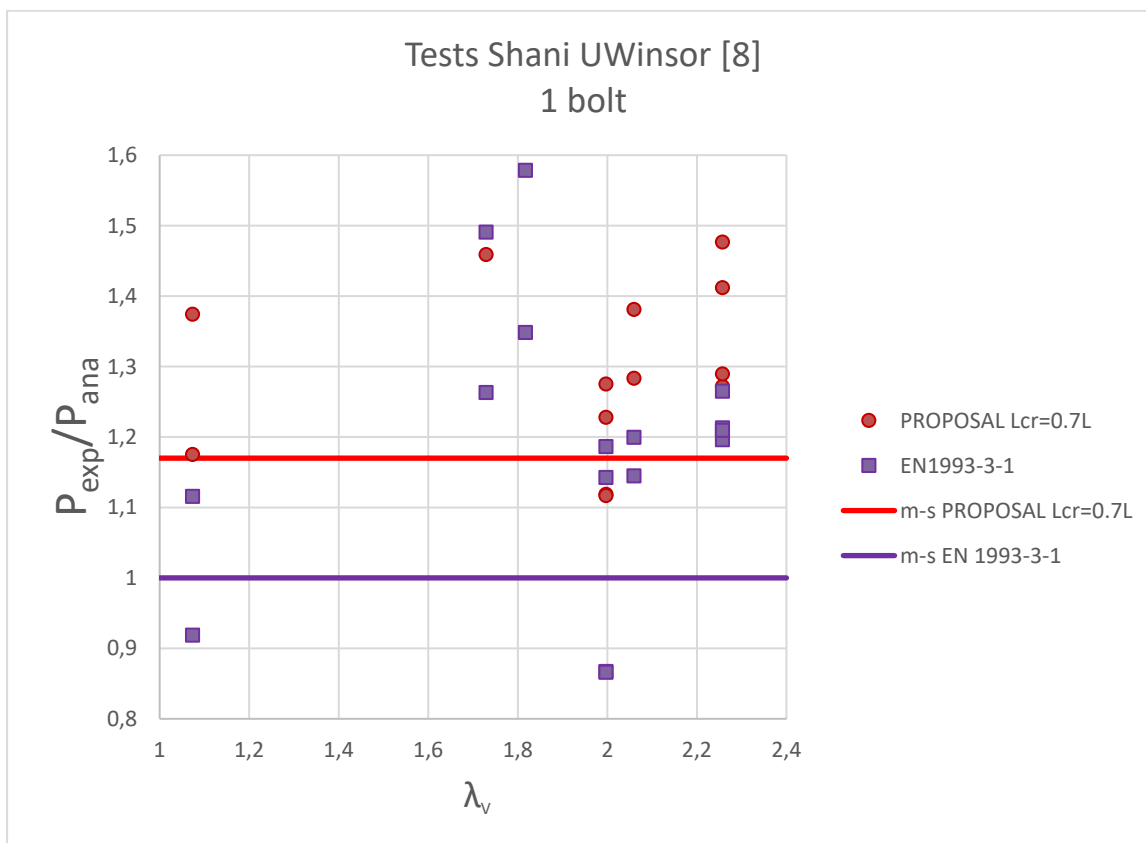
**Figure 3.6 Ratio between experimental and analytical load for the Shani/UWindsor tests setting $L_{cr}=0,7L$**
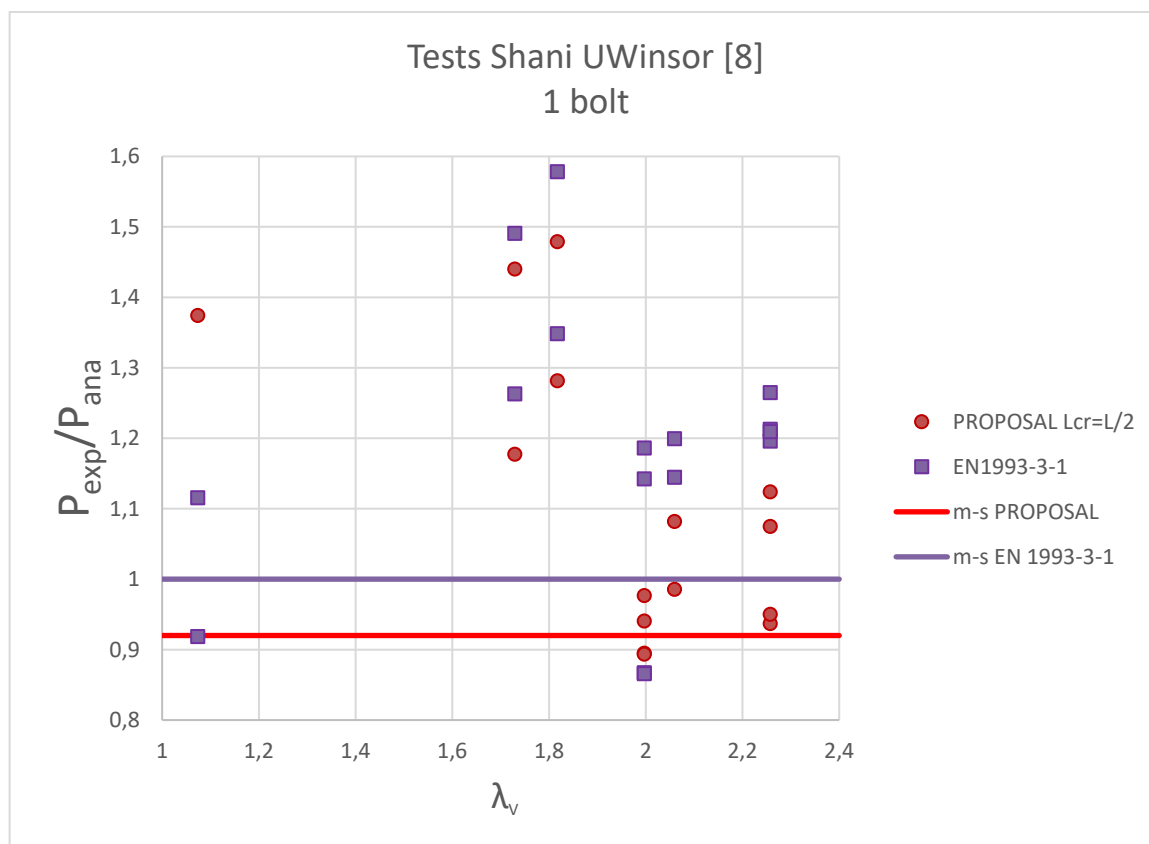


**Figure 3.7 Ratio between experimental and analytical load for the Shani/UWindsor tests setting $L_{cr}=0,5L$**

Following observations can be made:

1. Figure 3.6 shows that the current proposal gives for all tests a safe prediction for the angle capacity, while EN 1993-3-1 [4] provides safe estimations for all but two tests.

2. Figures 3.6 and 3.7 show that the buckling length of angles connected to one bolt may be reduced to 70% (**not** 50%) of the system length when fixity is provided at end supports.

3. The statistical estimates of the design rules are well on the safe side for the current proposal and exactly at the verge of safety for the provisions of EN 1993-3-1.

## 3.3   Tests at NIS Nagpur [10]

Bhilawe J, Gupta performed at the Visvesvaraya National Institute of Technology, Nagpur, India, 24 compression tests on equal angle sections loaded eccentrically in one leg [10]. The angles were connected to gusset plates through one bolt, two bots or welds. The cross sections were L50.6, L60.5 and L65.6. The material was steel S 350. Figure 3.9 illustrates the end support conditions. Although the test description and the specimen properties in [10] are ambiguous, the tests are reviewed here for reasons of comparison between methods.
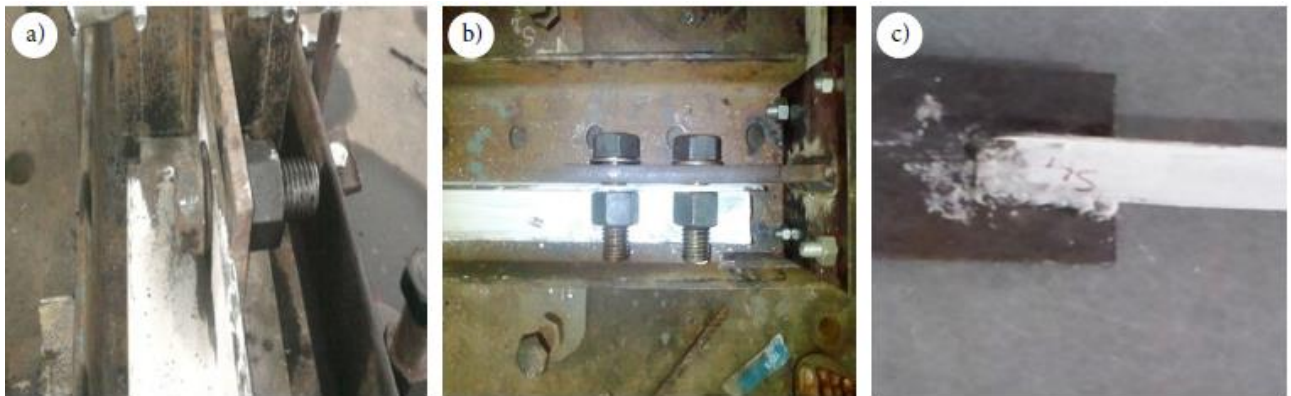


**Figure 3.8 End support conditions with one bolt, two bolts and welds for the NIS Nagpur tests [10]**

Figure 3.9 to Figure 3.11 present the ratio between experimental and analytical load for the tests as a function of the weak axis slenderness $\lambda_v$. The analytical load was determined according to the proposed method setting the buckling length equal to 70% of the system length for the connection with one bolt and weld and 50% of the system length for the connection with two bolts.  The calculations were made using the actual geometrical and material properties, as far as they were understood from the report, without safety factors.

No comments are made to the results due to the ambiguity of the input data. However it seems that the design with the current proposal provided results more on the safe side compared with EN 1993-3-1 for the bolted end connections, while the opposite holds for the welded connections.
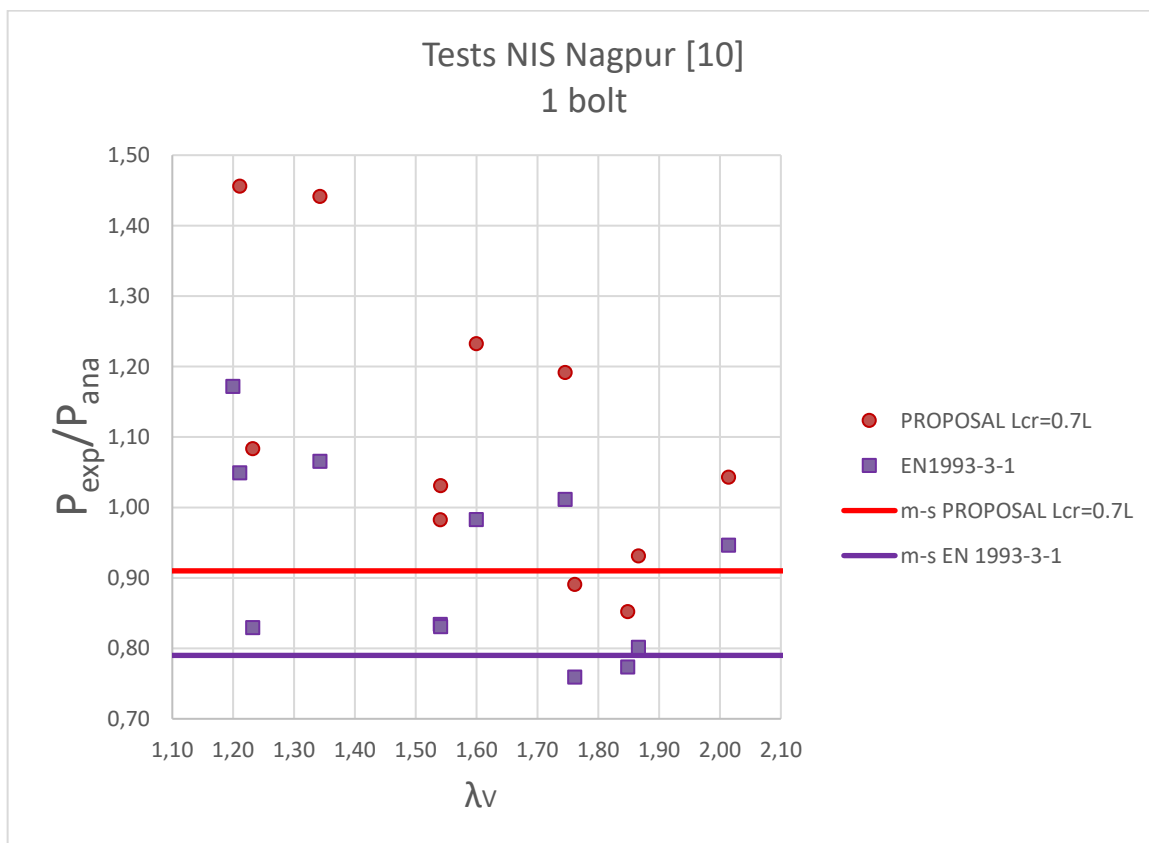
**Figure 3.9 Ratio between experimental and analytical load for the NIS Nagpur tests [10] for connection with one bolt**
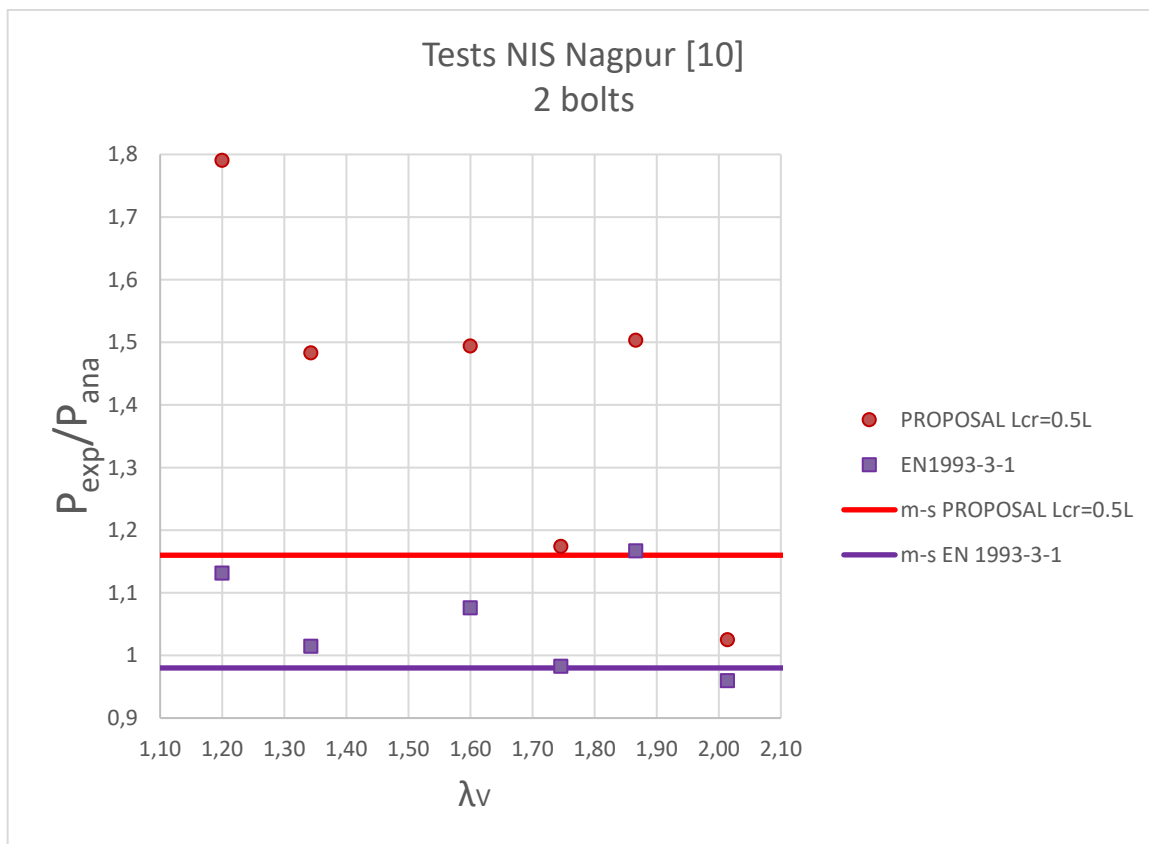


**Figure 3.10 Ratio between experimental and analytical load for the NIS Nagpur tests [10] for connection with two bolts**
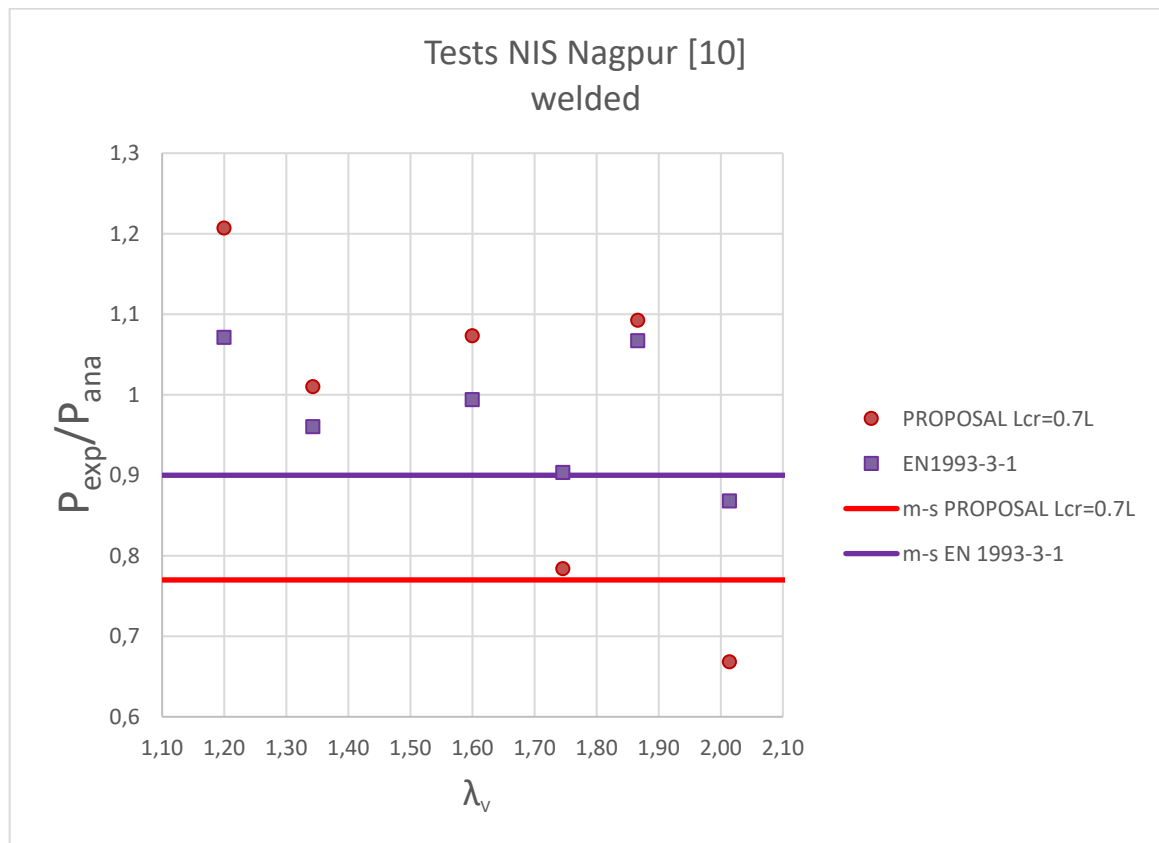
**Figure 3.11 Ratio between experimental and analytical load for the NIS Nagpur tests [10] for connection with welds**

# 4 Alternative analysis and design models for lattice towers without FRP strengthening

## 4.1 Level I – models

**Level I** – models mirror the state of design mostly applied in current Engineering practice in Europe. It is anchored in the provisions of the current versions of the Eurocodes, especially [4] and [5]. The properties of **Level I** models are summarized in the following.

### 4.1.1 Numerical models

The basic assumptions for the **Level I** numerical models may be summarized as following:

- Towers are modelled as 3D pin-jointed lattice girders;
- Members are represented by truss elements;
- Members eccentricities are ignored;
- Legs are considered to be pinned supported in the foundation;
- Forces are introduced or directly transferred to the nodes;
- Linear analysis in respect to material and geometry is employed (LA).

### 4.1.2 Design
Design is made along the following lines:

- Legs and bracing members are designed to pure compression.
- Connection eccentricities are taken into account by consideration of effective slenderness ratios.
- Member design considers the number of bolts at member ends and is presented in the following, where reference is made to EN 1993-3-1 [4].
  - **Chord members**
    - Effective slenderness                             Table G.1

      In plane buckling (v)    $L_{cr} = L$             $\bar{\lambda}_{eff,v} = 0{,}10 + 0{,}8\bar{\lambda}_v$

      Out of plane buckling (y or z)   $L_{cr} = L$      $\bar{\lambda}_{eff,y} = \bar{\lambda}_y$
    - Design to compression

      $$N_{Ed} \leq \frac{\chi\,A\,f_y}{\gamma_{M1}}$$

  - **Bracing members connected through two bolts on both sides**
    - Effective slenderness                             Table G.2

      In plane buckling (v)  $L_{cr} = L$             $\bar{\lambda}_{eff,v} = 0{,}35 + 0{,}7\bar{\lambda}_v$

      Out of plane buckling (y or z)       $L_{cr} = L$     $\bar{\lambda}_{eff,y} = 0{,}40 + 0{,}7\bar{\lambda}_y$

- o   Design to compression

$$N_{Ed} \leq \frac{\chi \, A \, f_y}{\gamma_{M1}}$$

- **Bracing members connected through one and two bolts**          BB.1.2(2)B
  - o   Effective slenderness                                                   Table G.2

    In plane buckling (v)        $L_{cr} = L$                    $\bar{\lambda}_{eff,v} = 0{,}35 + 0{,}7\bar{\lambda}_v$

    Out of plane buckling (y or z)   $L_{cr} = L$              $\bar{\lambda}_{eff,y} = 0{,}40 + 0{,}7\bar{\lambda}_y$

  - o   Design to compression

$$N_{Ed} \leq \frac{0{,}9 \, \chi \, A \, f_y}{\gamma_{M1}}$$                    G.1(3)

- **Bracing members connected through one bolt on both sides**          BB.1.2(2)B
  - o   Effective slenderness        Table G2

    In plane buckling (v-v)                              $\bar{\lambda}_{eff,v} = 0{,}35 + 0{,}7\bar{\lambda}_v$

    Out of plane buckling (y-y  or z-z)                 $\bar{\lambda}_{eff,y} = 0{,}58 + 0{,}7\bar{\lambda}_y$

  - o   Design to compression

$$N_{Ed} \leq \frac{0{,}8 \, \chi \, A \, f_y}{\gamma_{M1}}$$                    G.1(3)

- **Bolted connections** in bracing members are checked against the design axial force $N_{Ed}$

## 4.2  Level II – models

In **Level II**, the numerical models are refined in the recognition of the fact that the legs run continuously over the height of the tower. In addition, loads are implemented over the entire length of members, reflecting the actual loading conditions. This implies the introduction of beam elements to represent members in order to allow the development of bending moments arising through the continuity or the type of distributed loading. Eccentricities at member connections are accounted for in the models. The properties of **Level II** models are summarized in the following.

### 4.2.1  Numerical models
The basic assumptions for the **Level II** numerical models may be summarized as following:

- Structures are modelled as a 3D structure;

- Members are represented by 6DOF (degree of freedom) beam elements;

- Member eccentricities are accounted for;

- Legs run continuously over the height and are considered as pinned or clamped supported in the foundation according to the real design of the support condition;

- Bracing members are pin connected at their ends about the geometric axis;

- Distributed and/or point loads are introduced in the beam elements;

- Linear analysis in respect to material and geometry is employed (LA).

### 4.2.2 Design

Design is made along the following lines:

- **Bending moments in leg members** are introduced by the analysis

- **Bending moments in bracing members** due to connection eccentricities are calculated in the analysis.

- Buckling lengths for legs are determined numerically from linear buckling analysis (LBA), but $L_{cr} \geq 0,65L$.

  As an alternative, they may be set equal to $L_{cr} = 0,9L$, L = system length

- Buckling lengths, $L_{cr}$, for bracing members attached to stiff legs are reduced in comparison to clear length between bolts, $L_{clear}$:

  o  $\frac{L_{cr}}{L_{clear}} = 0,7$  for connection with two bolts

  o  $\frac{L_{cr}}{L_{clear}} = 0,85$ for connection with one bolt.

- Legs and bracing angle members are **designed** to compression and bending by interaction formulae, as proposed in Deliverable 2.4 for steel-FRP members correspondingly and expressed by the following equations:

  o  $\left( \frac{N_{Ed}}{N_{bv,Rd}} + k_{vu} \frac{M_{u,Ed}}{M_{u,Rd}} \right)^{\xi} + k_{vv} \frac{M_{v,Ed}}{M_{v,Rd}} \leq 1$    weak axis

  o  $\left( \frac{N_{Ed}}{N_{bu,Rd}} + k_{uu} \frac{M_{u,Ed}}{M_{u,Rd}} \right)^{\xi} + k_{uv} \frac{M_{v,Ed}}{M_{v,Rd}} \leq 1$   strong axis

- **Bolted connections** in bracing members are checked against the design axial force $N_{Ed}$, neglecting the eccentricity effects.

## 4.3 Level III – models

**Level III** numerical models consider more effects in analysis compared with the models of the preceding level, such as member eccentricities and geometrical imperfections. In addition, geometrical non-linear analysis is employed making simpler the design.

### 4.3.1 Numerical models

The basic assumptions for the **Level III** numerical models may be summarized as following:

- Structures are modelled as a 3D structure;

- Members are represented by 6DOF (degree of freedom) beam elements;

- Member eccentricities are considered;

- Legs run continuously over the height and are considered as pinned supported in the foundation;

- Bracing members are pin connected at their end;

- Distributed and/or point loads are introduced in the beam elements;

- Geometric non-linear analysis accounting for geometrical member imperfections is employed (GNIA).

### 4.3.2 **Design**

Design is simpler since only cross sections are required to be checked.

- **Cross section** design to combined forces and moments should be performed;

- **Bolted connections** in bracing members are checked against the design axial force $N_{Ed}$, neglecting the eccentricity effects.

## 4.4 **Level IV – models**

**Level IV** are the most refined numerical models considering in addition to geometrical structural imperfections and geometrical and material non-linear analysis. Design is fully covered by numerical analysis.

### 4.4.1 **Numerical models**

The basic assumptions for the **Level IV** numerical models may be summarized as following:

- Structures are modelled as a 3D structure.

- Members are represented by 6DOF (degree of freedom) beam elements.

- Member eccentricities are considered.

- Legs run continuously over the height and are considered as pinned supported in the foundation.

- Bracing members are pin connected at their ends

- Distributed and/or point loads are introduced in the beam elements.

- Geometric and material non-linear analysis accounting for geometrical and structural imperfections, or alternatively equivalent geometrical imperfections is employed (GMNIA).

4.4.2 **Design**

Design is fully covered by analysis.

- Tower resistance corresponds to peak load obtained from the simulation.

- **Bolted connections** in bracing members are checked against the design axial force $N_{Ed}$, neglecting the eccentricity effects.

# 5   Proposed analysis and design models for steel lattice towers, strengthened by FRP plates

A fully validated numerical model for angle section members strengthened by FRPs has not been developed yet. Furthermore, existing Code provisions apply to steel cross sections. Finally, material non-linear effects occur in the steel section only, while the FRP material remains elastic. For all these reasons, only **Level I** and **Level II** models, similar to those defined in the previous section 4, are proposed here and summarized below.

## 5.1   Level I – models

**Level I** – models mirror the state of design mostly applied in current Engineering practice in Europe. It is anchored in the provisions of the actual versions of the Eurocodes, especially [4] and [5]. The properties of **Level I** models are summarized in the following.

### 5.1.1   Numerical models

The basic assumptions for the **Level I** numerical models may be summarized as following:

- Towers are modelled as 3D pin-jointed lattice girders.

- Members are represented by truss elements.

- Members eccentricities are ignored.

- Legs are considered to be pinned supported in the foundation.

- Forces are introduced or directly transferred to the nodes.

- Linear analysis in respect to material and geometry is employed (LA)

### 5.1.2   Design

Design is made along the following lines:

- Legs and bracing members are designed to pure compression.

- Connection eccentricities are taken into account by consideration of effective slenderness ratios.

- Member design considers the number of bolts at member ends and is presented in the following, where reference is made to EN 1993-3-1 [4].

  - **Chord members**
    - Effective slenderness                                                Table G.1

    In plane buckling (v)    $L_{cr} = L$                    $\bar{\lambda}_{eff,v} = 0,10 + 0,8\bar{\lambda}_v$

    Out of plane buckling (y  or z)   $L_{cr} = L$          $\bar{\lambda}_{eff,y} = \bar{\lambda}_y$

    - Design to compression

    $$N_{Ed} \leq \frac{\chi \, A \, f_y}{\gamma_{M1}}$$

- **Bracing members connected through two bolts on both sides**
  - Effective slenderness                                                   Table G.2

    In plane buckling (v)  $L_{cr} = L$                                   $\bar{\lambda}_{eff,v} = 0,35 + 0,7\bar{\lambda}_v$

    Out of plane buckling (y or z)         $L_{cr} = L$          $\bar{\lambda}_{eff,y} = 0,40 + 0,7\bar{\lambda}_y$

  - Design to compression

  $N_{Ed} \leq \dfrac{\chi\, A\, f_y}{\gamma_{M1}}$

- **Bracing members connected through one and two bolts**          BB.1.2(2)B
  - Effective slenderness                                                  Table G.2

    In plane buckling (v)        $L_{cr} = L$                            $\bar{\lambda}_{eff,v} = 0,35 + 0,7\bar{\lambda}_v$

    Out of plane buckling (y or z)   $L_{cr} = L$                 $\bar{\lambda}_{eff,y} = 0,40 + 0,7\bar{\lambda}_y$

  - Design to compression

  $N_{Ed} \leq \dfrac{0,9\, \chi\, A\, f_y}{\gamma_{M1}}$                                        G.1(3)

- **Bracing members connected through one bolt on both sides**          BB.1.2(2)B
  - Effective slenderness       Table G2

    In plane buckling (v-v)                                          $\bar{\lambda}_{eff,v} = 0,35 + 0,7\bar{\lambda}_v$

    Out of plane buckling (y-y  or z-z)                      $\bar{\lambda}_{eff,y} = 0,58 + 0,7\bar{\lambda}_y$

  - Design to compression

  $N_{Ed} \leq \dfrac{0,8\, \chi\, A\, f_y}{\gamma_{M1}}$                                        G.1(3)

- **Bolted connections** in bracing members are checked against the design axial force $N_{Ed}$

## 5.2  Level II – models

In **Level II**, the numerical models are refined in the recognition of the fact that the legs run continuously over the height of the tower. In addition, loads are implemented over the entire length of members, reflecting the actual loading conditions. This implies the introduction of beam elements to represent members in order to allow the development of bending moments arising through the continuity or the type of distributed loading. In contrast to non strengthened Towers the eccentricities at member connections are ignored in the models and the bending moments acting in the bracing members are determined by a supplementary calculation step as presenter in section 5.2.2. The properties of **Level II** models are summarized in the following.

### 5.2.1  Numerical models

The basic assumptions for the **Level II** numerical models may be summarized as following:

- Structures are modelled as a 3D structure.

- Members are represented by 6DOF (degree of freedom) beam elements.

- Member eccentricities are ignored.

- Legs run continuously over the height and are considered as pinned supported in the foundation.

- Bracing members are pin connected at their ends

- Distributed and/or point loads are introduced in the beam elements.

- Linear analysis in respect to material and geometry is employed (LA)

### 5.2.2 **Design**

Design is made along the following lines:

- **Bending moments in leg members** are introduced by the analysis

- **Bending moments in bracing members** due to connection eccentricities are calculated as following:

  $M_{Ed(u,v)} = N_{Ed} \cdot e(u,v)$

  where:

  $N_{Ed}$ is the axial force in the member from analysis

              e is the connection eccentricity

- Buckling lengths for legs are determined numerically from linear buckling analysis (LBA), but $L_{cr} \geq 0,65L$.

  As an alternative, they may be set equal to $L_{cr} = 0,9L$, L = system length

- Buckling lengths, $L_{cr}$, for bracing members attached to stiff legs are reduced in comparison to clear length between bolts, $L_{clear}$:

  o   $\frac{L_{cr}}{L_{clear}} = 0,7$ for connection with two bolts

  o   $\frac{L_{cr}}{L_{clear}} = 0,85$ for connection with one bolt.

- Legs and bracing angle members are **designed** to compression and bending by interaction formulae, as proposed in Deliverable 2.4 for steel-FRP members correspondingly and expressed by the following equations:

  o   $\left(\frac{N_{Ed}}{N_{bv,Rd}} + k_{vu}\frac{M_{u,Ed}}{M_{u,Rd}}\right)^{\xi} + k_{vv}\frac{M_{v,Ed}}{M_{v,Rd}} \leq 1$    weak axis

  o   $\left(\frac{N_{Ed}}{N_{bu,Rd}} + k_{uu}\frac{M_{u,Ed}}{M_{u,Rd}}\right)^{\xi} + k_{uv}\frac{M_{v,Ed}}{M_{v,Rd}} \leq 1$   strong axis

- **Bolted connections** in bracing members are checked against the design axial force $N_{Ed}$, neglecting the eccentricity effects.

# 6   Validation of the proposed models to the tested tower

## 6.1   General

The tested towers are presented in detail in deliverable D2.5. It should be noted that the numbering of the towers used hereafter is the one also used in D2.5. Out of the six (6) towers, four (4) are composed of steel members and two (2) are partly reinforced by FRP plates. Accordingly, full validation for all levels is applied to the four (4) towers (see section 6.2), while only **Level I** and **Level II** validation is applied to the remaining two (2) towers (see section 6.3). The relevant matrix is shown in Table 6.1. The software package used for analysis is presented in Table 6.2.

Actual values of geometrical properties and material parameters were used in analysis and design.

**Table 6.1 Matrix of tower validation**

| No of Tower Type | Validation models | Experimental failure load | Experimental natural frequency |
|---|---|---|---|
| 1<br>O-1 | Level I | 39 kN | 19,4 Hz |
|  | Level II |  |  |
|  | Level III |  |  |
|  | Level IV |  |  |
| 2<br>O-2 | Level I | 105 kN | 19,0 Hz |
|  | Level II |  |  |
|  | Level III |  |  |
|  | Level IV |  |  |
| 3<br>O-1S | Level I | 54,5 kN | 22,8 Hz |
|  | Level II |  |  |
| 4<br>D-1 | Level I | 38,5 kN | 19,9 Hz |
|  | Level II |  |  |
|  | Level III |  |  |
|  | Level IV |  |  |
| 5<br>D-2 | Level I | 78 kN | 16,6 Hz |
|  | Level II |  |  |
|  | Level III |  |  |
|  | Level IV |  |  |
| 6<br>D-2S | Level I | 81,5 kN | 14,5 Hz |
|  | Level II |  |  |

**Table 6.2 Matrix of software used for tower validation**

| No/Type of Tower | Validation models | Software package |
|---|---|---|
| 1<br><br>O-1 | Level I | ANSYS |
| | Level II | ANSYS |
| | Level III | ANSYS |
| | Level IV | FINELG |
| 2<br><br>O-2 | Level I | ANSYS |
| | Level II | ANSYS |
| | Level III | ANSYS |
| | Level IV | FINELG |
| 3<br><br>O-1S | Level I and II | SOFISTIK |
| 4<br><br>D-1 | Level I | ANSYS |
| | Level II | ANSYS |
| | Level III | ANSYS |
| | Level IV | FINELG |
| 5<br><br>D-2 | Level I | ANSYS |
| | Level II | ANSYS |
| | Level III | ANSYS |
| | Level IV | FINELG |
| 6<br><br>D-2S | Level I and II | SOFISTIK |

## 6.2   Un-strengthened steel towers

### 6.2.1   Level I approach

#### 6.2.1.1   Description of the numerical model for steel towers

The steel towers are modelled using the commercial software package ANSYS Mechanical v18.2. Nonetheless, the conclusions are not specific to the software but they are specific to the modelling assumptions. For the **Level I** approach, the tower members are modelled by truss elements possessing three degrees of freedom (displacements along x-, y-, and z-axis) at their two nodes. Owing to the use of truss elements, each physical member is modelled by only one single finite element. One may also note that the truss elements possess only axial stiffness. Therefore, the sole input variable is their area.

The numerical model is represented in Figure 6.1.
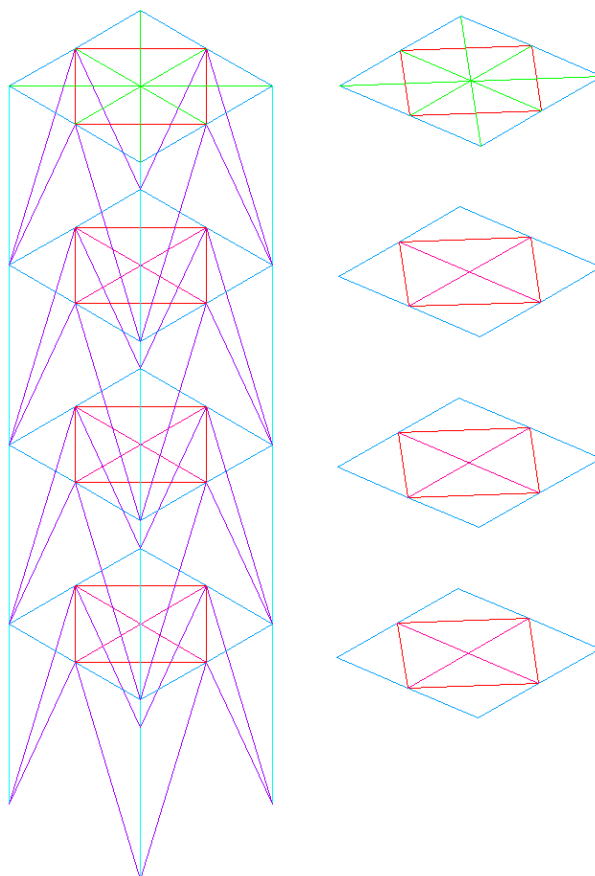
a) Tower model          b) Horizontal diaphragms

**Figure 6.1 Numerical model of tower – Level I approach**

It should be noted that the numerical model is stable only if the horizontal bracings are modified compared to the physical tower. In fact, comparing Figure 6.1b) and Figure 6.2, one may note that additional diagonal elements are introduced to stabilize the model. In the upper level, where the loading is introduced in the laboratory tests, these elements are represented in light green in Figure 6.1a) and Figure 6.1b). In order to create a diaphragm, the fictitious elements are modelled to be stiff (these elements are referred to as stiff elements in the following). This corresponds to the real load introduction that is done by a steel plate attached to the four horizontal members of upper level. In the intermediate levels, the fictitious diagonal elements are represented in pink. These elements are modelled as flexible as they should only add a minimal stiffness to stabilize the model. Hereafter, the sensitivity of the results to the stiffness of the fictitious truss elements is studied for tower O-1 (see Deliverable 2.5 for the description of the tower).
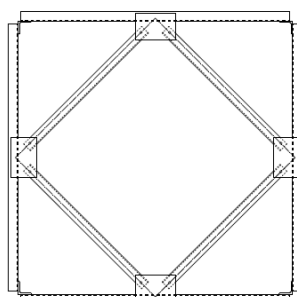


**Figure 6.2 Design of horizontal bracings**

In order to study the effect of the stiffness of the fictitious elements, the tower is subjected to two point loads of 1 000 kN applied at the top and acting along the y-axis respectively x-axis in order to generate a resulting action acting in the diagonal direction.
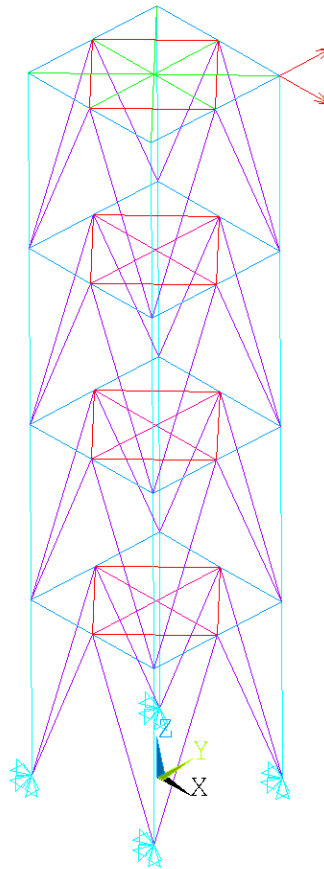


**Figure 6.3 Tower loaded by two point loads at top level**

Table 6.3 shows the maximum displacement at the top level depending on the stiffness of the fictitious elements generated in the intermediate levels. Clearly, the stiffness of these elements has no effect on the resulting displacement. This observation can be easily understood, as the fictitious elements are fully free of internal forces and do not influence the distribution of axial forces in the other members. However, their presence is necessary in order to add a minimum stiffness about the y- respectively x-axis at nodes representing the intersection between the vertical bracing and the horizontal members.

**Table 6.3: Effect of fictitious elements on the maximum displacement**

| Area of fictitious elements /Area of diagonals of vertical bracing | Area of rigid elements /Area of diagonals of vertical bracing | Maximum displacement at the upper level (mm) |
|---|---|---|
| no flexible elements | $10^8$ | model is instable |
| $10^{-5}$ | $10^8$ | 445,546 |
| $10^{-1}$ | $10^8$ | 445,546 |
| 1 | $10^8$ | 445,546 |
| $10^5$ | $10^8$ | 445,546 |

In contrast to the stiffness of the fictitious elements, the stiffness of the "rigid" elements has an effect on the maximum displacement at the upper level as shown in Table 6.4. The difference results from the deformability of the upper level. For the studied load case, the differences are however rather small (approximately 2% between the lowest and highest stiffness).

**Table 6.4: Effect of stiff elements on the maximum displacement**

| Area flexible elements /Area of diagonals of vertical bracing | Area rigid elements /Area of diagonals of vertical bracing | Maximum displacement at the upper level |
|---|---|---|
| 1 | $10^{-4}$ | 454,059 |
| 1 | $10^{-2}$ | 453,943 |
| 1 | 1 | 449,257 |
| 1 | $10^{2}$ | 445,617 |
| 1 | $10^{6}$ | 445,546 |
| 1 | $10^{8}$ | 445,546 |

In the following simulations, the flexible elements are modelled with an area **equal to the area of the diagonals of the vertical bracing** and the stiff elements are modelled with an area equal to **$10^{6}$ times the area of these diagonals**.

### 6.2.1.2 Analysis of the towers tested in the laboratory

In the following, the **Level I** design approach is applied to the towers tested in the laboratory. The tower is consequently modelled using truss elements neglecting all eccentricities in the analysis. The effect of the eccentricities is taken into account through the modification of the member slenderness and the reduction of the factor $\chi$ is accounted for as the diagonal is connected through only one bolt at both ends (see paragraph 4.1). The towers are loaded at the top level at a central node that is linked through the rigid fictitious elements to the legs as shown in Figure 6.4. The loads leading to buckling of the first element are summarised for the four towers in Table 6.5. Additionally, this table indicates the failure mode predicted by the **Level I** design approach.

Figure 6.5 to Figure 6.8 represent detailed results for the tested towers. In particular, the value of the axial forces (negative indicates compression) acting in the members and the results of the design checks are provided. The design load has been obtained by increasing the applied load up to the point that the first member check equals 1,0.
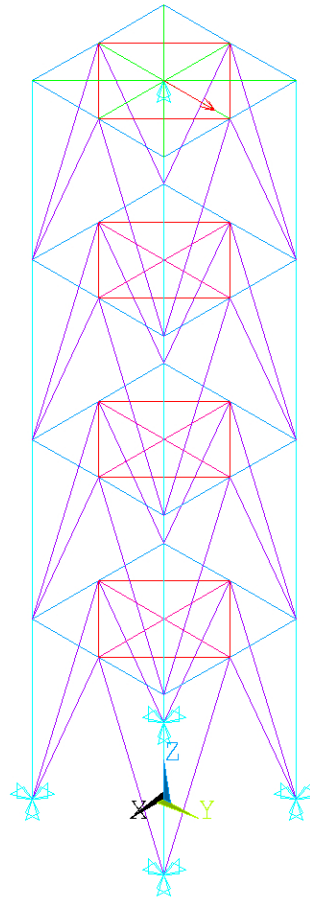
**Figure 6.4 Tower loaded by a horizontal point load at top level**

**Table 6.5: Summary of predicted design loads for Level I approach**

| Tower | Numerical model | | Laboratory test |
|---|---|---|---|
| | Design load (kN) | Failure mode | Maximum load (kN) |
| O-1 | 29,38 | Buckling of diagonals | 39,00 |
| O-2 | 67,97 | Buckling of lower legs | 106,5 |
| D-1 | 25,06 | Buckling of diagonals | 38,50 |
| D-2 | 48,06 | Buckling of lower legs | 78,50 |

a) Axial forces (kN)                                    b) Result of design checks
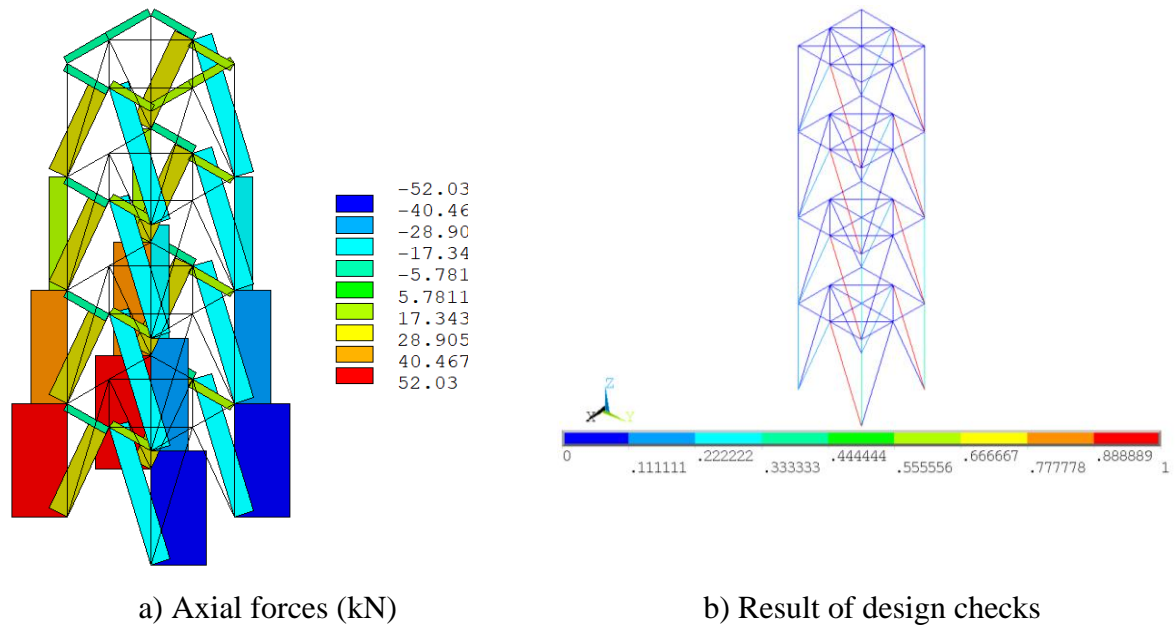
**Figure 6.5 Results for tower O-1**



a) Axial forces (kN)                                    b) Result of design checks
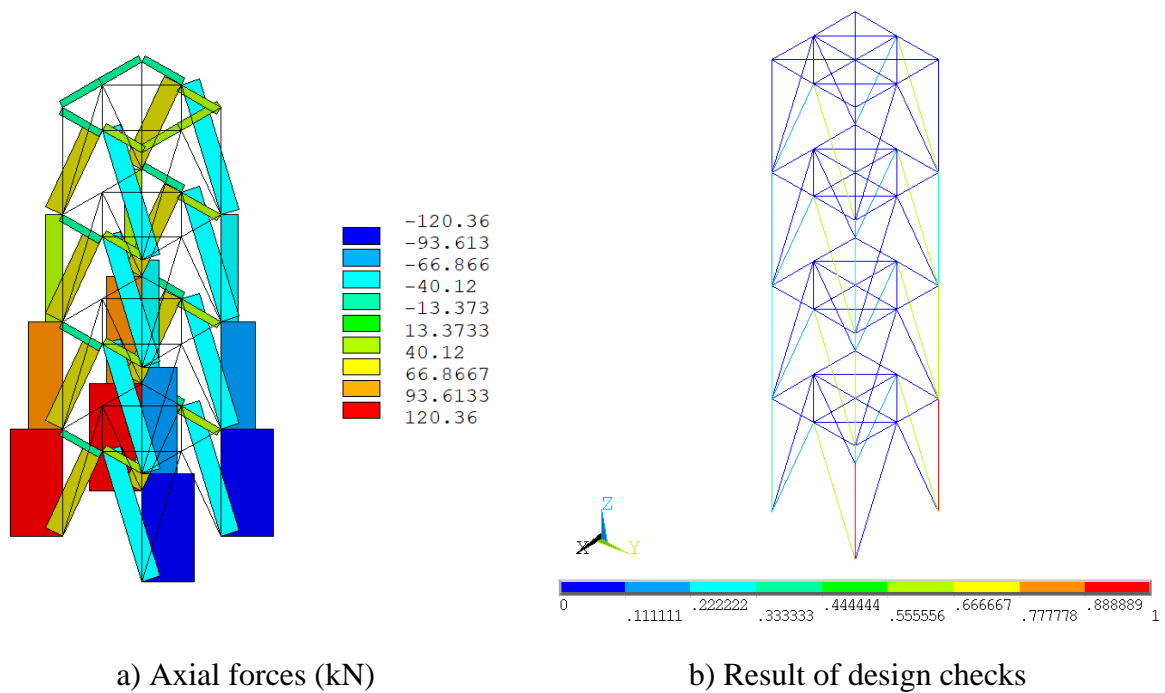
**Figure 6.6 Results for tower O-2**

| | |
|---|---|
| a) Axial forces (kN) | b) Result of design checks |
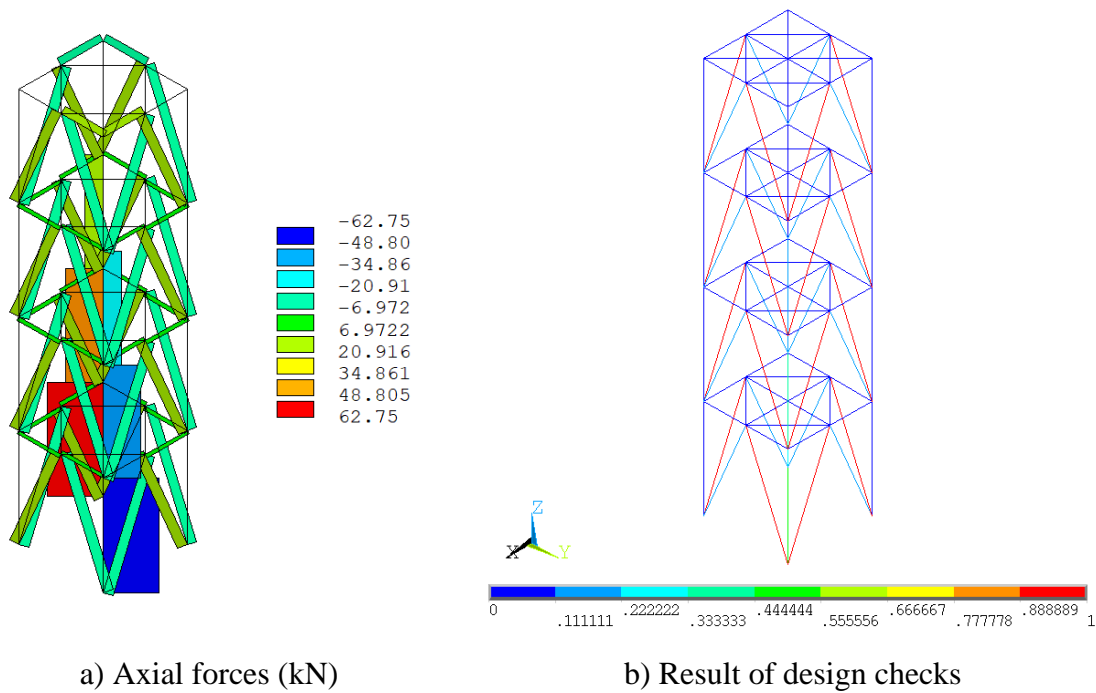
**Figure 6.7 Results for tower D-1**



| | |
|---|---|
| a) Axial forces (kN) | b) Result of design checks |
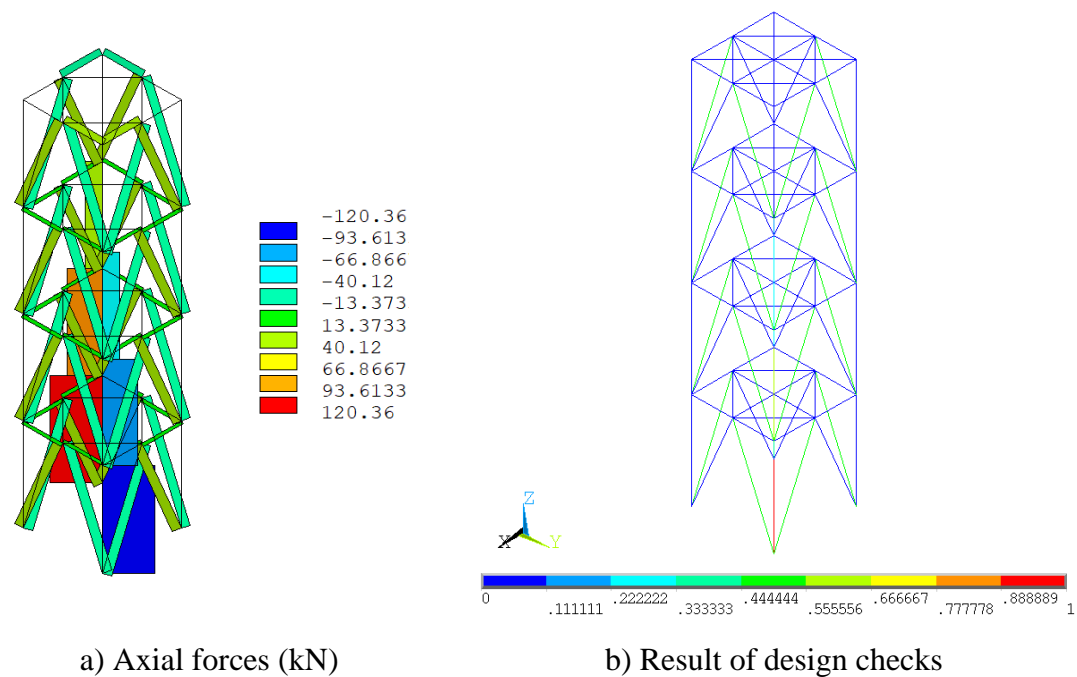
**Figure 6.8 Results for tower D-2**

Additionally to the resistance of the towers, it is interesting to compare the eigen frequencies as they characterise the stiffness of the tower. All eigen frequencies refer to a flexural vibration mode for both, the laboratory tests and the numerical simulations. One may note that the numerical model leads to slightly lower eigen frequencies than the real tower. However, the differences seem acceptable.

**Table 6.6: Summary of predicted eigen frequencies for Level I approach**

| Tower | Eigen frequency – Level I model (Hz) | Eigen frequency – Laboratory test (Hz) |
|---|---|---|
| O-1 | 17,08 | 19,4 |
| O-2 | 18,07 | 19,0 |
| D-1 | 16,06 | 19,9 |
| D-2 | 17,94 | 16,6 |

## 6.2.2   **Level II approach**

### 6.2.2.1   **Description of the numerical model for steel towers**

Hereafter, the **Level II** design approach is applied to the towers tested in the laboratory. The tower is modelled using beam elements with 6 degrees of freedom and the eccentricities are accounted for as precisely as possible in a beam element model. The bolted connections are represented by fictitious elements possessing a very low torsional stiffness, which is calibrated hereafter. The loads are introduced at the extremities of the legs in the top level.

Figure 6.9 to Figure 6.11 represent the modelling details for the connections between the legs and the bracings as well as the connection between the vertical bracing and the horizontal members (Figure 6.11).
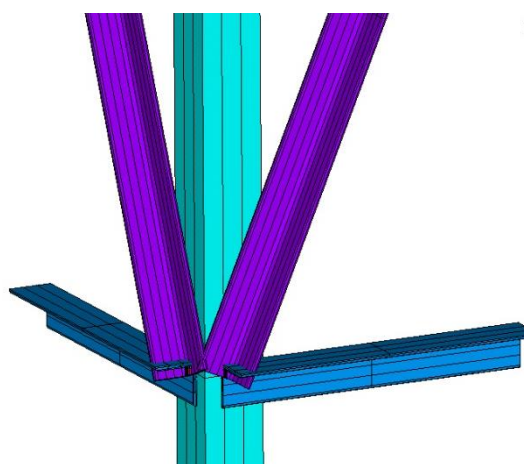


**Figure 6.9 Tower model Level II approach – Detail of connection between vertical bracing and leg**
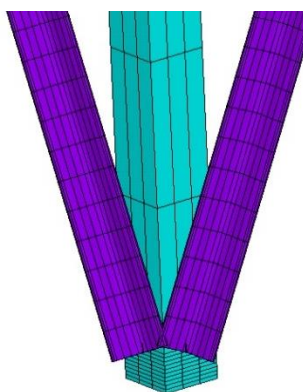


**Figure 6.10 Tower model Level II approach – Detail of connection between vertical bracing and leg at base level**

In Figure 6.11, one may observe that the gusset plate is modelled through a beam finite element (green element in Figure 6.11). Consequently, the eccentricity between the horizontal member and the diagonals is accounted for. The gusset plate, welded in the physical specimens to the horizontal members, is modelled as clamped to the horizontal members. The diagonals are connected to the gusset plate by the fictitious elements of low torsional stiffness reproducing a pinned "one bolt" connection.



a) Isometric view



b) Side view

c) Front view
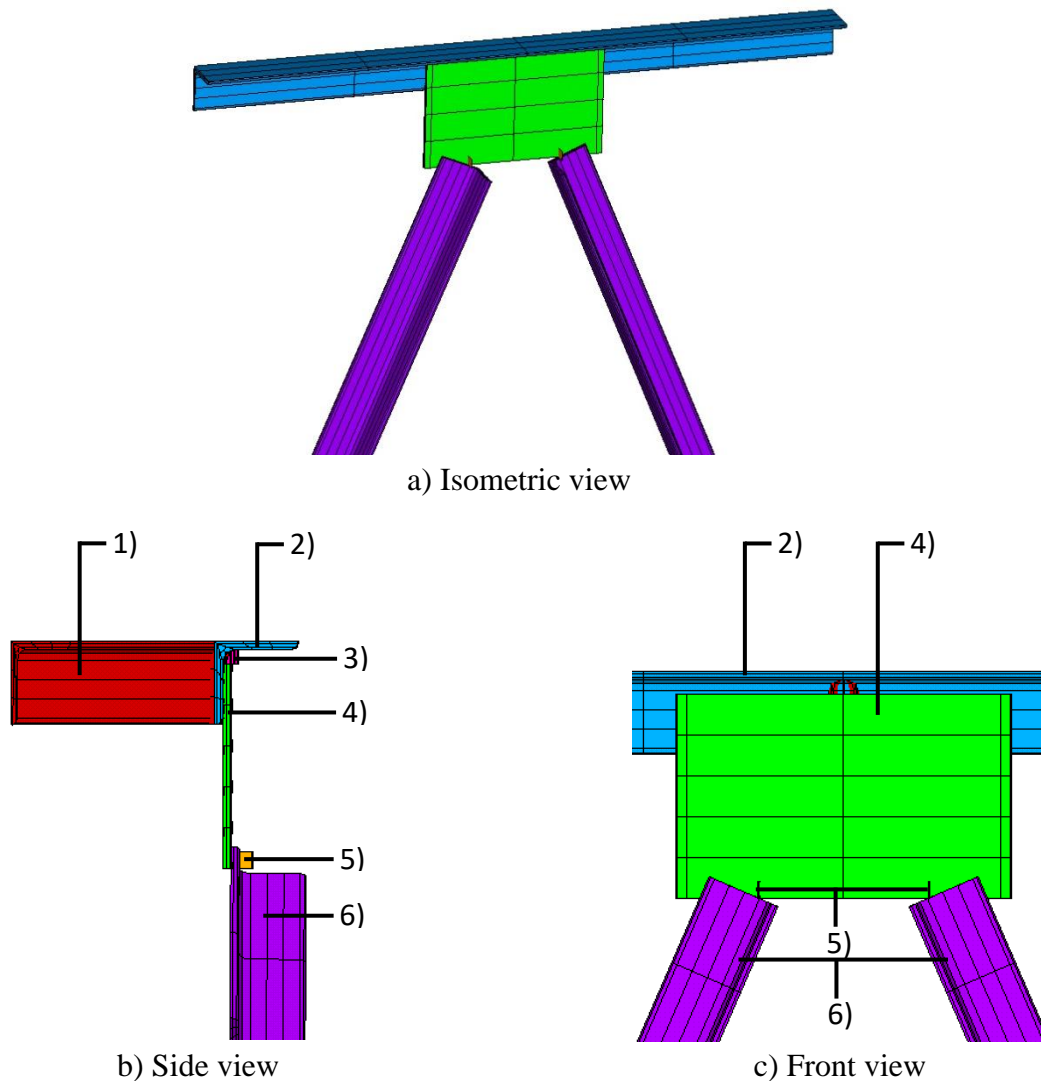
1) Horizontal bracing members
2) Transversal members
3) Rigid beam element connecting centroid of transversal member to gusset plate
4) Gusset plate
5) Equivalent bolt element connecting gusset plate to centroid of vertical bracing member
6) Vertical bracing member

**Figure 6.11 Tower model Level II approach – Detail of connection between vertical bracing and horizontal members**

Next, the torsional stiffness of the fictitious "bolt" elements is calibrated through the sub model presented in Figure 6.12. The sub model is composed of:

1) the angle section pinned to the gusset plate through the fictitious beam element representing the bolt;
2) the gusset plates clamped at the ends (all degrees of freedom are restrained).

The member possesses a length of 1 m and it is subject to a point load of 10 kN.

Obviously, this sub-model is not completely representative of the diagonal in the structure, but it is appropriate to study the influence of the connection stiffness.
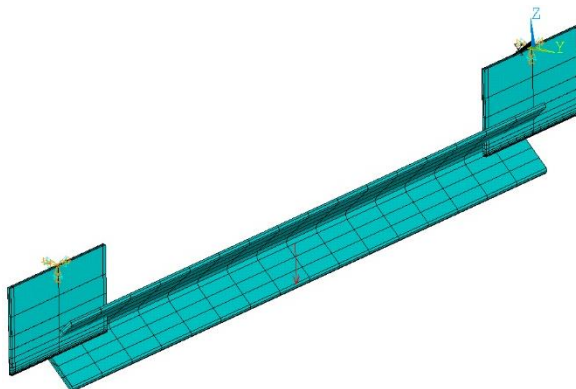


**Figure 6.12 Single angle with gussets – Loading about major-axis**

The torsional stiffness of the fictitious beam elements is varied and expressed as a multiple of the flexural stiffness $EI_u/L$ of the angle section member ($E$ is the Young's modulus, $I_u$ the 2nd moment of area about major-axis and $L$ is the member length). The other section properties (material, area, second moment of areas about major- and minor-axis) are considered equal to the properties of the angle section leading to a rigid connection of the displacements and the rotations between the gusset plate and the angle section.

Table 6.7 presents the bending moment acting in the member depending on the torsional stiffness of the "bolt" elements (equal to $GI_t/L$). The studied member is subject to a point load applied at mid span acting about the major-axis. The first line of the table represents the results obtained for stiff "bolt" elements generating a clamped connection. The torsional stiffness of the bolts is then decreased and starting from a stiffness approximately equal to $0,01EI_u/L$, a perfect hinged connection may be considered. Nonetheless, hereafter a stiffness equal to $10^{-3}EI_u/L$ is used to generate the hinged bolt connection. The exact torsional stiffness of the beam element representing the bolt is recalculated from its length assuming a shear modulus equal to 80 770 MPa.

**Table 6.7: Major-axis bending moment distribution depending on connection stiffness**

| Stiffness $GI_t/L$ | Bending moment distribution about major-axis (kNm) |
|---|---|
| $25EI_u/L$ |  |
| $EI_u/L$ |  |

| $0,5 EI_u/L$ |  |
| $0,1 EI_u/L$ |  |
| $0,01 EI_u/L$ |  |
| $10^{-3} EI_u/L$ |  |
| $10^{-4} EI_u/L$ |  |
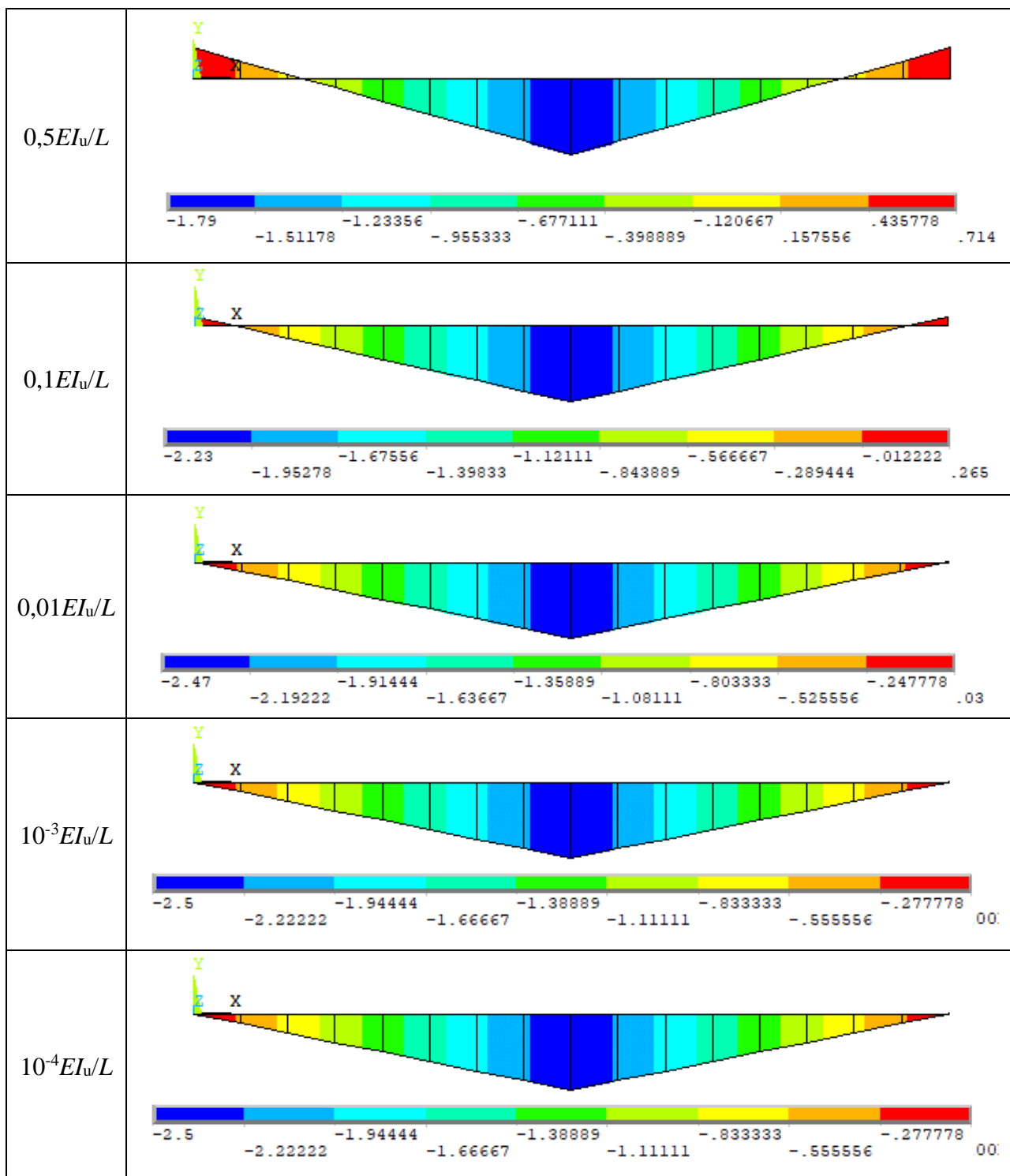
Next, the same member is studied under a point load applied about the minor-axis as shown in Figure 6.13 Single angle with gussets – Loading about minor-axis. Again the load is equal to 10 kN and the member length is equal to 1 m. The fictitious bolt elements are modelled with a torsional stiffness equal to $10^{-3} EI_u/L$.
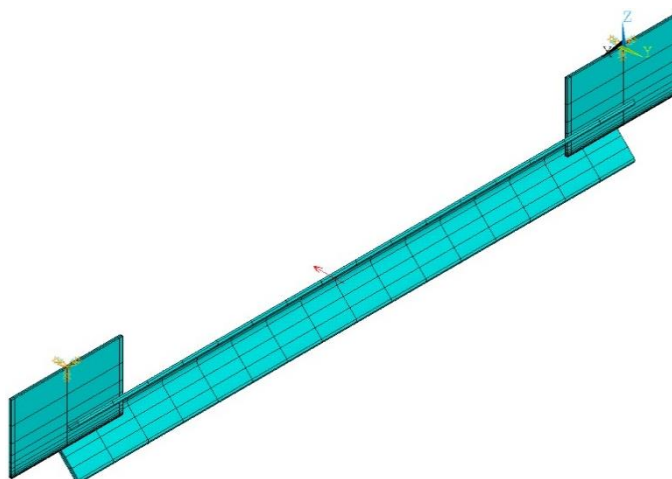
**Figure 6.13 Single angle with gussets – Loading about minor-axis**

Figure 6.14 represents the minor-axis bending moment acting along the member. One may observe that the bending moment is close to the case of a member with hinged connections. Yet, owing to the (small) torsional stiffness of the gusset plates, a small bending moment arises at the connections.
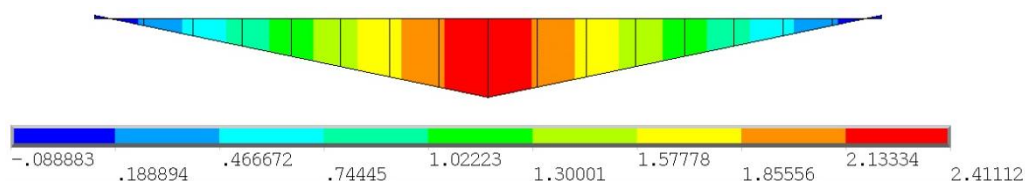


**Figure 6.14 Minor-axis bending**

Finally, the angle section member is studied in its real position, i.e. it is oriented with a leg parallel to the gusset plates. The member is therefore subject to a load that acts along to the geometric axis rather than along the major- or minor-axis.
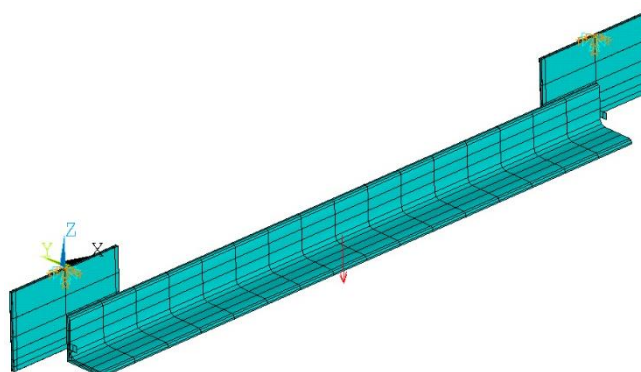


**Figure 6.15 Single angle with gussets – Loading along geometric axis z-z**

Figure 6.16 and Figure 6.17 present the bending moment diagram resulting from applied load. One may observe that the geometric axis loading generates bending moments about both, the minor- and the major-axis. Additionally, even if the "bolt" elements possess a very low torsional stiffness creating a hinge, the bending moment diagrams do not correspond to a perfectly hinged member as the hinge does not act about the major- or the minor-axis.
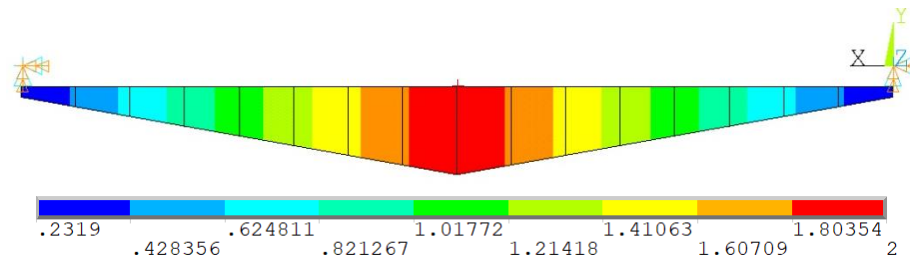
**Figure 6.16 Major-axis bending moment $M_u$ – Loading along geometric axis z-z**
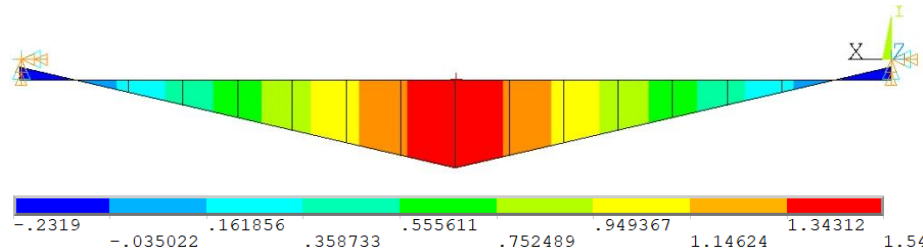


**Figure 6.17 Minor-axis bending moment $M_v$ – Loading along geometric axis z-z**

### 6.2.2.2 Analysis of the towers tested in the laboratory

The four towers are recalculated hereafter using the **Level II** approach. Two alternatives concerning the supports are investigated. First, the tower is supposed to be hinged. Generally, this assumption is also used in practice. However, the support conditions designed for the laboratory tests may be considered as rigid. Therefore, the towers are also analysed with clamped supports. Table 6.8 summarises the results obtained by applying the **Level II** approach, consisting in a first order elastic analysis followed by the application of the design equations provided in paragraph 4.2.

Table 6.8 clearly highlights the influence of the support conditions. Indeed, the design load for the towers failing by leg buckling increases. Inversely, the support conditions have practically no influence on the design load of towers failing by diagonal buckling. This conclusion does not seem surprising as presence of clamped supports does not affect much the distribution of internal forces and moments acting in the members and especially in the diagonals. Yet, the clamped supports decrease the buckling length of the legs and therefore lead to an increase of the legs' buckling strength and hence of the strength of towers O-2 and D-2.

It is interesting to note that the **Level I** and **Level II** approaches predict the same failure mode and provide close failure loads for towers O-1 and D-1 as well as for towers O-2 and D-2 if the supports are considered as hinged. The difference is only in a range of 5-10%.

**Table 6.8: Summary of predicted design loads for Level II approach**

| Tower | Design load (kN) – Level II approach with hinged supports | Design load (kN) – Level II approach with clamped supports | Failure mode | Maximum load (kN) – Laboratory test |
|---|---|---|---|---|
| O-1 | 32,06 | 32,06 | Buckling of diagonals | 39,00 |
| O-2 | 66,11 | 82,62 | Buckling of lower legs | 106,5 |
| D-1 | 27,57 | 27,55 | Buckling of diagonals | 38,50 |
| D-2 | 48,85 | 60,31 | Buckling of lower legs | 78,50 |

Figure 5.16 to Figure 5.19 show the detailed results obtained for the four towers considered with clamped supports, including the internal forces and moments. It is recalled that the buckling lengths for the legs is calculated based on the eigenvalue of the first elastic buckling mode (see paragraph 4.2.2). Therefore, Figure 6.19 and Figure 6.22 represent the buckling modes of the tower O-2 and 4 subjected to the loads given in Table 6.8 (column Design Load – **Level II** approach with clamped supports). The diagonals are calculated with a buckling length of 0,85L.

For Tower O-1, one may observe that the compressed diagonals lead to failure of the tower. Owing to the clamped support, the lower diagonals are however slightly less loaded than the diagonals in the upper levels.

a) Axial forces (kN)

b) Major axis bending moment (kNm)

c) Minor axis bending moment (kNm)          d) Result of design checks
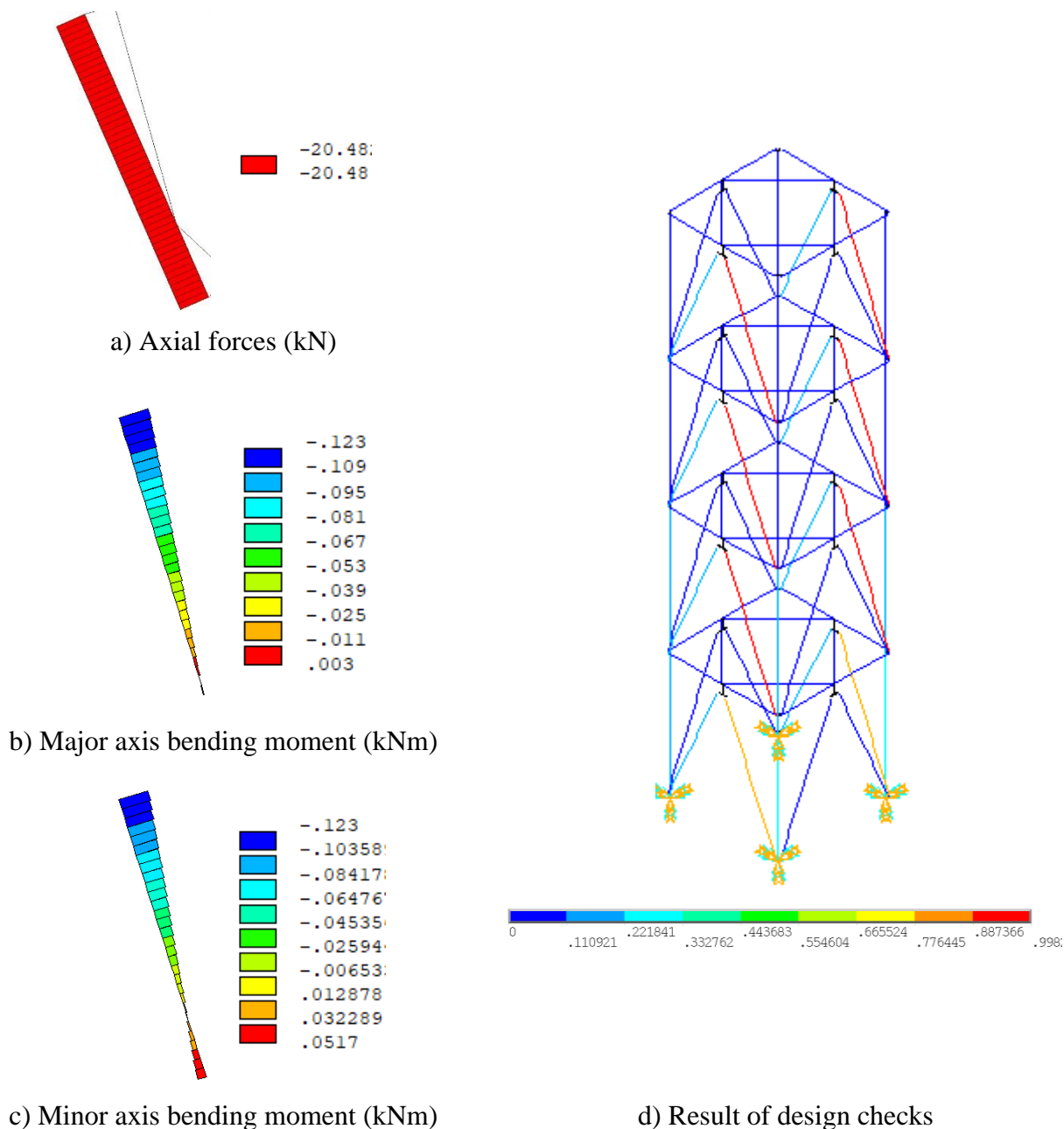
**Figure 6.18 Results for tower O-1**

Figure 6.19 shows the first buckling mode of the tower calculated under the failure load obtained with the **Level II** approach (82,62 kN). Based on the critical amplification factor $\alpha_{cr}$ equal to 2,06 and the axial force acting in the leg (= 145 kN), the buckling length of approximatively 1,10 m is obtained ($\beta = L_{cr}/L = 0,668$).
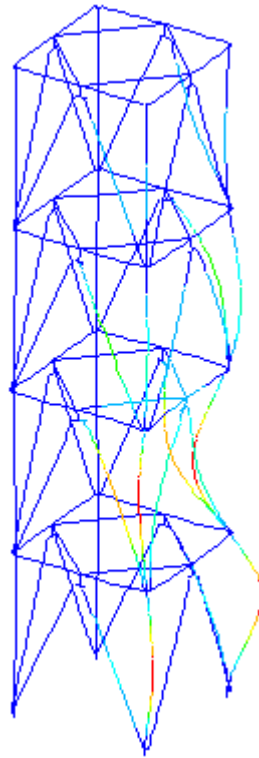
**Figure 6.19 1st buckling eigenmode – minor axis buckling of the compressed lower legs – $\alpha_{cr} = 2{,}06$**

Figure 6.20 shows the detailed results. It may be observed that the failure results from the cross-section interaction of the lower part of the leg situated between the support and the joints with the diagonals. The buckling check of the most compressed legs is equal to approximatively 0,9.

a) Axial forces (kN)



b) Major axis bending moment (kNm)



c) Minor axis bending moment (kNm)          d) Result of design checks
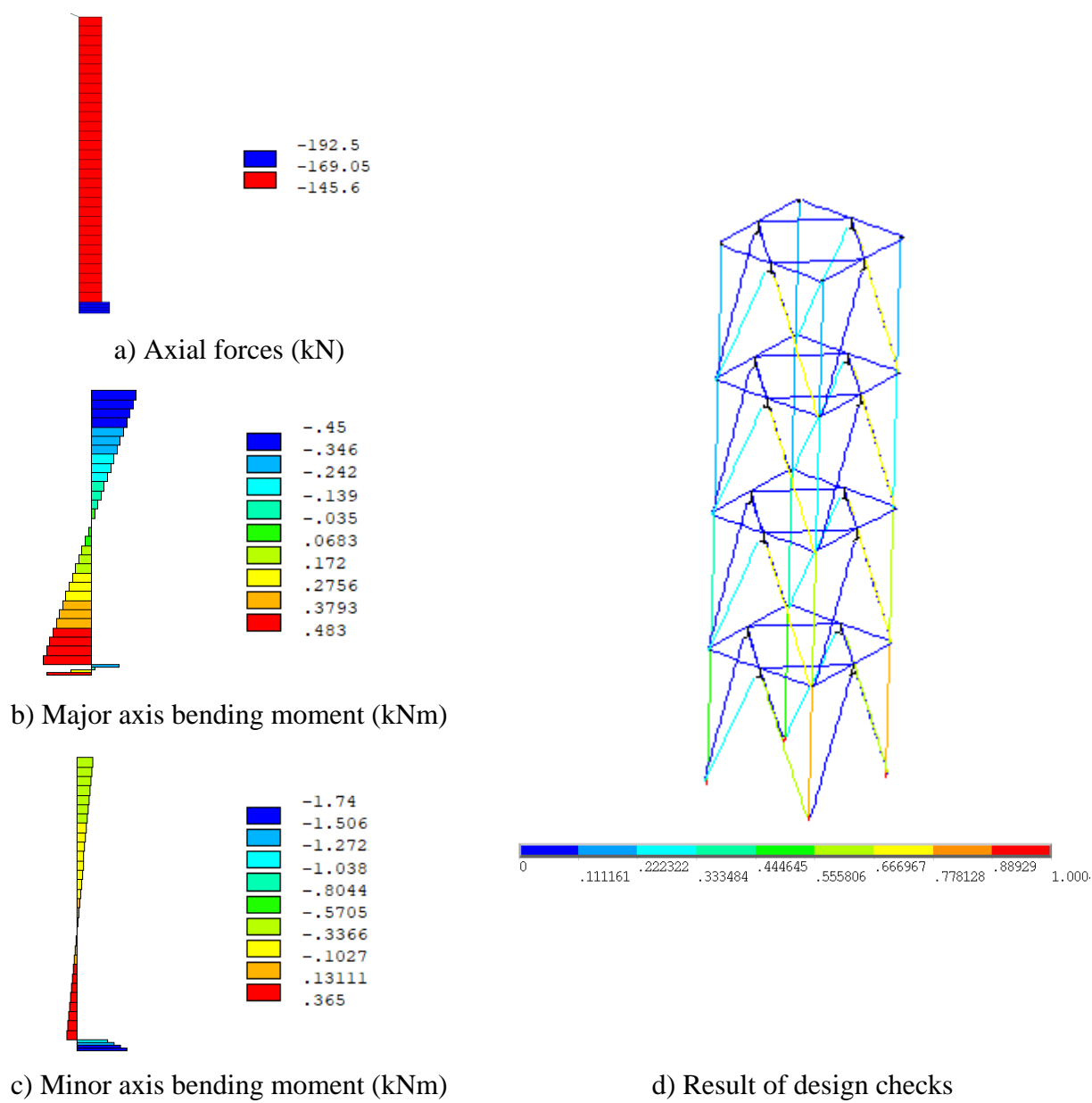
**Figure 6.20 Results for tower O-2**

Figure 6.21 represents the results of tower D-1. It may be noted that all compressed diagonals nearly attain a working ratio of 1,0. Owing to the clamped support, the diagonals in the lower level are however slightly less loaded (working degree ≈ 0,9).

a) Axial forces (kN)

b) Major axis bending moment (kNm)

c) Minor axis bending moment (kNm)                    d) Result of design checks
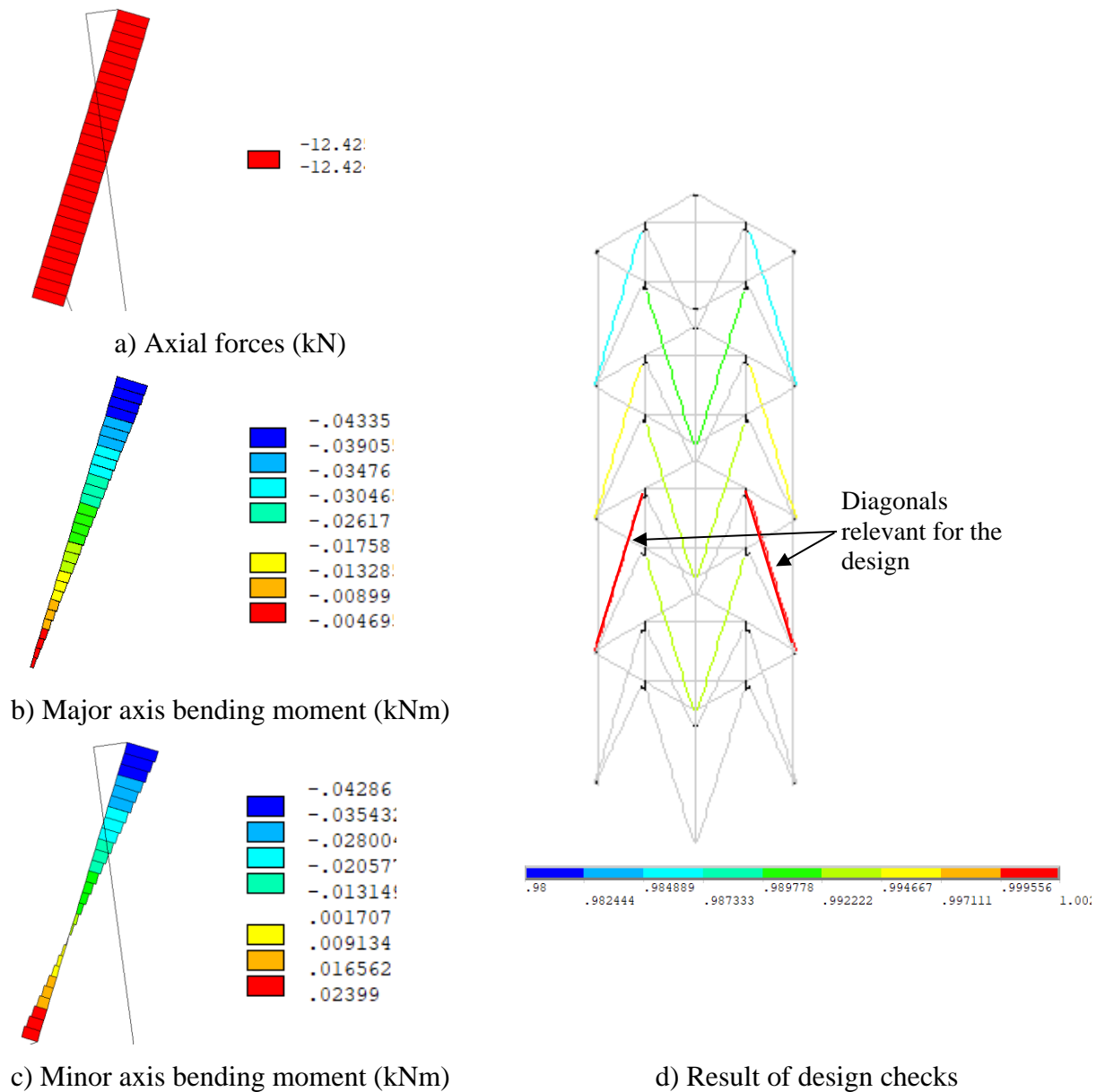
**Figure 6.21 Results for tower D-1**

Finally, Figure 6.22 and Figure 6.23 represent the results for tower D-2. First, the buckling length of the lower leg is determined based on the critical load factor $\alpha_{cr}$. The resulting buckling length is again (as for tower O-2) equal to approximately 1,10 m leading to a ratio $\beta = L_{cr}/L$ of 0,663.
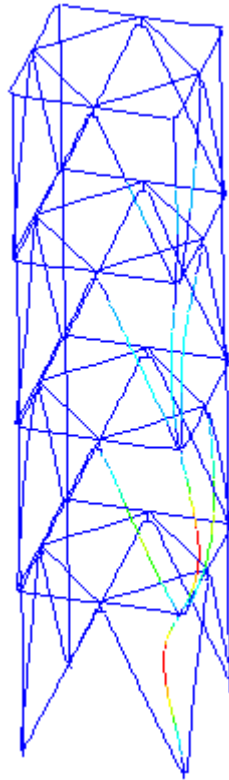
**Figure 6.22 1st buckling eigenmode – minor axis buckling of the most compressed lower leg –**
$\alpha_{cr} = 2{,}025$

Figure 6.23 shows the results of the design checks. One may observe that the design load is attained when the buckling check of the compressed lower leg becomes relevant.

a) Axial forces (kN)



b) Major axis bending moment (kNm)



c) Minor axis bending moment (kNm)

d) Result of design checks
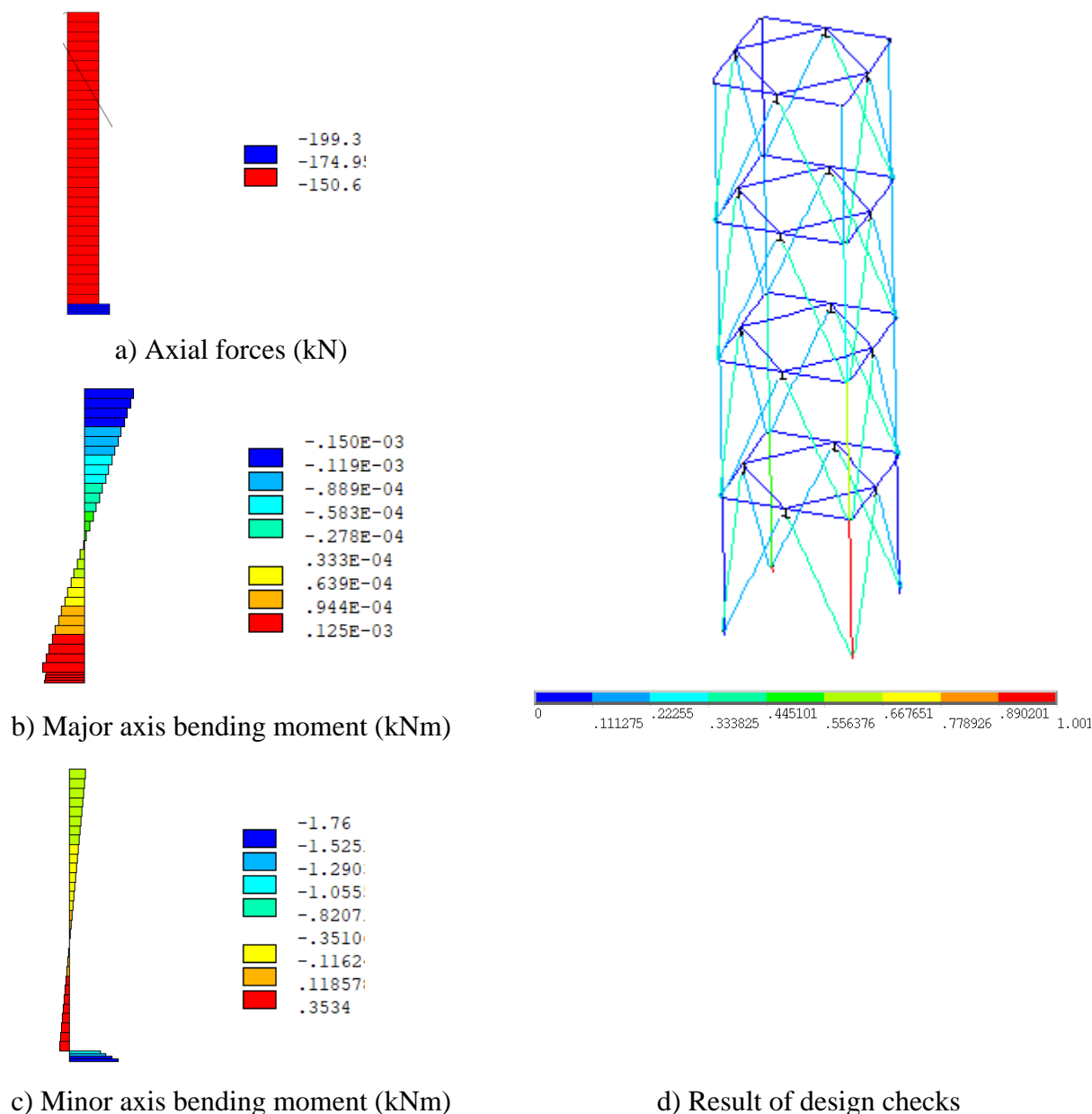
**Figure 6.23 Results for tower D-2**

Again, it is interesting to compare the eigen frequencies. This comparison is shown in Table 6.9. The results of Table 6.9 indicate that the **Level II** model seems to be less stiff than the **Level I** model. This seems understandable as the **Level II** model includes bending of the members reducing the stiffness of the tower.

**Table 6.9 Summary of predicted eigen frequencies for Level II approach**

| Tower | Eigen frequency – Level II model (Hz) | Eigen frequency – Level I model (Hz) | Eigen frequency – Laboratory test (Hz) |
|-------|---------------------------------------|--------------------------------------|----------------------------------------|
| O-1   | 15,51                                 | 17,08                                | 19,4                                   |
| O-2   | 16,14                                 | 18,07                                | 19,0                                   |
| D-1   | 14,91                                 | 16,06                                | 19,9                                   |
| D-2   | 16,10                                 | 17,94                                | 16,6                                   |

## 6.2.3  Level III approach

### 6.2.3.1  Description of the numerical model for steel towers

The **Level III** approach consists in an elastic $2^{nd}$ order calculation considering an equivalent geometrical imperfection. Residual stresses are not included in the numerical model. Nonetheless, owing to the consideration of $2^{nd}$ order effects and member imperfection, the members may be designed using the cross section resistance as reference. A buckling reduction needs not to be calculated as the effect of buckling is included through the geometric non-linear analysis. According to prEN 1993-1-1:2019, the imperfection may be based on different assumptions. It is possible to introduce a member imperfection according to a half sine wave with an amplitude depending on the cross section verification:

- Members are designed using an elastic interaction: $e_0 = 0,34L/(200\varepsilon)$;
- Members are designed using a plastic interaction:   $e_0 = 0,34L/(68\varepsilon)$.

However, one may note that the values have been calibrated based on investigations on I and H sections. The direct use of these values for angle sections may admittedly be questioned.

As an alternative, an imperfection according to the buckling eigenmode of the structure may be considered. In this case, the amplitude should be chosen as:

$$\eta_{init}(x) = e_{0,m}\frac{N_{cr,m}}{EI_m|\eta_{cr}^{II}|}\eta_{cr}(x)$$

With:

$$e_{0,m} = \alpha_m(\bar{\lambda}_m - 0,2)\frac{M_{Rk,m}}{N_{Rk,m}}$$

$$\bar{\lambda}_m = \sqrt{\frac{N_{Rk,m}}{N_{cr,m}}}$$

Where:

| | |
|---|---|
| m: | is the index denoting the critical cross section of the structure |
| $N_{cr,m}$: | is the critical axial force of the member in which the critical cross section m is situated |
| $\alpha_m$: | is the imperfection factor applicable for cross section m (=0,34 for buckling curve b applicable to angle sections) |
| $M_{Rk,m}$: | is the characteristic value of the bending moment resistance of cross section m |
| $N_{Rk,m}$: | is the characteristic value of the axial force resistance of cross section m |
| $\eta_{cr}$: | is the buckling eigenmode |
| $\eta_{init}$ | is the geometric imperfection |

This second approach does not include a differentiation between elastic and plastic cross-section design. In fact, a linear interaction should be used based on elastic or plastic cross-section characteristics. Yet, plastic cross section resistances have to be limited to 1,25 times the elastic ones. One may note that it is not clearly stated which modal bending moment ($EI_m\eta_{cr}^{II}$) should be used. Neither it is stated if the major or minor axis bending moment resistance should be used for $M_{Rk,m}$. However, it is admitted that this method is intended to be used for plane structures. Nonetheless, it is applied hereafter and as the members of the studied towers mainly fail by weak-axis buckling, the

quantities $EI_m\eta^{II}_{cr}$ and $M_{Rk,m}$ are used with reference to the weak axis bending moments in the following.

In the next sections, the three different possibilities for the definition of the member imperfections are used for the four towers. One may note that the value of the coefficient $\varepsilon$ is calculated based on the measured yield stress. Finally, it should be noted that the tower is modelled as for the **Level II** approach including fictitious elements used to model the "one bolt" pinned connection of the diagonals to the legs and to the horizontal members.

### 6.2.3.2 Analysis of the towers tested in the laboratory

Table 6.10 represents the synthesis of the results for both, the elastic and plastic cross-section resistance verification in case of an imperfection introduced as sine half wave on all members in compression and for the case of the eigenmode affine imperfection.

It appears that the results vary highly depending on the chosen shape of imperfection (half sine wave vs eigenmode affine) and on the chosen direction of imperfection. Additionally, it seems that a sine wave affine imperfection leads in most cases to higher resistances than the eigenmode affine imperfection. This observation is however not surprising as the amplitude of the imperfection is for all towers higher if the analysis is based on the eigenmode as imperfection. Still, the eigenmode affine imperfection leads to very satisfactory results for the buckling of the diagonals (towers O-1 and D-1). For these towers, the half sine wave imperfection is unsafe. For towers failing by leg buckling (towers O-2 and D-2) both imperfection types seem suitable. It should be noted that the half sine wave imperfection directed inwards leads to the failure mode observed in the laboratory for towers O-2 and D-2 (inward leg buckling). If the imperfection is directed inwards according to the observed failure mode, the half sine wave imperfection approach is slightly safer than the eigenmode affine imperfection. A more detailed analysis of the results is given in the next paragraphs.

**Table 6.10 Summary of predicted design loads for Level III approach**

| Tower | Design load (kN) – Level III | | | | | Design load (kN) – Level II approach | Maximum load (kN) – Laboratory test |
| | Half sine wave outwards | | Half sine wave inwards | | Eigenmode affine imperfection (number of mode) | clamped supports | |
| | Elastic CS design | Plastic CS design | Elastic CS design | Plastic CS design | | | |
|---|---|---|---|---|---|---|---|
| O-1 | 55,75 | 52,98 | 43,11 | 47,52 | 38,93 (1) | 32,06 | 39,00 |
| O-2 | 92,27 | 110,0 | 77,47 | 81,31 | 84,84 (1) | 82,62 | 106,5 |
| D-1 | 50,87 | 41,95 | 41,23 | 40,53 | 37,62 (2) | 27,55 | 38,50 |
| D-2 | 67,61 | 80,96 | 62,30 | 65,40 | 65,61 (1) | 60,31 | 78,50 |

The detailed results for all towers are provided in the following figures.

Tower O-1:

Table 6.11 represents the first buckling eigenmode of tower O-1 in the first column. This eigenmode represents (minor-axis) flexural buckling of the lower compressed diagonals. The following columns represent the design checks (red indicates a working degree of 1,0) obtained depending on the applied imperfection. The lowest value is obtained for an elastic design imperfection directed inwards. However, even the lowest value of 43,11 kN is approximatively 10% higher than the ultimate load obtained by the laboratory test (39 kN). The highest value is obtained for an elastic design imperfection directed outwards. It is somewhat astonishing that this value is even higher than the design resistance based on plastic resistance. Yet, the reason for this observation is that the elastic design imperfection compensates partially the applied minor-axis bending moment whereas the plastic design imperfection (of higher amplitude) creates a minor-axis bending moment of opposite sign and higher absolute value. The buckling direction is therefore different.

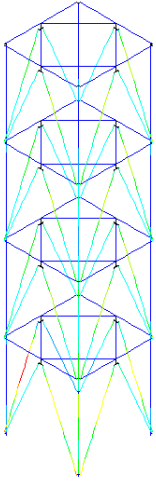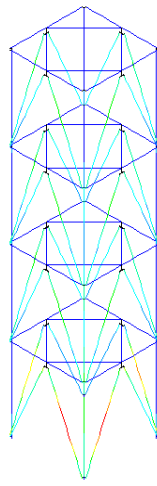**Table 6.11 Tower O-1 design results based on half sine wave imperfection**
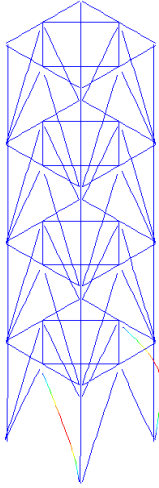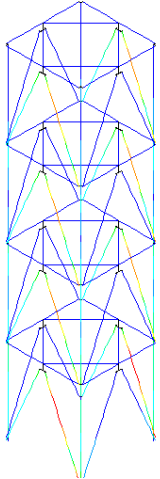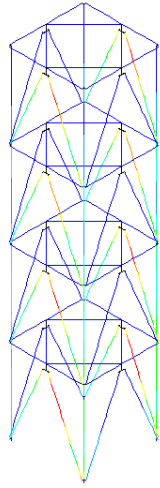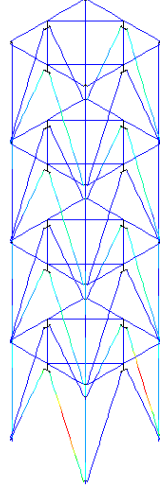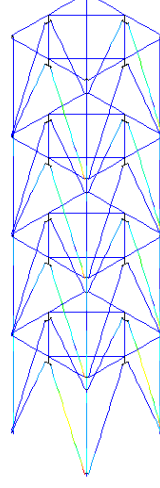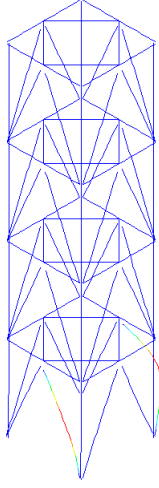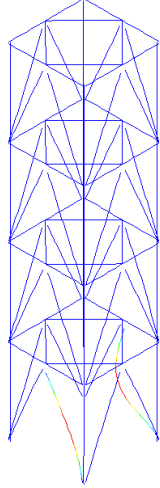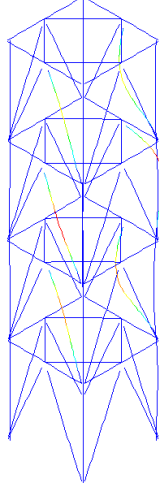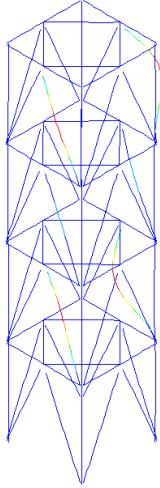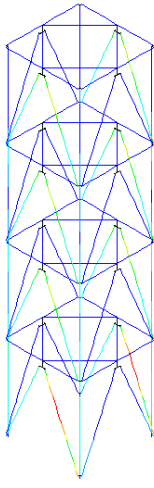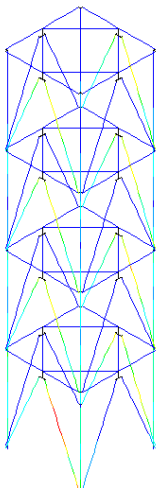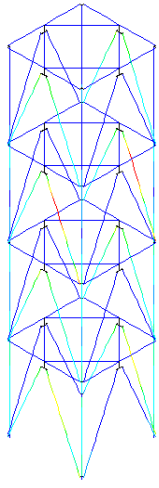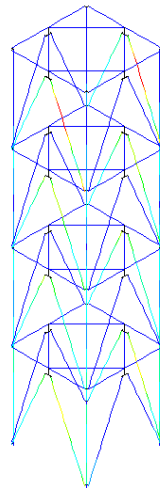
| Shape of $1^{st}$ Buckling eigenmode | Elastic design and half sine wave outwards | Elastic design and half sine wave inwards | Plastic design and half sine wave outwards | Plastic design and half sine wave inwards |
|---|---|---|---|---|
|  |  |  |  |  |
| Critical load = 65,13 kN | Design load = 55,75 kN | Design load = 43,11 kN | Design load = 52,98 kN | Design load = 47,52 kN |

Table 6.12 represents the design loads obtained with an eigenmode affine imperfection followed by an elastic cross-section verification. It can be observed that for the three different imperfections, the design loads are rather close. Certainly, this results from the fact that the first four critical loads are also very close for Tower O-1. The imperfection affine to the first eigenmode leads to lower design loads than the sine wave imperfection. However, this second imperfection approach leads to results that are very close to laboratory test.
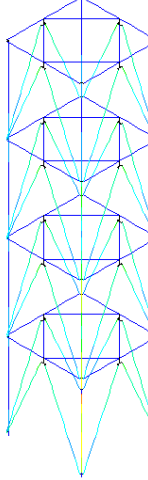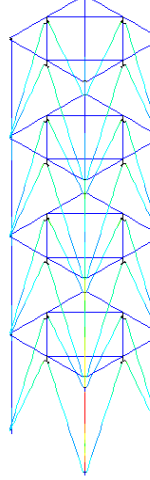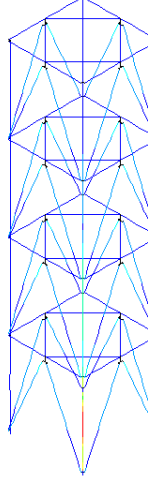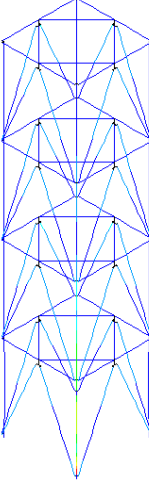
**Table 6.12 Tower O-1 design results based on eigenmode affine imperfection**

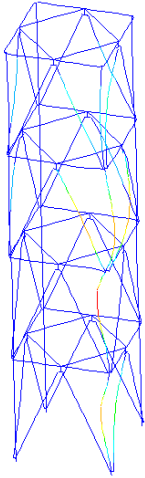|  | Eigenmode 1 | Eigenmode 2 | Eigenmode 3 | Eigenmode 4 |
|---|---|---|---|---|
| Shape of Eigenmode |  |  |  |  |
| Critical load (kN) | 65,13 kN | 65,83 kN | 74,53 kN | 75,98 kN |
| Amplitude imperfection (mm | 5,94 | 5,96 | 5,46 | 5,43 |
| Design Check |  |  |  |  |
| Design load (kN) | 38,93 | 44,43 | 41,59 | 41,39 |

Tower O-2:

Next, Table 6.13 and Table 6.14 represent the results obtained for Tower O-2 failing by leg buckling. In case of an imperfection according to a half sine wave, the numerical analysis leads to satisfactory results in both cases, elastic and plastic cross-section verification. Generally, the plastic cross-section interaction leads to higher design loads. It should be noted that the tower fails by inward leg buckling. This failure mode is only represented if the imperfection is directed inwards. Therefore, it seems most consistent to compare the values of 77,47 kN (obtained with elastic design imperfection) and of 81,31 kN (obtained with plastic design imperfection) to the laboratory test result of 106,5 kN. The difference is therefore of about 20%, which seems however acceptable owing to the complexity of the structure.

**Table 6.13: Tower O-2 design results based on half sine wave imperfection**
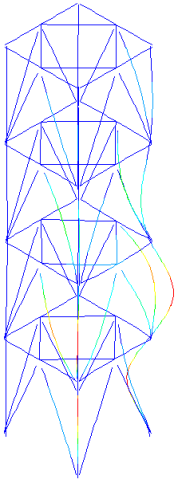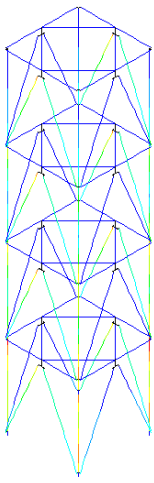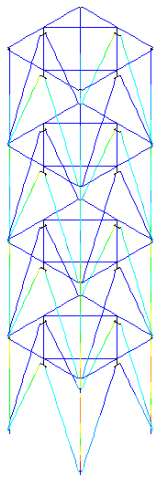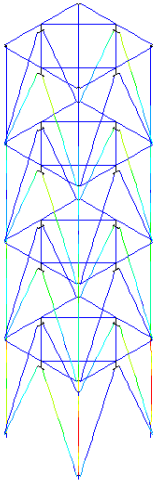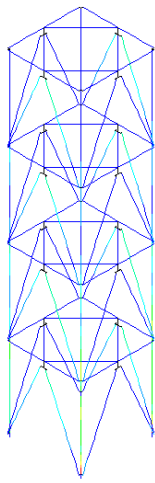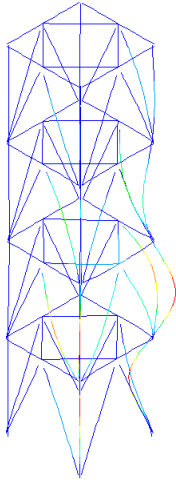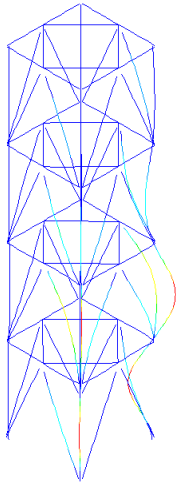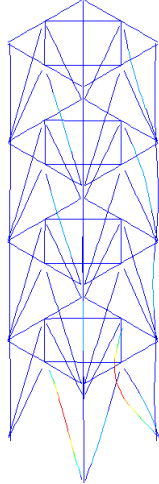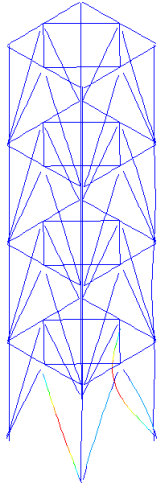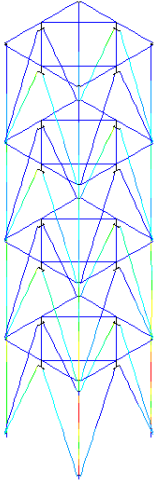
| Shape of 1st Buckling eigenmode | Elastic design and half sine wave outwards | Elastic design and half sine wave inwards | Plastic design and half sine wave outwards | Plastic design and half sine wave inwards |
|---|---|---|---|---|
|  |  |  |  |  |
| Critical load = 166,89 kN | Design load = 93,27 kN | Design load = 77,47 kN | Design load = 110,00 kN | Design load = 81,31 kN |

Table 6.14 shows the results obtained with an eigenmode affine imperfection. One may note that only the first eigenmode is used as the higher modes are linked to much higher critical amplification factors. Additionally, eigenmode 3 and eigenmode 4 do not represent the failure mode observed in the laboratory.

In contrast to Tower O-1, the cross-section verification is performed with an elastic cross-section interaction and, as alternative, with linear plastic cross section interaction. One may observe that the elastic cross-section interaction leads to a rather conservative design load of 69,18 kN. If the linear plastic cross-section interaction is applied, the design load is again sufficiently close to the laboratory test. The use of a non linear plastic imperfection could potentially increase further on the design load and therefore lead to lower difference between laboratory test and numerical simulation. Nonetheless, it should be recalled that the eigenmode affine imperfection should only be used with an elastic cross-section interaction or a linear plastic interaction according to Eurocode 3Part 1-1.

**Table 6.14 Tower O-2 design results based on eigenmode affine imperfectio**

| | Eigenmode 1 | Eigenmode 2 | Eigenmode 3 | Eigenmode 4 |
|---|---|---|---|---|
| Shape of Eigenmode |  |  |  |  |
| Critical load (kN) | 166,89 | 181,05 | 223,11 | 228,98 |
| Amplitude imperfection (mm) | 5,28 | | | |
| Design Check |  | - | - | - |
| Design load (kN) – elastic interaction | 69,18 | - | - | - |
| Design load (kN) – linear plastic interaction | 84,84 | - | - | - |

<u>Tower D-1:</u>

Table 6.15 and Table 6.16 represent the design results for Tower D-1 failing by diagonal buckling under a load applied along a diagonal. In Table 6.15, the obtained design loads are given for the half sign wave imperfection.

**Table 6.15 Tower D-1 design results based on half sine wave imperfection**
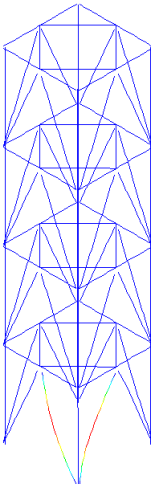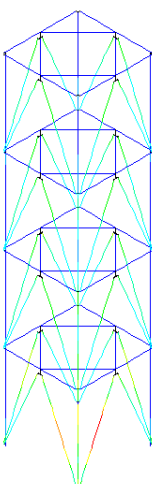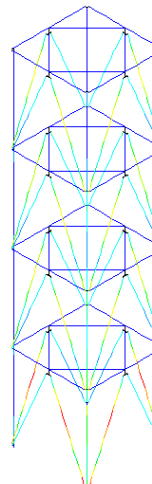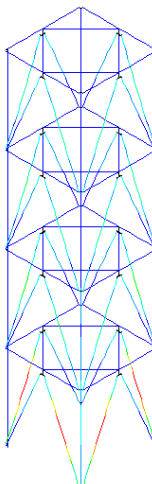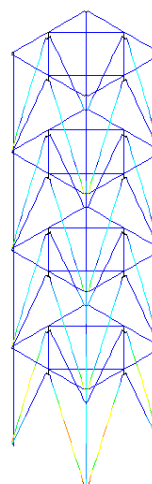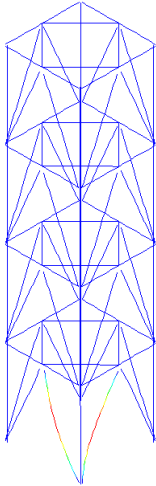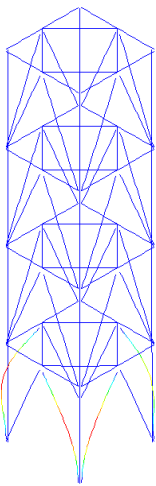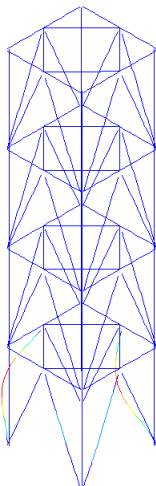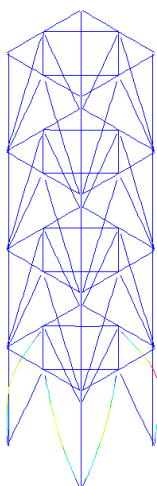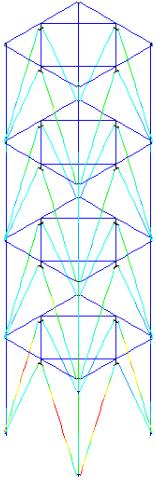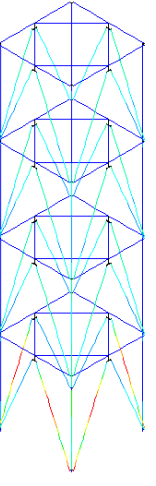
| Shape of 1st Buckling eigenmode | Elastic design and half sine wave outwards | Elastic design and half sine wave inwards | Plastic design and half sine wave outwards | Plastic design and half sine wave inwards |
|---|---|---|---|---|
|  |  |  |  |  |
| Critical load = 52,52 kN | Design load = 50,88 kN | Design load = 41,23 kN | Design load = 41,94 kN | Design load = 41,24 kN |

Table 6.16 represents the design loads obtained based on eigenmode affine imperfections. First, one may observe that the first four eigenmodes are very close. The design loads are obtained with a linear elastic cross-section interaction and one may observe that they are again slightly higher than the critical loads. This observation results as before from elastic redistribution of the internal forces and moments. Finally, it should be noted that the design load obtained with an imperfection affine to eigenmode 1 is safe sided and very close to the laboratory test result.
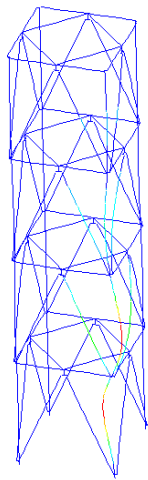
**Table 6.16 Tower D-1 design results based on eigenmode affine imperfection**

| | Eigenmode 1 | Eigenmode 2 | Eigenmode 3 | Eigenmode 4 |
|---|---|---|---|---|
| Shape of Eigenmode |  |  |  |  |
| Critical load (kN) | 52,52 | 54,50 | 54,69 | 54,94 |
| Amplitude imperfection (mm) | 6,58 | 6,60 | 6,58 | 6,59 |
| Design Check |  |  |  |  |
| Design load (kN) | 37,79 | 41,49 | 44,76 | 39,94 |

Tower D-2:
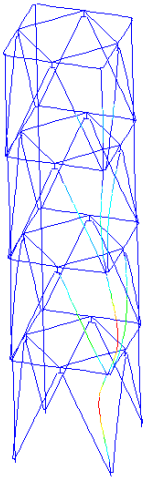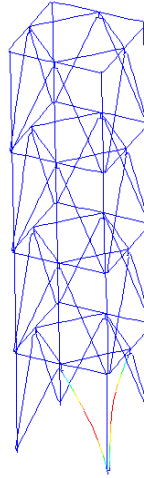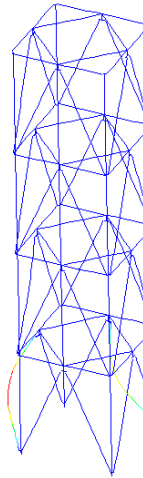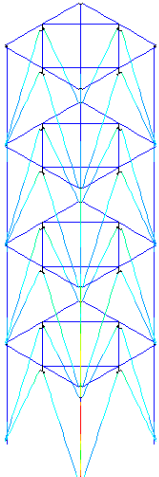
Last, Table 6.17 and Table 6.18 represent the results obtained for Tower D-2 failing by buckling of the most compressed diagonal. In the laboratory, buckling was observed to develop to the inside of the tower for a load of 78,5 kN. It can observed that the half sine wave imperfection leads in general to acceptable results. In particular, one may observe that the results obtained for the elastic and plastic design imperfection directed inwards are on the safe side. The difference of 20% seems to be acceptable again.

**Table 6.17 Tower D-2 design results based on half sine wave imperfection**

| Shape of 1st Buckling eigenmode | Elastic design and half sine wave outwards | Elastic design and half sine wave inwards | Plastic design and half sine wave outwards | Plastic design and half sine wave inwards |
|---|---|---|---|---|
|  |  |  |  |  |
| Critical load = 119,6 kN | Design load = 67,61 kN | Design load = 62,30 kN | Design load = 80,96 kN | Design load = 65,40 kN |

The results obtained based on an eigenmode affine imperfection are represented in Table 6.18. Again the first four eigenmodes are represented but the numerical simulation is only performed for an imperfection according to eigenmode 1 as the others are linked to much higher critical load amplification factors. Again, the use of the linear plastic cross section interaction leads to satisfactory results. The elastic cross section interaction seems however to be too safe sided for the case of leg buckling.

**Table 6.18 Tower D-2 design results based on eigenmode affine imperfection**

| | Eigenmode 1 | Eigenmode 2 | Eigenmode 3 | Eigenmode 4 |
|---|---|---|---|---|
| Shape of Eigenmode |  |  |  |  |
| Critical load (kN) | 119,6 | 190,6 | 190,7 | 237,0 |
| Amplitude imperfection (mm | 5,24 | | | |
| Design Check |  | - | - | - |
| Design load (kN) – elastic interaction | 53,51 | - | - | - |
| Design load (kN) – linear plastic interaction | 65,61 | - | - | - |

### 6.2.3.3   Conclusions on Level III approach

In this section, an important number of numerical results has been presented. It may be noted that many combinations between shape of the imperfection, amplitude of the imperfection and choice of the cross-section design method are possible. Based on the comparisons between numerical simulations and laboratory tests some interesting conclusions may be drawn:

- Using an eigenmode affine imperfection generally leads to satisfactory results;

- The geometric imperfection should not be based exclusively on the first eigenmode but several shapes should be investigated especially if the eigenmodes are close (as here for the case of buckling of the diagonals);
- For the case of leg buckling the linear plastic cross-section interaction seems suitable if it is used with an eigenmode affine imperfection;
- For the case of buckling of diagonals, the elastic interaction should be used with the eigenmode affine imperfection;
- The half sine wave imperfection generally leads to slightly unsafe design loads for buckling of the diagonals;
- For the buckling of the legs the half sine wave imperfection leads to satisfactory results in both cases of elastic and plastic cross-section imperfection;
- Several imperfection directions should be investigated also if the half sine wave imperfection is applied.

In case of the eigenmode affine imperfection, it seems first surprising that the linear plastic interaction can be used in case of leg buckling but not for the case of buckling of the diagonals. The major difference is in fact the slenderness of the members. The legs failing in case of Towers O-2 and D-2 possess a relative slenderness for minor-axis buckling of about 1,0 whereas the diagonals failing in case of Towers O-1 and D-1 possess a relative slenderness of nearly 2,0. Consequently, it seems that the choice of the cross-section interaction should be linked to the relative slenderness of the studied member. For members of low slenderness, it appears consistent to authorize even the use of a non-linear plastic interaction in order to ensure the continuity between members failing by buckling and members failing by cross section yielding.

## 6.2.4   **Level IV approach**

### 6.2.4.1   **Description of the numerical model for steel towers**

The **Level IV** design approach, which consists in a full non-linear analysis, is therefore applied to the towers tested in the laboratory. The tower is modelled with FINELG software [11] using beam elements with 6 degrees of freedom and the eccentricities are accounted for as precisely as possible in a beam element model (Figure 6.24). The bolted connections are represented by fictitious elements possessing a very low torsional stiffness, as for **Level II** and **III** models. The eccentricity between the horizontal member and the diagonals is taken into account through the gusset plate. The plate, welded in the physical specimens to the horizontal members, is modelled as clamped to the horizontal members. The diagonals are connected to the gusset plate by the fictitious elements of low torsional stiffness reproducing a pinned "one bolt" connection. The self-weight of the structure (W) is calculated automatically by the software, while the horizontal loads (H) are introduced at the extremities of the legs at the top level. The tower is assumed to be clamped at the ground, so as to represent better the actual support conditions of the laboratory tests.
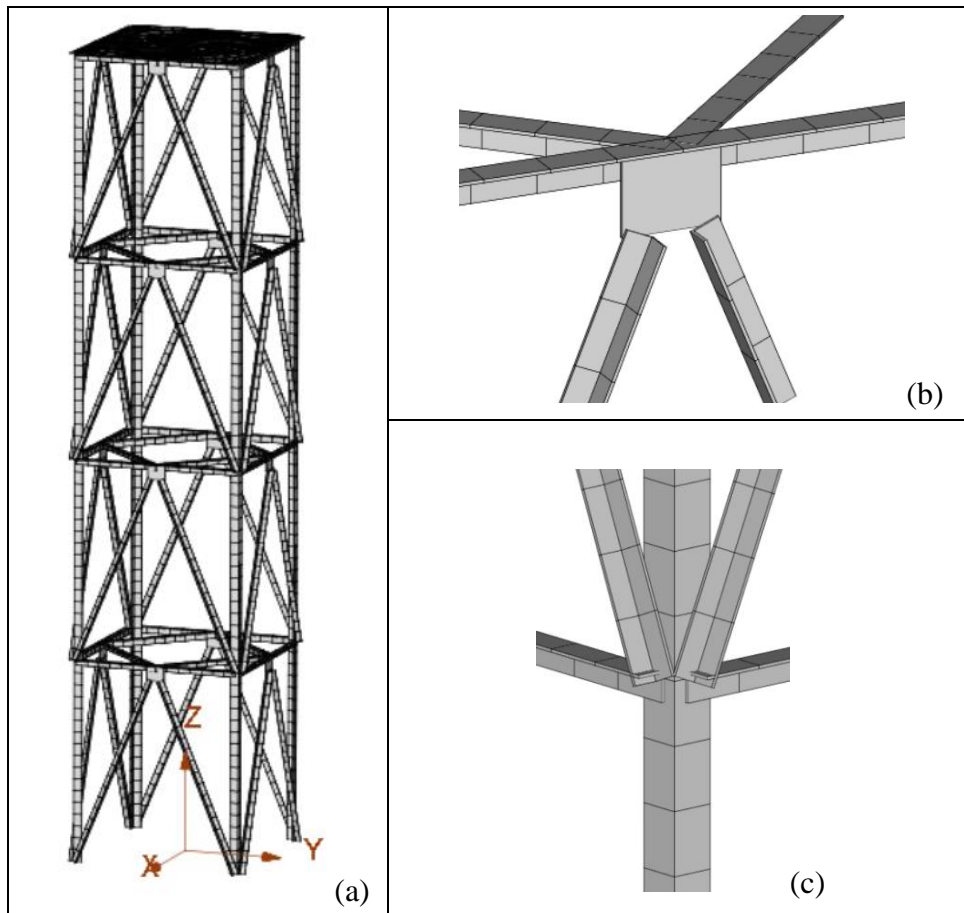
**Figure 6.24 (a) 3-D tower model at Level IV approach, (b) Detail of connection between horizontal and vertical bracings, (c) Detail of connection between vertical bracings and leg**

The FINELG finite element analysis adopting the GMNIA method is performed considering:

- an initial imperfection (shape in accordance with the first buckling mode and amplitudes as they determined in 6.2.3.1);
- a linear elastic - perfectly plastic material law without strain hardening, based on the measured yield stresses.
- residual stresses resulting from the hot-rolling procedure. The selected pattern (see Figure 6.25) is issued from previous studies [12] in which appropriate measurements have been realized; this pattern is a rather common one for angles;
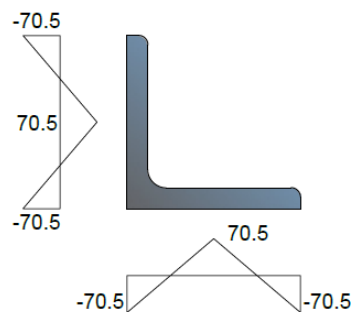


**Figure 6.25 Assumed pattern of residual stresses [12]**

### 6.2.4.2   Analysis of the towers tested in the laboratory

The detailed results for all towers are provided in the following figures and tables. For each tower, the following analyses are performed:

- an elastic instability analysis with load combination $a_{cr}(W+H_{exp})$

- a modal analysis
- a full non-linear analysis, in which the gravity loads (W) are first applied and then the horizontal load is increasing (W+λH) until failure of the tower occurs. This load sequence simulation is closer to the test procedure.

Tower O-1:

**Table 6.19 Tower O-1 design results based on eigenmode affine imperfection for Level IV approach**
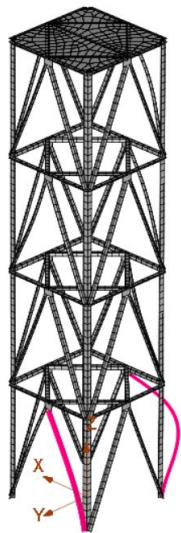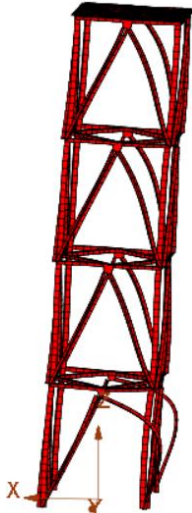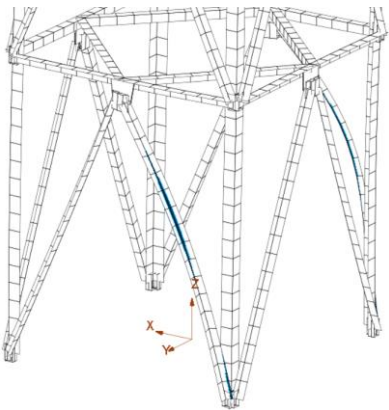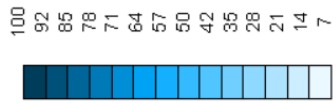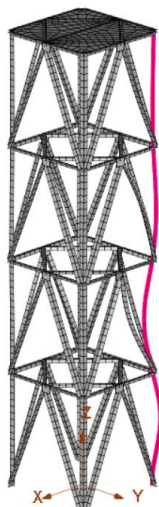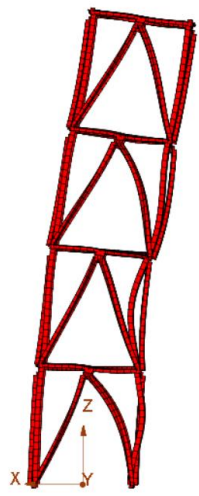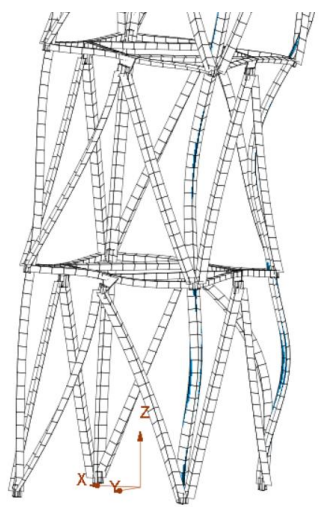
| Elastic instability analysis | Full non-linear analysis | |
|---|---|---|
| Shape of 1st Buckling mode | Deformation shape at ULS | Level of yielding |
|  |  |  |
| Critical load = 62,01 kN (a$_{cr}$=1,590) | Design load= 40,70 kN | |

Table 6.19 includes the results for the Tower O-1. The first buckling mode (shape and critical load) of Tower O-1, that is a minor-axis flexural buckling of the lower compressed diagonals same as in **Level III** model, is presented in the first column of the table. The following columns represent the deformation shape of the tower at the ultimate limit state, the design load and the distribution of yielding at the members of the tower. The design load is equal to 40,70kN and is a bit higher (4,3%) than the ultimate load obtained by the laboratory test, but is acceptable. The failure occurs at the lower compressed diagonals and the difference between the numerical model and the experiment is the direction of buckling (inwards/outwards).

Tower O-2:

Table 6.20 represents the results obtained for Tower O-2 failing by leg buckling. It should be noted that the tower fails by inward leg buckling during the laboratory test in contrast with the analysis that fails by outward leg buckling. The design load is equal to 101,620 kN and is a quite close to the ultimate load obtained by the laboratory test. It might be said that the results of the **Level IV** design approach are covering better the plasticity effects (yielding) than the **Level III** design approach.
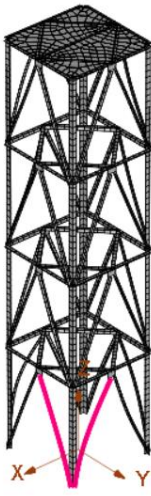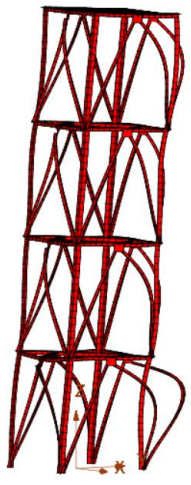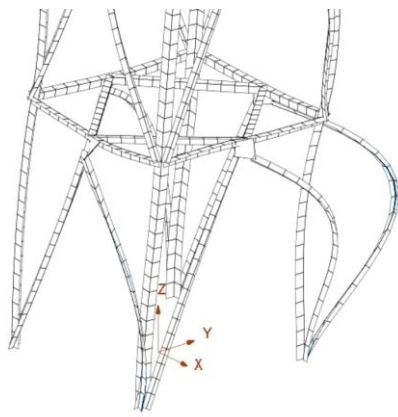
**Table 6.20 Tower O-2 design results based on eigenmode affine imperfection for Level IV approach**

| Elastic instability analysis | Full non-linear analysis | |
|---|---|---|
| Shape of 1st Buckling mode | Deformation shape at ULS | Level of yielding |
|  |  |  |
| Critical load = 162,41 kN ($a_{cr}$=1,525) | Design load= 101,62 kN | |
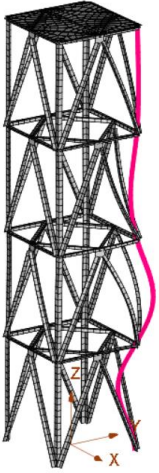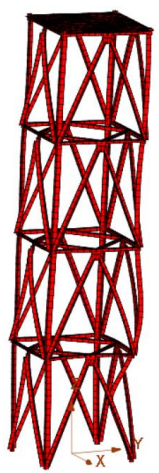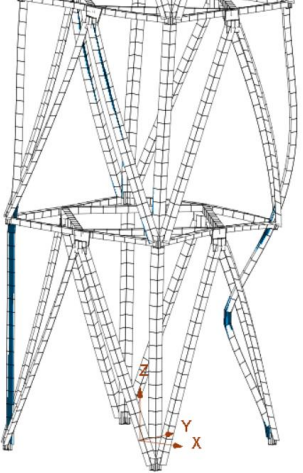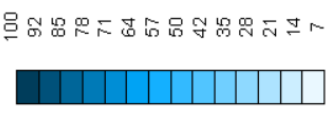
Tower D-1:

For the Tower D-1, the results are summarized in In Table 6.21 and the failure occurs due to a diagonal buckling. The design load equals 38,50kN and is a just bit higher (0,34%) than the ultimate load obtained by the laboratory test. It can be observed that both analyses concerning a diagonal buckling failure, give results rather close to the tests but on the unsafe side. This could be explained by the low level of yielding at the buckling diagonals.

**Table 6.21 Tower D-1 design results based on eigenmode affine imperfection for Level IV approach**

| Elastic instability analysis | Full non-linear analysis | |
|---|---|---|
| Shape of 1st Buckling mode | Deformation shape at ULS | Level of yielding |
|  |  |  |
| Critical load = 58,83 kN ($a_{cr}$=1,528) | Design load= 38,50 kN | |

Tower D-2:

**Table 6.22 Tower D-2 design results based on eigenmode affine imperfection for Level IV approach**

| Elastic instability analysis | Full non-linear analysis | |
|---|---|---|
| Shape of 1st Buckling mode | Deformation shape at ULS | Level of yielding |
|  |  |  |
| Critical load = 119,16 kN (a$_{cr}$=1,518) | Design load= 74,68 kN | |

The results for Tower D-2, obtained based on an eigenmode affine imperfection, are represented in Table 6.22. The tower fails due to a buckling of the most compressed diagonal with a design load equal to 74,68kN. The buckling is observed to develop to the inside of the tower same as the experimental test.

Furthermore, Figure 6.26 illustrates the load-displacement curves of the numerical simulations for the four towers. The horizontal axis represents the absolute displacement of the top of the tower, associated with the load direction (i.e. u$_x$ for towers O-1, O-2 and $\sqrt{u_x^2 + u_y^2}$ for towers D-1, D-2). One can observe that the results are in line with the physical expectations (eccentricity of the members, stiffness of the tower, etc.).
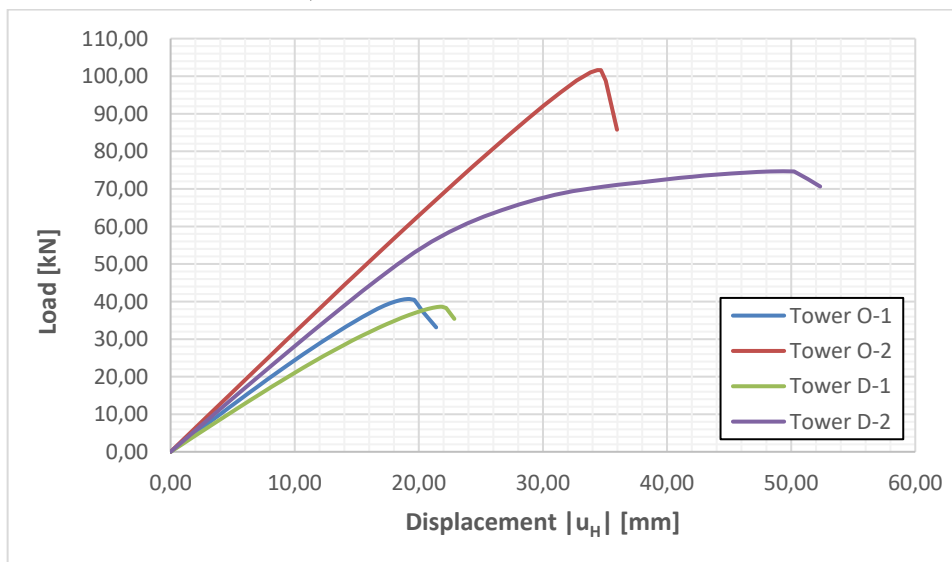


**Figure 6.26 Load – displacement curves for the four towers through the numerical simulations**

Finally, a comparison between the eigen frequencies is shown in Table 6.23Table 6.9. The results indicate that the **Level IV** model seems to be rather close with the results of **Level II** model. This was expected as both level approaches have almost the same assumptions for the modelling of the structure.

**Table 6.23 Summary of predicted eigen frequencies for Level VI approach**

| Tower | Eigen frequency – Level II model (Hz) | Eigen frequency – Level IV model (Hz) | Eigen frequency – Laboratory test (Hz) |
|---|---|---|---|
| O-1 | 15,51 | 14,73 | 19,4 |
| O-2 | 16,14 | 15,31 | 19,0 |
| D-1 | 14,91 | 14,01 | 19,9 |
| D-2 | 16,10 | 15,18 | 16,6 |

### 6.2.5  **Summary**

Table 6.24 summarises the main results presented in section 6.2. One may observe that the very simple **Level I** approach leads to safe sided results. However, the design results appear to be very conservative and the use of **Level I**, especially if an optimisation of the tower is intended, cannot be recommended. **Level II** approach is also safe sided but much less than the **Level I** approach. The difference between the **Level II** design result and the laboratory tests is of about 20%. This difference seems acceptable as the **Level II** approach sufficiently simple to treat the complex structure of an angle section lattice tower. The **Level III** approach with an eigenmode affine imperfection leads to results that are very close to the laboratory tests in case of diagonal member buckling and sufficiently close to the laboratory tests in case of leg buckling. It should however be noted that supplementary investigations on the **Level III** approach seem necessary in order to clearly define for which members a plastic cross-section interaction may be used and for which members the design should be limited to an elastic cross-section interaction. Finally, the **Level IV** approach, considering an eigenmode affine imperfection, gives very satisfying results that are quite close to the tested towers.

**Table 6.24 Results of different design approaches**

| Tower | Ultimate load – Laboratory test | Level I Design load | Level II Design load | Level III Design load – Eigenmode affine imperfection | Level IV Design load – Eigenmode affine imperfection |
|---|---|---|---|---|---|
| O-1 | 39,00 | 29,38 | 32,06 | 38,93 | 40,70 |
| O-2 | 106,5 | 67,97 | 82,62 | 84,84 | 101,62 |
| D-1 | 38,50 | 25,06 | 27,55 | 37,62 | 38,63 |
| D-2 | 78,50 | 48,06 | 60,31 | 65,61 | 74,68 |

## 6.3 Reinforced steel towers

### 6.3.1 Validation of tower 3 type 0-1S

#### 6.3.1.1 Level I model

**Modelling and Analysis**

The tower is modelled as 3D pin-jointed frame implemented in the SOFISTIK software, Figure 6.27. All members are represented by beam elements with hinges at their end and are stressed by axial forces only. The legs are considered to be simply supported at the base. The top diaphragm plate is modelled through rigid links between the nodes of the top floor, illustrated with yellow in Figure 6.27a). Loads include the self-weight of the structure, the weight of the diaphragm plate and a horizontal force applied at the middle of the top beam, Figure 6.27a).

Dynamic analysis provides eigenvalues and eigenforms of the tower, illustrated in Figure 6.27 b) and c).
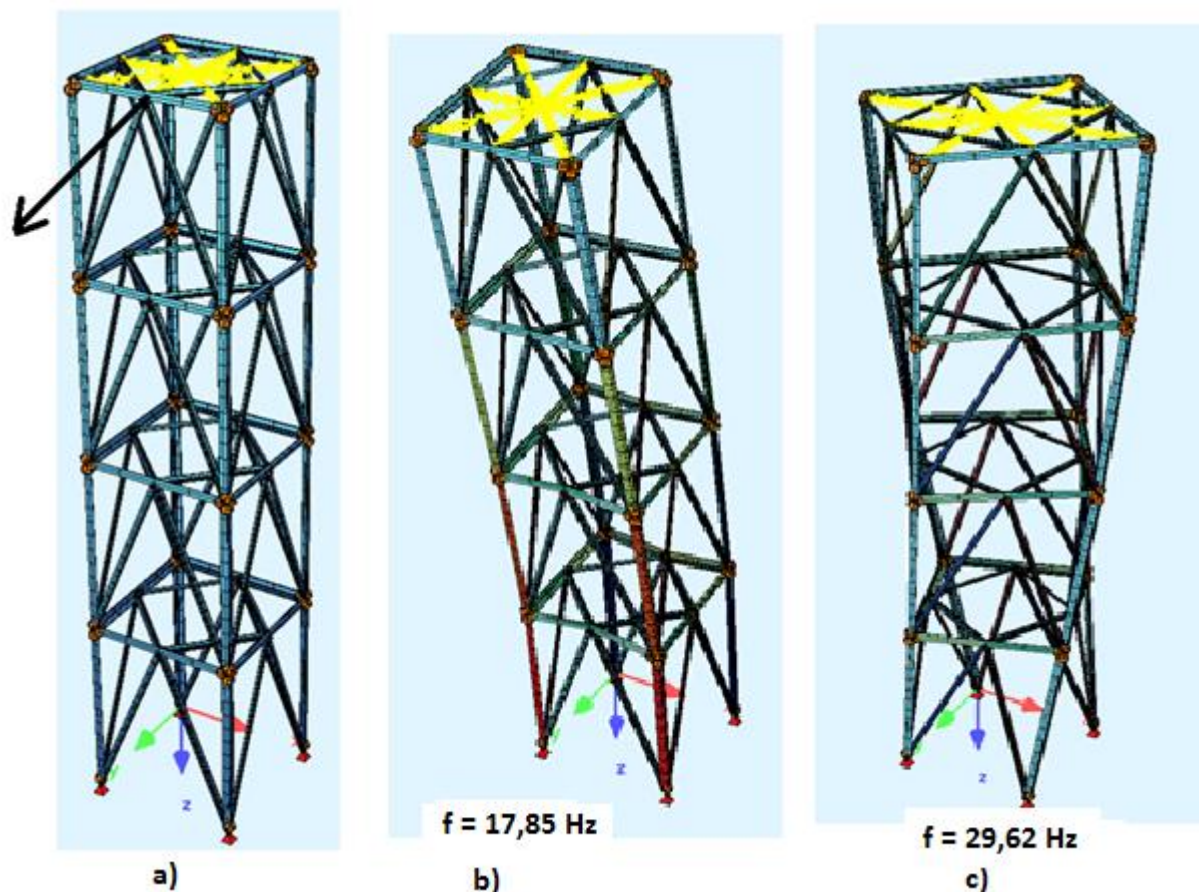


**Figure 6.27 Level I model Tower O-1S. a) Applied force, b) translational vibration mode (1st and 2nd), c) torsional vibration mode (3rd)**

The braces are angle sections L45.45.5, with external leg strengthening with FRP strips 50x1.2 mm.

### 6.3.1.1.1 Design

**Braces L45.45.5+FRP**

Design refers to the failed compression braces composed of angle sections L45.45.5 strengthened by FRP strips 50x1.2 mm that were applied on the external side of their legs. In **Level I** braces are checked for buckling due to axial compression with modified slenderness.

- **Material properties**

Actual material properties for design are as follows:

Steel $f_y$ = 286,7 MPa     $f_u$ = 416,67 MPa FRP  $f_{f,actual}$ = 3187 MPa

- **Cross section properties**

Since the width of the FRP, 50 mm, is wider that the width of the legs, 45 mm, only the portion of the FRP attached to steel is considered in analysis and design, as shown in Figure 6.28.
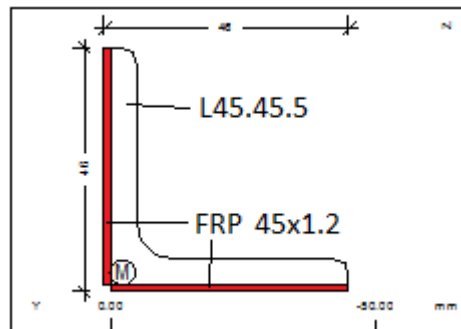


**Figure 6.28 Brace cross section used for analysis and design**

The properties of this hybrid cross section are determined according to the procedures described in Deliverable 2.4 and are summarized in Table 6.25

**Table 6.25 Properties of the hybrid cross section of Figure 6.28**

| Cross section area | Second moment of area, strong axis | Second moment of area, weak axis | Plastic axial force *calculated with $f_f$= $f_{f,actual}/2$ |
|---|---|---|---|
| A = 519 mm$^2$ | $I_u$ = 124355 mm$^4$ | $I_v$ = 32855 mm$^4$ | *$N_{pl}$ = 295 kN |

The buckling resistance to axial compression is determined according to section 5.1.2 and is summarized in Table 6.26.

**Table 6.26 Buckling resistance of the hybrid brace cross section**

| Buckling length | Euler buckling load | Relative slenderness $$\bar{\lambda}_v = \sqrt{\dfrac{N_{pl}}{N_{cr}}}$$ | Effective slenderness $\bar{\lambda}_{eff,v}$ $= 0,35 + 0,7\bar{\lambda}_v$ | Reduction factor, curve b | Buckling resistance $$N_R = \dfrac{0,8\,\chi\,A\,f_y}{\gamma_{M1}}$$ |
|---|---|---|---|---|---|
| $L_{cr} = L =$ 183,8 cm | $N_{cr,v} = 20,13$ kN | $\bar{\lambda}_v = 3,83$ | $\bar{\lambda}_{eff,v} = 3,03$ | $\chi_v = 0,1086$ | $N_R = 25,6$ kN |
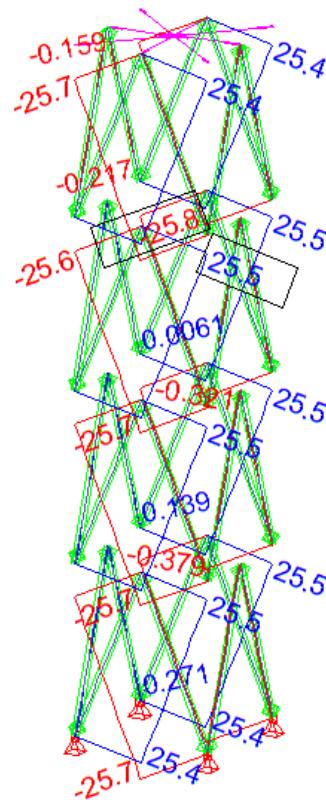


**Figure 6.29 Brace forces $N_E$ for horizontal force on the tower F = 38,93 kN**

## Bolted connection of braces L45.45.5

The connection is with one bolt M12 10.9.

Bolt properties: d = 12 mm, $d_0$ = 13 mm, $A_s$ = 84,3 mm$^2$, $f_{ub}$ = 1000 MPa

For angle section: Thickness t = 5 mm, $f_u$ = 416,67 MPa

Geometry of connection: $e_1$ = 25 mm, $e_2$ = 20 mm  $\alpha_d$ = 25/(3·13) = 0,64, $k_1$ = 2,5, $\alpha_b = \alpha_d$

Shear capacity:  $F_{V,R} = 0,5 \cdot f_{ub} \cdot A_s = 42,15$ kN

Bearing capacity: $F_{b,R} = \dfrac{2,5 \cdot 0,64 \cdot 416 \cdot 12 \cdot 5}{1000} = 40,1$ kN

Critical for the bolted connection is the bearing capacity, $F_{Bolt,R}$ = 40,1 kN

### Legs L70.70.7

- **Material properties**

Actual material properties of the cross section: $f_y = 308,3$ MPa

### Cross section properties

**Table 6.27 Properties L 70.70.7**

| Cross section area | Second moment of area, strong axis | Second moment of area, weak axis | Plastic axial force |
|---|---|---|---|
| A = 940 mm$^2$ | $I_u$ = 671000 mm$^4$ | $I_v$ = 17600 mm$^4$ | $N_{pl}$ = 289 kN |

The buckling resistance to axial compression is determined according to section 5.1.2 above and is summarized in Table 6.28.

**Table 6.28 Buckling resistance of the leg**

| Buckling length | Euler buckling load | Relative slenderness $$\bar{\lambda}_v = \sqrt{\frac{N_{pl}}{N_{cr}}}$$ | Effective slenderness $\bar{\lambda}_{eff,v}$ $= 0,1 + 0,8\bar{\lambda}_v$ | Reduction factor, curve b | Buckling resistance $$N_R = \frac{0,8\,\chi\,A\,f_y}{\gamma_{M1}}$$ |
|---|---|---|---|---|---|
| $L_{cr} = L =$ 170,6 cm | $N_{cr,v}$ = 125,2 kN | $\bar{\lambda}_v = 1,52$ | $\bar{\lambda}_{eff,v} = 1,31$ | $\chi_v = 0,4101$ | $N_R$ = 118,7 kN |

The axial force of the leg is $N_E = 79,1$ kN $< N_R = 118,7$ kN

The results are summarized in Table 6.29. The **Level I** failure load is 38,93 kN.

**Table 6.29 Summary of the Level I design checks for tower 3 Type O-1S**

| | Leg | Diagonal | Connection |
|---|---|---|---|
| $F_E$ | 79,1 | 25,6 | 25,6 |
| $F_R$ | 118,7 | 25,6 | 40,1 |
| Utilization grade | 0,67 | 1 | 0,64 |
| Level I Failure Load/test load | 38,9 / 54,5 = 0,71 | | |

### 6.3.1.2   Level II model

### 6.3.1.2.1   Modelling and Analysis

The tower model is similar to the **Level I** model, with the difference that all legs run continuously over the height, Figure 6.30)a.  Dynamic analysis provides eigenvalues and eigenforms of the tower, illustrated in Figure 6.30b) and c). They are nearly identical with those of **Level I** model.
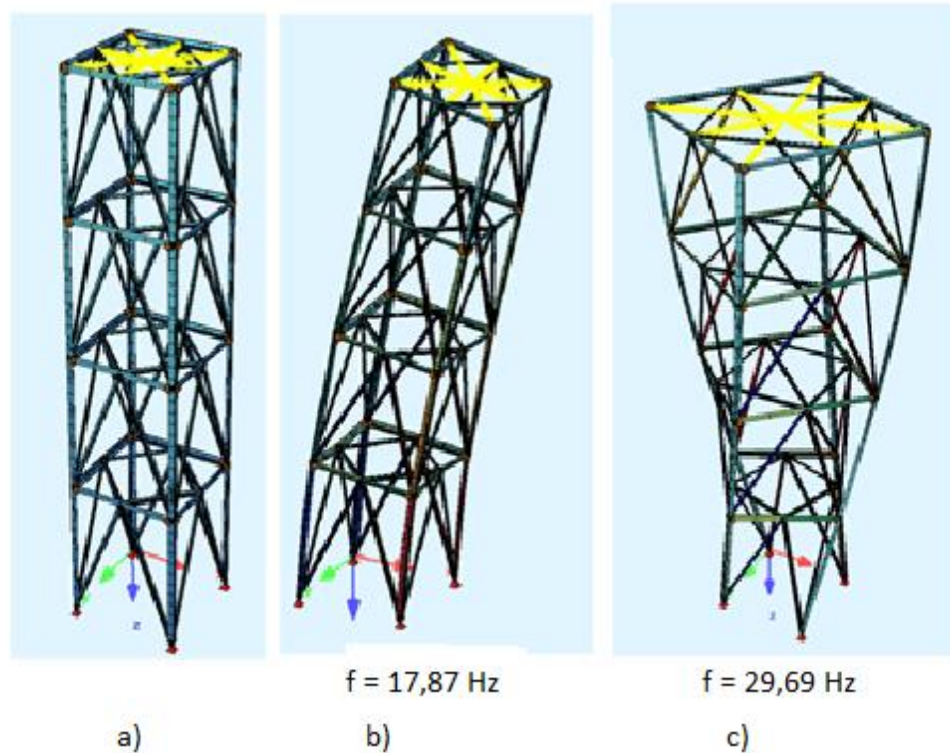


**Figure 6.30 Level II model of tower O-1S. a) model, b) translational vibration mode (1st and 2nd), c) torsional vibration mode (3rd)**

### 6.3.1.2.2   Design

**Braces L45.45.5+FRP**

In **Level II** design braces are checked for buckling due to compression and bending as resulting from the eccentric connection of the bolts. Material and cross section properties are the same as described in section 6.2.2.1. The load eccentricity is calculated according to Deliverable 2.2 from the position of the bolts in the legs and the distance of the centroid from the angle heel which are shown in Figure 6.31. The relevant eccentricities are:

$$e_v = \frac{e}{\sqrt{2}} - u_G = 0{,}0223 \text{ mm} \quad \text{and} \quad e_u = e/\sqrt{2} = 17{,}68 \text{ mm}$$

The end moments are calculated from:

$$M_u = N \cdot e_u \quad \text{and} \quad M_v = N \cdot e_v$$

where N ist he acting axial force.
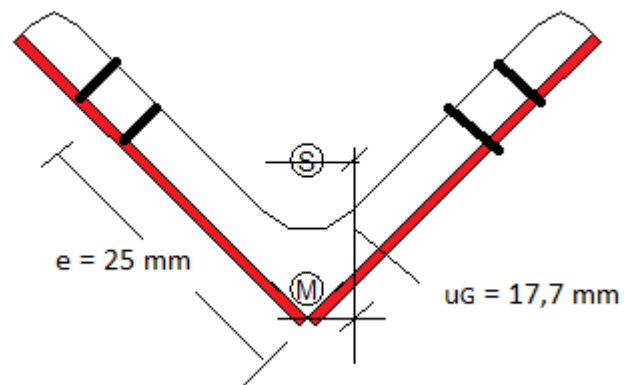
**Figure 6.31 Position of bolts and eccentricities**

The tower is subjected to a horizontal force at the top equal to 50,71 kN. The resulting forces for braces are shown in Figure 6.32.
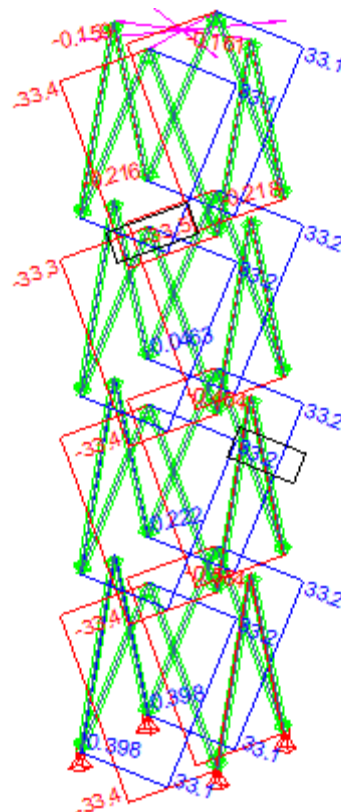


**Figure 6.32 Brace forces $N_E$ for horizontal force on the tower F = 50,71 kN**

The design to axial compression and bending is determined according to section 5.1.2 above and is summarized in Table 6.30.

**Table 6.30 Design summary for the hybrid brace L45.45.5+FRP to compression and bending**

|  |  | v-v | u-u |
|---|---|---|---|
| Acting forces and moments | $N_{Ed} = 35,4$ kN | $M_{v,Ed} = 0,00159$ kNm | $M_{u,Ed} = 0,62579$ kNm |
| Clear length | L m | 1,67 | 1,67 |
| Buckling factor | β | 0,85 | 0,85 |
| Buckling length | $L_{cr}$ m | 1,419 | 1,419 |
| Critical load | $N_{cr}$ kN | 33,8 | 127,8 |
| Relative slenderness | λ | 2,96 | 1,52 |
| Reduction factors | χ | 0,113 | 0,337 |
| Ratio of end moments | ψ | 1 | 1 |
| Factors | C | 1 | 1 |
| Factors | k | $k_{vv} = k_{uv} = 93,5$ | $k_{uu} = k_{vu} = 1,354$ |
| Elastic-plastic resistances | 295 kN | 149,6 kNm | 459,0 kNm |
| Interaction | Interaction | 1,00 | 0,115 |

**Bolted connection of braces L45.45.5+FRP**

The connection is identical as in **Level I** analysis, their capacity being equal to

$F_{Bolt,R} = 40,1$ kN

**Legs**

The acting forces and moments and the fundamental buckling form of the tower according to linear analysis (LA) are presented in Figure 6.33. The transformation of the geometric axes moments to the principal axis moments is according to:

$$M_v = \frac{M_y + M_z}{\sqrt{2}}$$

$$M_u = \frac{M_y - M_z}{\sqrt{2}}$$
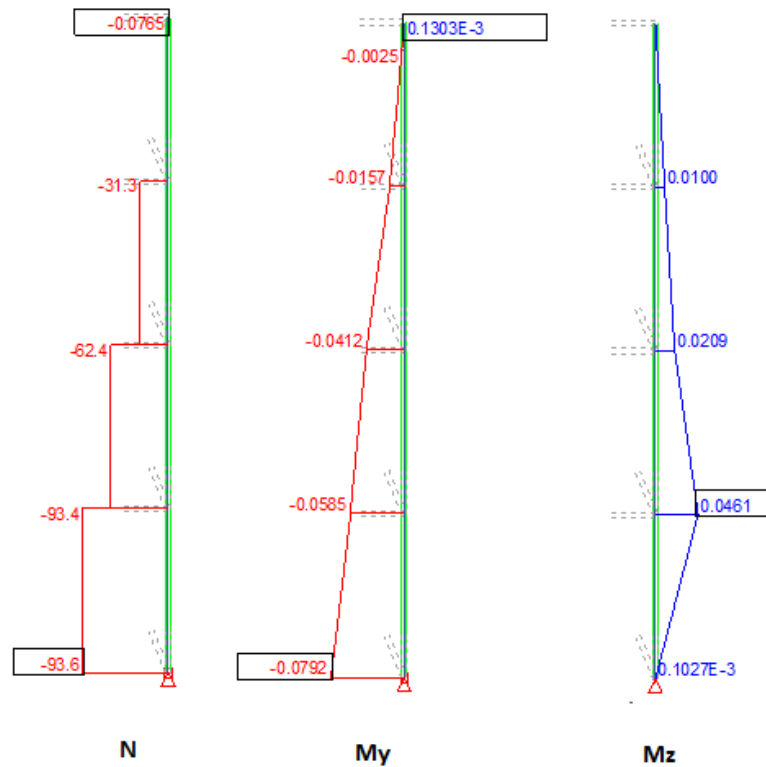
**Figure 6.33 Acting forces and moments for the leg**

The critical buckling length of the leg may be determined from linear buckling analysis (LBA). Figure 6.34 shows the fundamental buckling form in which the leg buckles in respect to the weak axis vv. The critical buckling factor due to application of the horizontal force, H=50,71 kN, is $\alpha_{cr}$ = 3,34. The axial force of the leg determined from global analysis due to this force is $N_E$ = 93,4 kN, Figure 6.33.

The critical buckling load of the leg is $\alpha_{cr}$-times this force, $N_{cr}= \alpha_{cr} \cdot N_E$.

The critical buckling load is in general given by: $N_{cr} = \dfrac{\pi^2 EI}{(\beta L)^2}$

Equating the right sides of the two formulae, the equivalent buckling length factor β may be determined. The results in the relation:

$$\beta = \sqrt{\dfrac{\pi^2 EI}{\alpha_{cr} \cdot N_E}} \,/L$$

where:

E modulus of elasticity

I second moment of area in respect to the buckling axis that corresponds to the buckling form

$\alpha_{cr}$ critical buckling factor as determined from LBA due to the applied loads

$N_E$ axial force in the leg from LA due to the applied loads

L system length of the leg.

The application of the above formula in the case study gives:

$$\beta = \sqrt{\frac{\pi^2 \, 21000 \cdot 17,6}{3,32 \cdot 93,4}}/170,6 = 0,635 > 0,65. \text{ Accordingly } \beta = 0,65$$
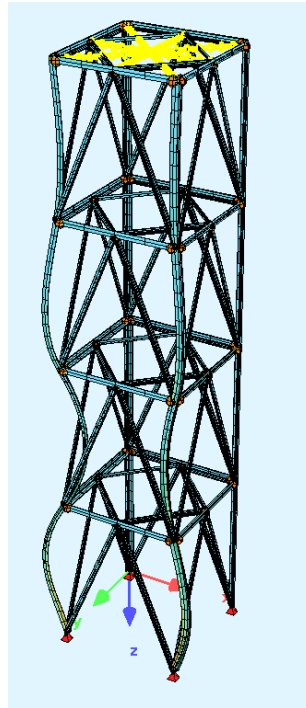


**Figure 6.34 Fundamental buckling form of the tower, $\alpha_{cr} = 3,32$**

The design to axial compression and bending of the compression leg is determined according to section 5.1.2 above and is summarized in Table 6.31.

**Table 6.31 Design summary for the leg L70.70.7 to compression and bending**

|  |  | v-v | u-u |
|---|---|---|---|
| Acting forces and moments | $N_{Ed}$ = 93,6 kN | $M_{v,Ed}$ = 0,056 kNm | $M_{u,Ed}$ = 0,074 kNm |
| Clear length | L m | 1,706 | 1,706 |
| Buckling factor | β | 0,65 | 0,65 |
| Buckling length | $L_{cr}$ m | 1,109 | 1,109 |
| Critical load | $N_{cr}$ kN | 296 | 1129 |
| Relative slenderness | λ | 0,989 | 0,506 |
| Reduction factors | χ | 0,573 | 0,918 |
| Ratio of end moments | ψ | 0,157 | 0,757 |
| Factors | C | 0,66 | 0,90 |
| Factors | k | $k_{vv} = k_{uv}$ = 1,320 | $k_{uu}= k_{vu}$ = 0,722 |
| Plastic resistances Npl, Mpl | 290 kN | 325 | 632 |
| Interaction | Interaction | 0,318 | 0,124 |

The results are summarized in Table 6.32. The **Level II** failure load is 50,71 kN.

**Table 6.32 Summary of the Level II design checks for tower 3 Type O-1S**

|  | Leg | Diagonal | Connection |
|---|---|---|---|
| $F_E$ | 93,6 | 33,4 | 33,4 |
| $F_R$ | 166 | 33,4 | 40,1 |
| Utilization grade | 0,56 | 1 | 0,83 |
| Level I Failure Load/test load | 50,71 / 54,5 = 0,93 | | |

Figure 6.35 gives for all floors the experimental and numerical load - displacement curves. It may be seen that the numerical analysis underestimates by a high degree the actual displacements as recorded in the tests. This is due to the fact that the numerical analysis does not account for any flexibility of connections, joints, base structures etc.
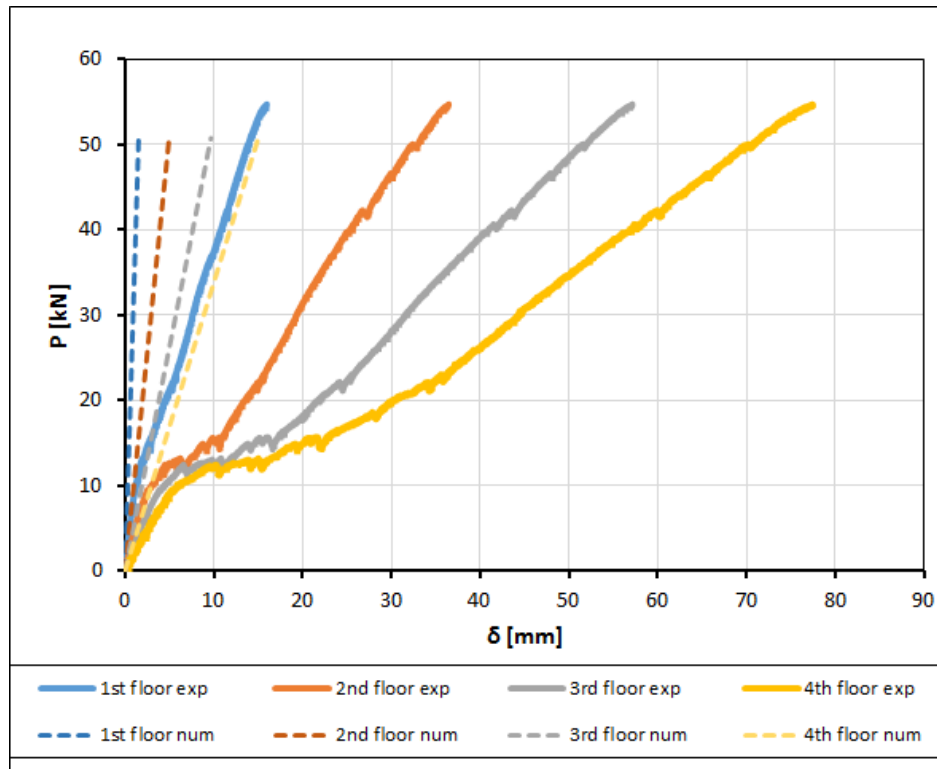


**Figure 6.35 Experimental vs numerical force – displacement curves**

The results of tower 3 for all calculation methods are summarized in Table 6.33.

**Table 6.33 Summary of all design checks for tower 3 Type O-1S**

|  | Experimental | Level I method | Level II method |
|---|---|---|---|
| Failure load | 54,5 kN | 38,9 kN | 50,71 kN |
| Critical member | Compression brace | Compression brace | Compression brace |
| Fundamental vibration frequency | 22,8 Hz | 17,85 Hz | 17,87 Hz |
| Top displacement at 50 kN horizontal force | 70,0 mm | 14,78 mm | 14,78 mm |

6.3.2   **Validation of tower 6 type D-2S**

**6.3.2.1   Level I model**

**6.3.2.1.1   Modelling and Analysis**

This tower has one leg strengthened in the two lower floors and four (4) strengthened compression diagonals at the top floor. Strengthening of the angle sections is with FRP strips 50x1.2 mm, applied externally to the angle legs.

The structure is modelled as 3D pin-jointed frame implemented in the SOFISTIK software, Figure 6.36. All members are represented by beam elements with hinges at their end and are stressed by axial forces only. The legs are considered to be simply supported at the base. The top diaphragm plate is modelled through rigid links between the nodes of the top floor, illustrated with yellow in Figure 6.36a). Loads include the self-weight of the structure, the weight of the diaphragm plate and a horizontal force applied at the corner of the top floor, Figure 6.36a).

Dynamic analysis provides eigenvalues and eigenforms of the tower, illustrated in Figure 6.36b) and c).
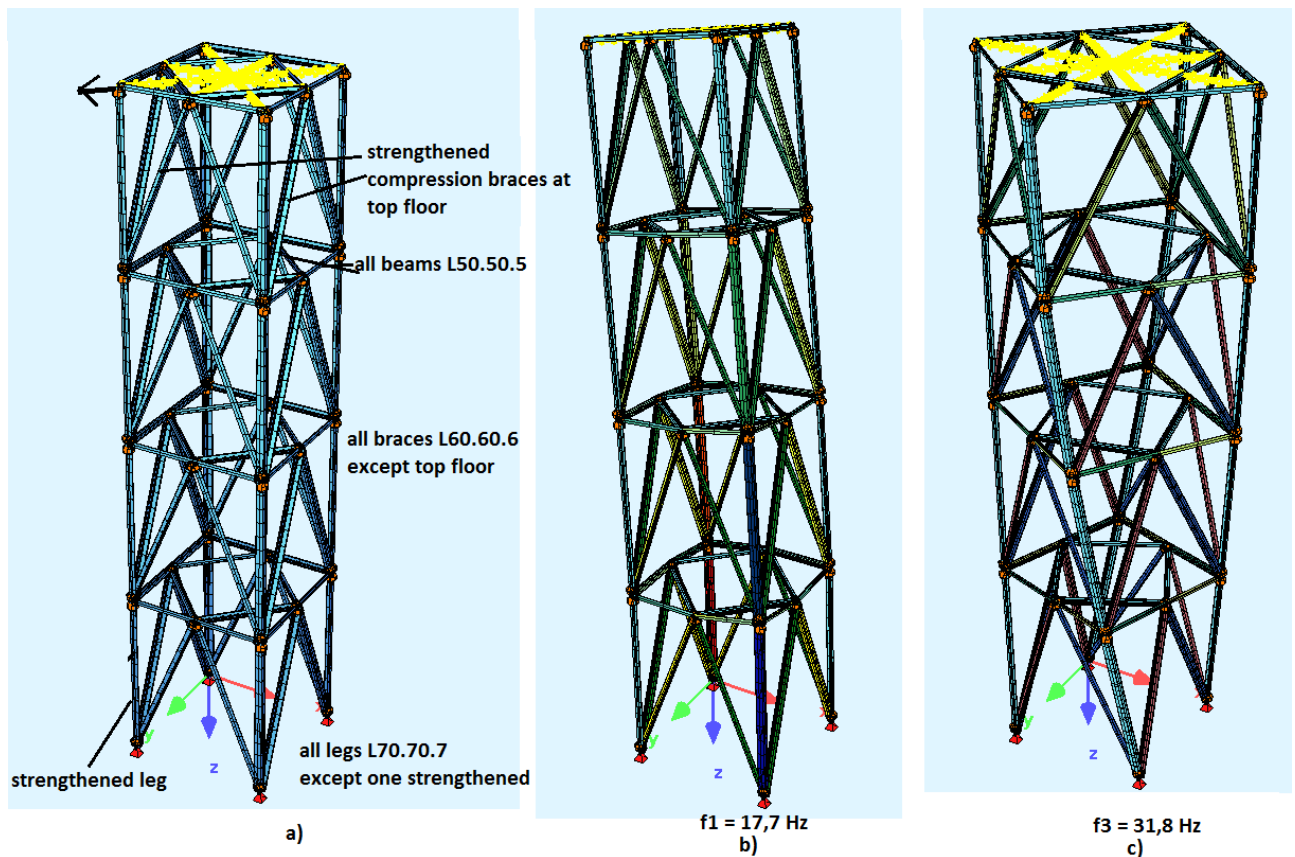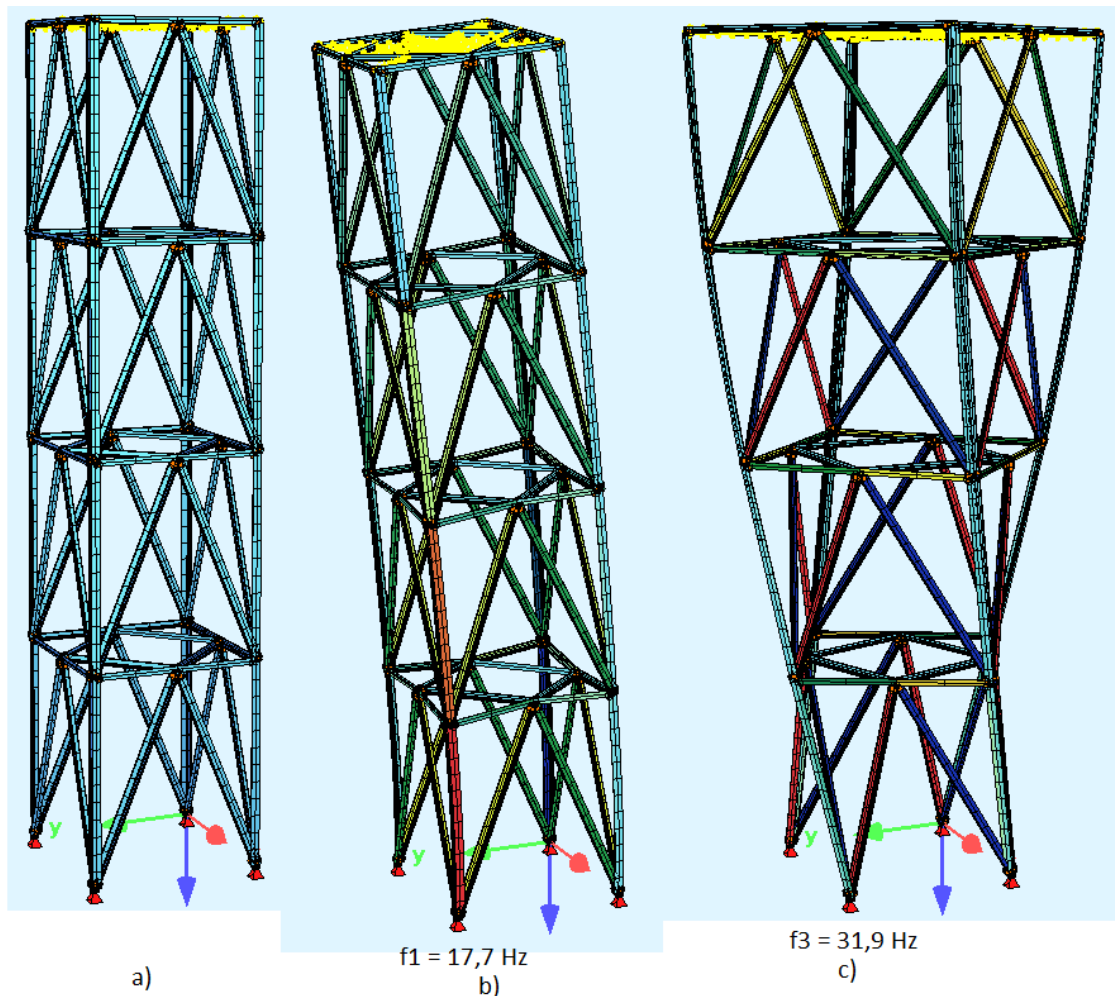


**Figure 6.36 Level I model Tower D-2S. a) Applied force, b) translational vibration mode (1st and 2nd), c) torsional vibration mode (3rd)**

### 6.3.2.1.2  Design
**Leg L70.70.7+FRP**

Design refers to the failed compression leg composed of angle sections L45.45.5 strengthened by
FRP strips 50x1.2 mm that were applied on the external side of their legs. In **Level I** legs are
checked for buckling due to axial compression with modified slenderness.

- **Material properties**

Actual material properties for design are as follows:

Steel $f_y = 308,3$ MPa      $f_u = 435,7$ MPa      FRP  $f_{f,actual} = 3187$ MPa

- **Cross section properties**

Since the width of the FRP, 50 mm, is wider that the width of the legs, 45 mm, only the portion of
the FRP attached to steel is considered in analysis and design, as shown in Figure 6.37.
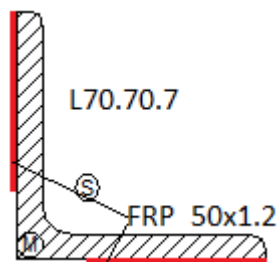


**Figure 6.37 Leg cross section used for analysis and design**

The properties of this hybrid cross section are determined according to the procedures described in
Deliverable 2.4 and are summarized in Table 6.34.

**Table 6.34 Properties of the hybrid cross section of Figure 6.37**

| Cross section area | Second moment of area, strong axis | Second moment of area, weak axis | Plastic axial force <br> *calculated with $f_f = f_{f,actual}/2$ |
|---|---|---|---|
| A = 1037 mm$^2$ | $I_u = 691349$ mm$^4$ | $I_v = 196349$ mm$^4$ | *$N_{pl} = 470,4$ kN |

The buckling resistance to axial compression is determined according to section 5.1.2 above and is
summarized in Table 6.35.

**Table 6.35 Buckling resistance of the hybrid leg cross section**

| Buckling length | Euler buckling load | Relative slenderness $\bar{\lambda}_v = \sqrt{\dfrac{N_{pl}}{N_{cr}}}$ | Effective slenderness $\bar{\lambda}_{eff,v} = 0,1 + 0,8\bar{\lambda}_v$ | Reduction factor, curve b | Buckling resistance $N_R = \dfrac{0,8\,\chi\,A\,f_y}{\gamma_{M1}}$ |
|---|---|---|---|---|---|
| $L_{cr} = L = 170{,}6$ cm | $N_{cr,v} = 139{,}7$ kN | $\bar{\lambda}_v = 1{,}84$ | $\bar{\lambda}_{eff,v} = 1{,}57$ | $\chi_v = 0{,}321$ | $N_R = 151{,}4$ kN |

The leg forces in the two opposite legs along the diagonal due to application of a horizontal force H = 55,9 kN at the top floor are shown in Figure 6.38. The axial forces in the other two legs are practically zero.
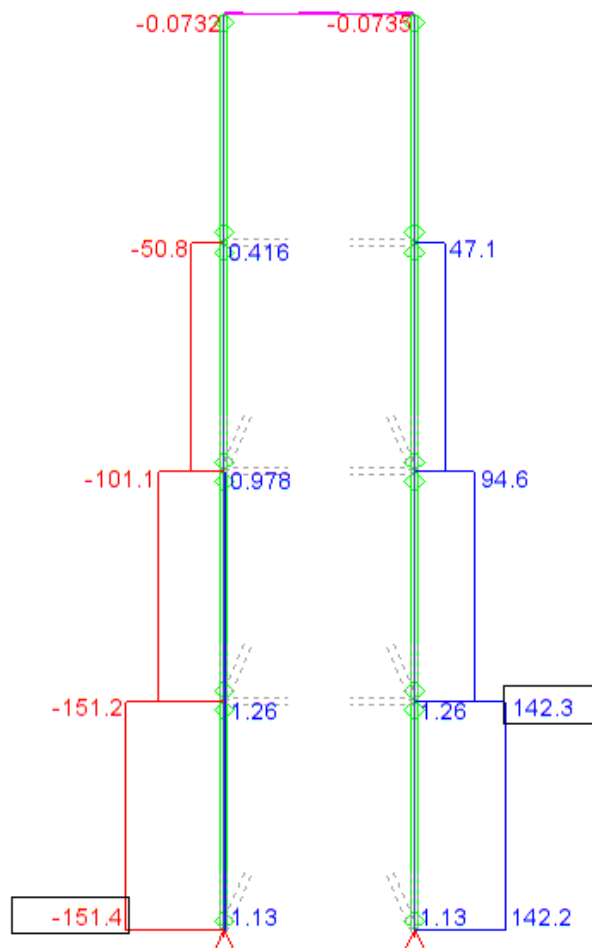


**Figure 6.38 Axial forces in along the diagonal legs due to applied force 57,5 kN**

**Bolted connection of braces L60.60.6**

The connection is with one bolt M12 10.9.

Bolt properties: d = 12 mm, d₀ = 13 mm, A_s = 84,3 mm², f_ub = 1000 MPa

For angle section: Thickness t = 6 mm, $f_u$ = 403,85 MPa

Geometry of connection: $e_1$ = 35 mm, $e_2$ = 20 mm  $\alpha_d$ = 35/(3·13) = 0,90, $k_1$ = 2,5, $\alpha_b$=$\alpha_d$

Shear capacity:  $F_{V,R}$ = 0,5· $f_{ub}$· $A_s$ = 42,15 kN

Bearing capacity: $F_{b,R} = \frac{2,5·0,90·403,85·12·6}{1000} = 65,2$ kN

Critical for the bolted connection is the shear capacity, $F_{Bolt,R}$ = 42,15 kN

The acting shear force on the bolts is 26,1 kN, equal to the axial force on the braces.

## Braces L60.60.6

- **Material properties**

Actual material properties of the cross section: $f_y$ = 280 MPa     $f_u$ = 403,85 MPa

**Cross section properties**

**Table 6.36 Properties L 60.60.6**

| Cross section area | Second moment of area, strong axis | Second moment of area, weak axis | Plastic axial force |
|---|---|---|---|
| A = 691 mm² | $I_u$ = 361000 mm⁴ | $I_v$ = 94300 mm⁴ | $N_{pl}$ = 194 kN |

The buckling resistance to axial compression is determined according to section 5.1.2 above and is summarized in Table 6.37.

**Table 6.37 Buckling resistance of the brace**

| Buckling length | Euler buckling load | Relative slenderness $\bar{\lambda}_v = \sqrt{\dfrac{N_{pl}}{N_{cr}}}$ | Effective slenderness $\bar{\lambda}_{eff,v} = 0,35 + 0,7\bar{\lambda}_v$ | Reduction factor, curve b | Buckling resistance $N_R = \dfrac{0,8\,\chi\,A\,f_y}{\gamma_{M1}}$ |
|---|---|---|---|---|---|
| $L_{cr}$ = L = 184,0 cm | $N_{cr,v}$ = 57,67 kN | $\bar{\lambda}_v$ = 1,83 | $\bar{\lambda}_{eff,v}$ = 1,63 | $\chi_v$ = 0,303 | $N_R$ = 47,0 kN |

The axial force of the braces is $N_E$ = 26,9 kN < $N_R$ = 47,0 kN

The results are summarized in Table 6.16. The **Level I** failure load is 57,5 kN.

**Table 6.38 Summary of the Level I design checks for tower 3 Type D-2S**

|  | Leg | Diagonal | Connection |
|---|---|---|---|
| $F_E$ | 151,4 | 26,1 | 26,9 |
| $F_R$ | 151,4 | 47,0 | 42,15 |
| Utilization grade | 1 | 0,56 | 0,64 |
| Level I Failure Load/test load | 57,5 / 81,8 = 0,70 |  |  |

### 6.3.2.2 Level II model

### 6.3.2.2.1 Modelling and Analysis

The tower model is similar to the **Level I** model, with the difference that all legs run continuously over the height, Figure 6.39a). Dynamic analysis provides eigenvalues and eigenforms of the tower, illustrated in Figure 6.39b) and c). They are close to those of **Level I** model.

**Figure 6.39 Level II model of tower D-2S. a) model, b) translational vibration mode (1$^{st}$ and 2$^{nd}$), c) torsional vibration mode (3$^{rd}$)**

### 6.3.2.2.2  Design

#### Compression leg L70.70.7+ FRP

The acting forces and moments and the fundamental buckling form of the tower according to linear analysis (LA) are presented in Figure 6.40. The transformation of the geometric axes moments to the principal axis moments is according to:

$$M_v = \frac{M_y + M_z}{\sqrt{2}}$$

$$M_u = \frac{M_y - M_z}{\sqrt{2}}$$
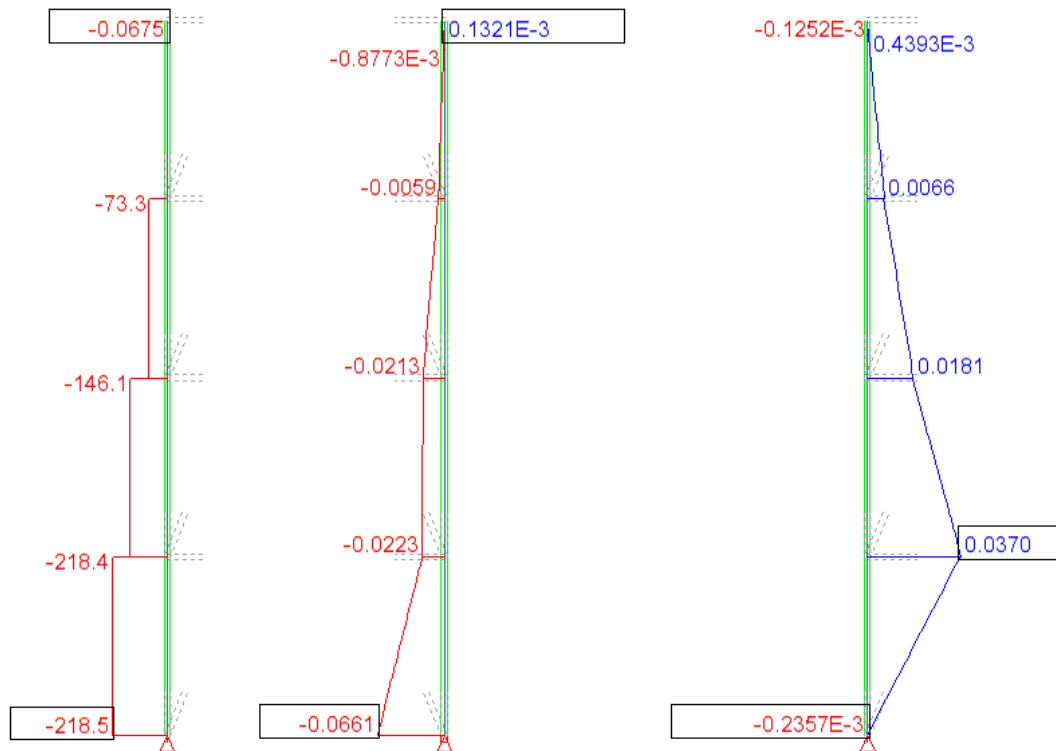
**Figure 6.40 Acting forces and moments for the leg**

The critical buckling length of the leg may be determined from linear buckling analysis (LBA).
Figure 6.41 shows the fundamental buckling form in which the leg buckles in respect to the weak
axis vv. The critical buckling factor due to application of the horizontal force, H=83,4 kN, is $\alpha_{cr}$ =
2,72. The axial force of the leg determined from global analysis due to this force is $N_E$ = 218,5 kN,
Figure 6.40.

The critical buckling load of the leg is $\alpha_{cr}$-times this force, $N_{cr}= \alpha_{cr} \cdot N_E$.

The critical buckling load is in general given by: $N_{cr} = \frac{\pi^2 EI}{(\beta L)^2}$

Equating the right sides of the two formulae, the equivalent buckling length factor $\beta$ may be
determined. The results in the relation:

$$\beta = \sqrt{\frac{\pi^2 EI}{\alpha_{cr} \cdot N_E}} \cdot L$$

where:

E modulus of elasticity

I second moment of area in respect to the buckling axis that corresponds to the buckling form

$\alpha_{cr}$ critical buckling factor as determined from LBA due to the applied loads

$N_E$ axial force in the leg from LA due to the applied loads

L system length of the leg.

The application of the above formula in the case study gives:

$$\beta = \sqrt{\frac{\pi^2 21000 \cdot 19{,}6}{2{,}72 \cdot 218{,}5}} \cdot 170{,}6 = 0{,}49 > 0{,}65. \text{ Accordingly } \beta = 0{,}65$$
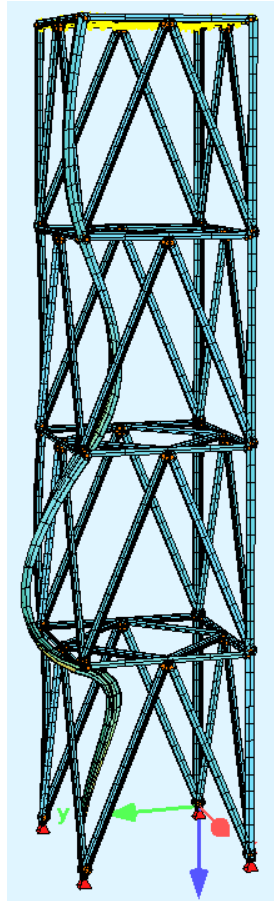


**Figure 6.41Fundamental buckling form of the tower, $\alpha_{cr} = 2{,}72$**

The design to axial compression and bending of the compression leg is determined according to section 5.1.2 above and is summarized in Table 6.39.

**Table 6.39 Design summary for the leg L70.70.7+FRP to compression and bending**

| | | v-v | u-u |
|---|---|---|---|
| Acting forces and moments | $N_{Ed}$ = 218,5 kN | $M_{v,Ed}$ = 0,045 kNm | $M_{u,Ed}$ = 0,045 kNm |
| Clear length | L | 1,706 m | 1,706 m |
| Buckling factor | β | 0,65 | 0,65 |
| Buckling length | $L_{cr}$ | 1,109 m | 1,109 m |
| Critical load | $N_{cr}$ | 311 kN | 1185 kN |
| Relative slenderness | λ | 3,05 | 1,56 |
| Reduction factors | χ | 0,107 | 0,323 |
| Ratio of end moments | ψ | 0,157 | 0,757 |
| Factors | C | 0,66 | 0,90 |
| Factors | k | $k_{vv}$ = $k_{uv}$ = 0,719 | $k_{uu}$= $k_{vu}$ = 1,292 |
| Elastic-plastic resistances | 470,4 kN | 605 kNm | 1264 kNm |
| Interaction | | 1,0 | 0,32 |

## Braces L60.60.6

In **Level II** design braces are checked for buckling due to compression and bending as resulting from the eccentric connection of the bolts. Material and cross section properties are the same as described in section 6.2.2.1.

The load eccentricity is calculated according to Deliverable 2.2 from the position of the bolts in the legs and the distance of the centroid from the angle heel which are shown in Figure 6.42. The relevant eccentricities are:

$e_v = \frac{e}{\sqrt{2}} - u_G$ = 0,849 mm  and   $e_u = e/\sqrt{2}$ = 24,7 mm

The end moments are calculated from:

$M_u = N \cdot e_u$  and  $M_v = N \cdot e_v$

where N ist he acting axial force.
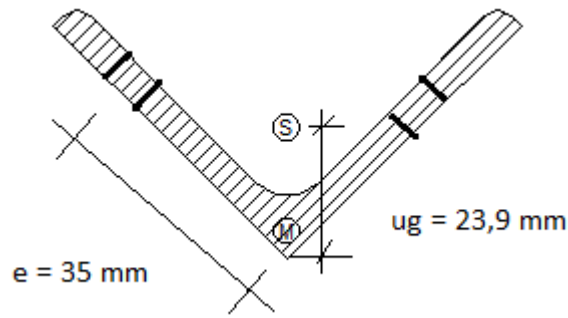
**Figure 6.42 Position of bolts and eccentricities for brace L 60.60.6**

The acting axial forces for braces are shown in Figure 6.43.
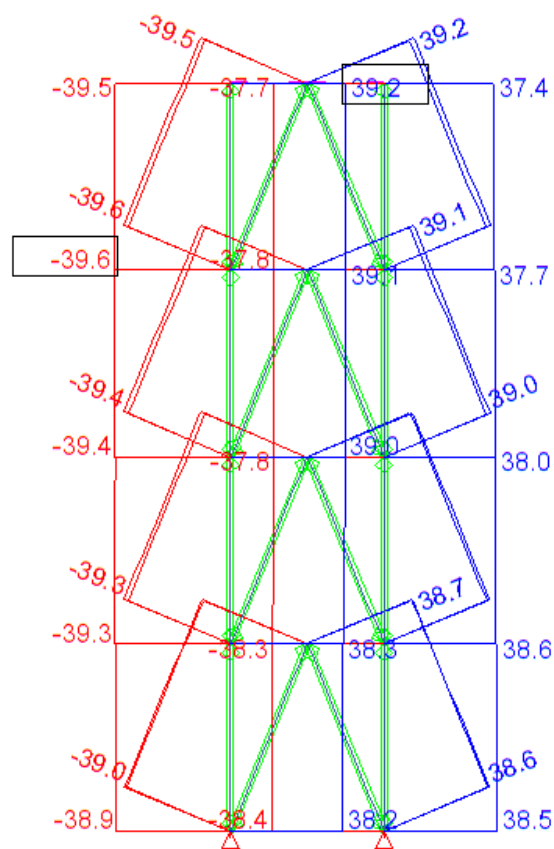


**Figure 6.43 Brace forces $N_E$ for horizontal force on the tower F = 83,4 kN**

The design to axial compression and bending is determined according to section 5.1.2 above and is summarized in Table 6.40.

**Table 6.40 Design summary for the hybrid brace to compression and bending**

| | | v-v | u-u |
|---|---|---|---|
| Acting forces and moments | $N_{Ed} = 39,6$ kN | $M_{v,Ed} = 0,0336$ kNm | $M_{u,Ed} = 0,980$ kNm |
| Clear length | L | 1,84 m | 1,84 m |
| Buckling factor | B | 0,65 | 0,65 |
| Buckling length | $L_{cr}$ | 1,56 m | 1,56 m |
| Critical load | $N_{cr}$ | 79,8 kN | 305,6 kN |
| Relative slenderness | λ | 1,556 | 0,796 |
| Reduction factors | χ | 0,325 | 0,700 |
| Ratio of end moments | ψ | 1 | 1 |
| Factors | C | 1 | 1 |
| Factors | k | $k_{vv} = k_{uv} = 1,984$ | $k_{uu} = k_{vu} = 1,149$ |
| Plastic resistances Npl, Mpl | 193 kN | 194 kNm | 380 kNm |
| Interaction | | 0,400 | 0,0878 |

## Bolted connection of braces L60.60.6

The connection is identical as in **Level I** analysis, their capacity being equal to

$F_{Bolt,R} = 42,15$ kN

**Table 6.41 Summary of the Level II design checks for tower 3 Type O-1S**

| | Leg | Diagonal | Connection |
|---|---|---|---|
| $F_E$ kN | 218,5 | 39,6 | 39,6 |
| $F_R$ kN | 218,5 | 62,9 | 42,15 |
| Utilization grade | 1 | 0,63 | 0,94 |
| Level I Failure Load/test load | 83,4 / 81,5 = 1,020 | | |

Figure 6.44 gives for all floors the experimental and numerical load - displacement curves. It may be seen that the numerical analysis underestimates by a high degree the actual displacements as recorded in the tests. This is due to the fact that the numerical analysis does not account for any flexibility of connections, joints, base structures etc.
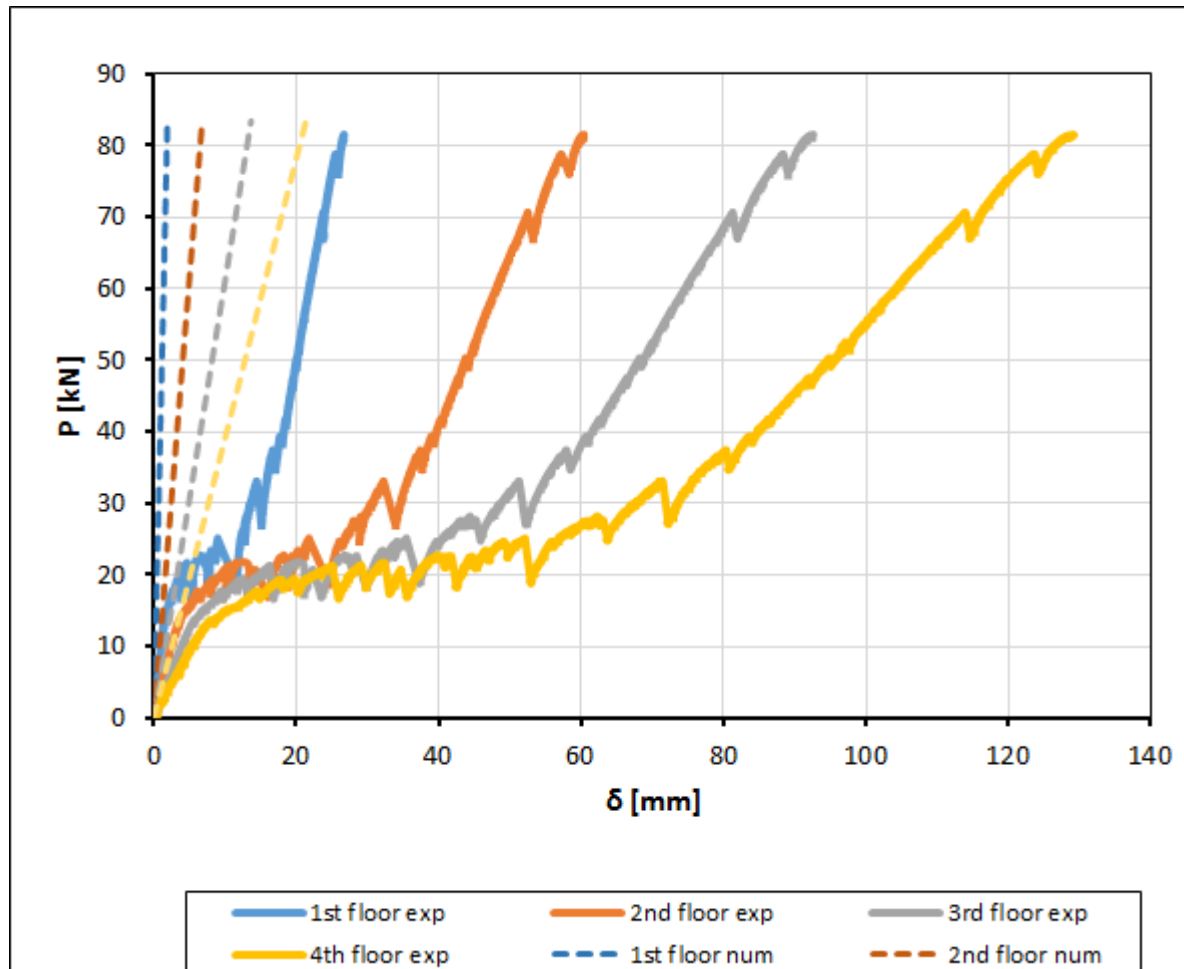


**Figure 6.44 Experimental vs numerical force – displacement curves**

The results of tower 3 for all calculation methods are summarized in Table 6.42.

**Table 6.42 Summary of all design checks for tower 3 Type D-2S**

|  | Experimental | Level I method | Level II method |
|---|---|---|---|
| Failure load | 81,5 kN | 57,5 kN | 83,4 kN |
| Critical member | Compression brace | Compression brace | Compression brace |
| Fundamental vibration frequency | 14,5 Hz | 17,7 Hz | 17,7 Hz |
| Top displacement at 81,5 kN horizontal force | 129 mm | 21 mm | 21 mm |

# References

[1] Dinkelbach K, Mors H (1985) Maste und Türme, Antennentragwerke, in Stahlbau Handbuch, Stahlbau-Verlagsgessellschaft mbH, Köln

[2] ECCS (1978) European Recommendation on Steel Structures

[3] ECCS (1976) Manual on Stability of Steel Structures

[4] EN 1993-3-1 (2006) Eurocode 3: Design of steel structures - Part 3-1: Towers, masts and chimneys – Towers and masts. CEN

[5] EN 1993-1-1 (2005) Eurocode 3: Design of steel structures - Part 1-1: General rules and rules for buildings. CEN

[6] EN 50341-1 (2001) Overhead electrical lines exceeding 45 kV – Part 1: General requirements – Common Specifications, CENELEC

[7] Haidar R. (1996) Compressive strength of steel single angles loaded through two-bolts in one leg. MSc Thesis, University of Windsor,

[8] Shani M. (1998) Compressive strength of eccentrically loaded steel angles. MSc Thesis, University of Windsor, 16 tests

[9] CSA (1994), CAN/CSA-S37-94, Antenna, towers and antenna supporting structures, Canadian Standards Association, Rexdale, Ont. Canada

[10] Bhilawe J, Gupta L (2015) Experimental investigation of steel equal angle subjected to compression, Engineering Structures and Technologies, Volume 7, Issue 2, pp. 55-66, 24 tests

[11] FINELG: Non-linear finite element analysis program, User's manual, Version 9.0, Greisch Ingeniere, 2003.

[12] Zhang L, Jaspart JP, Stability of members in compression made of large hot-rolled and welded angles, Research Report, University of Liège, 2013.

## List of Figures

## List of Tables